Investigation of Mechanistic Deterioration Modeling for Bridge Design and Management

Kyle Nickless, E.I.

Rebecca Atadero, Ph.D, P.E.

1. Report No. CDOT-2017-05	2. Government Accession No.	3. Recipient's Catalog No.
4. Title and Subtitle INVESTIGATION OF MECHANISTIC DETERIORATION MODELING FOR BRIDGE DESIGN AND MANAGEMENT		5. Report Date 04/2017
		6. Performing Organization Code
7. Author(s) Kyle Nickless, Rebecca Atadero		8. Performing Organization Report No. CDOT-2017-05
9. Performing Organization Name and Address Colorado State University 1373 Campus Delivery Fort Collins, CO 80523-1373		10. Work Unit No. (TRAIS)
		11. Contract or Grant No. Study No. 215-07
12. Sponsoring Agency Name and Address Colorado Department of Transportation - Research 4201 E. Arkansas Ave. Denver, CO 80222		13. Type of Report and Period Covered Final Report
		14. Sponsoring Agency Code
15. Supplementary Notes Prepared in cooperation with the US Department of Transportation, Federal Highway Administration		

16. Abstract

The ongoing deterioration of highway bridges in Colorado dictates that an effective method for allocating limited management resources be developed. In order to predict bridge deterioration in advance, mechanistic models that analyze the physical processes causing deterioration are capable of supplementing purely statistical models and addressing limitations associated with bridge inspection data and statistical methods. A review of existing analytical models in the literature was conducted. Due to its prevalence throughout the state of Colorado and frequent need for repair, corrosion-induced cracking of reinforced concrete (RC) decks was selected as the mode of deterioration for further study. A mechanistic model was developed to predict corrosion and concrete cracking as a function of material and environmental inputs. The model was modified to include the effects of epoxy-coated rebar, waterproofing membranes, asphalt overlays, joint deterioration, and deck maintenance. Probabilistic inputs were applied to simulate inherent randomness associated with deterioration. Model results showed that mechanistic models may be able to address limitations of statistical models and provide a more accurate and precise prediction of bridge degradation in advance. Preventive maintenance may provide longer bridge deck service life with fewer total maintenance actions than current methods. However, experimental study of specific deterioration processes and additional data collection are needed to validate model predictions. Maintenance histories of existing bridges are necessary to predicting bridge deterioration and improving bridge design and management in the future.

Implementation

To improve existing methods of bridge design and management, mechanistic models may be used as a supplement to current statistical models if additional data is collected. Maintenance history should be documented. Experimental study is necessary to provide timelines of deterioration and effectiveness of joints, waterproofing membranes, rebar coatings, and asphalt overlays. If model inputs are adjusted to reflect experimental results, and outputs are validated using condition and maintenance history, the model developed for this project can be used to predict deterioration for new and existing bridges.

17. Keywords bridge deck, mechanistic model, deterioration, bridge management, corrosion, maintenance.	18. Distribution Statement This document is available on CDOT's website http://www.coloradodot.info/programs/research/pdfs
19. Security Classif. (of this report) Unclassified	20. Security Classif. (of this page) Unclassified	21. No. of Pages 135	22. Price

Form DOT F 1700.7 (8-72)   Reproduction of completed page authorized

ACKNOWLEDGEMENTS

EXECUTIVE SUMMARY

The ongoing deterioration of highway bridges in Colorado dictates that an effective method for allocating limited management resources be developed. In order to predict bridge deterioration in advance, mechanistic models, which analyze the physical processes causing deterioration, are capable of supplementing purely statistical models and addressing limitations associated with bridge inspection data and statistical methods. A review of existing analytical models in the literature was conducted. Due to its prevalence throughout the state of Colorado and frequent need for repair, corrosion-induced cracking of reinforced concrete (RC) decks was selected as the mode of deterioration for further study. A mechanistic model was developed to predict corrosion and concrete cracking as a function of material and environmental inputs. The model was modified to include the effects of epoxy-coated rebar, waterproofing membranes, asphalt overlays, joint deterioration, and deck maintenance. Probabilistic inputs were applied to simulate inherent randomness associated with deterioration. Model results showed that mechanistic models may be able to address limitations of statistical models and provide a more accurate and precise prediction of bridge degradation in advance. Preventive maintenance may provide longer bridge deck service life with fewer total maintenance actions than current methods. However, experimental study of specific deterioration processes and additional data collection are needed to validate model predictions. Maintenance histories of existing bridges are necessary for predicting bridge deterioration and improving bridge design and management in the future.

TABLE OF CONTENTS

List of Figures

List of Tables

1. INTRODUCTION

1.1 Background

Bridge construction and maintenance are substantial components of asset management for transportation departments throughout the United States. According to the ASCE 2013 Infrastructure Report Card, roughly $12.8 billion is spent on bridge care annually in the U.S., and nearly 25% of the nation's bridges are structurally deficient or functionally obsolete (ASCE 2013). The State of Colorado's bridges are in better condition than national averages. As of the 8,624 Colorado bridges listed in the 2015 National Bridge Inventory (NBI), 521 (~6%) are structurally deficient (SD) and 851 (~10%) are functionally obsolete (FO). In 2009, the state established the Colorado Bridge Enterprise (CBE), a government owned business within the Colorado Department of Transportation (CDOT), to address the worst bridges in the state; those classified as SD or FO and rated in poor condition. As of 2015, of the192 bridges deemed eligible for CBE funds, 120 had already been repaired, reconstructed, or replaced.

While Colorado has taken specific steps to address the worst bridges in the state, the fact remains that, in Colorado and nationally, funding for repair and maintenance of bridges is limited, and current funding levels are not adequate to keep up with continued aging and degradation of bridges. Two strategies are available to improve the condition of the state's bridge infrastructure. One, the current level of federal (or state) funding for bridge maintenance could be increased. And two, the available funds could be used more efficiently, by altering the timing of resource allocation. While a combination of these strategies is likely necessary, this report focuses primarily on bridge asset management and strategy number two.

Bridge asset management starts with inspection. Modern bridge data collection, as mandated at the federal level by FHWA guidelines, requires bridge owners to record the condition of each bridge component during inspection. The deck, superstructure, and substructure must all receive ratings such that the bridge can be modeled as a combination of separate elements rather than as a single entity. Further, existing asset management software such as AASHTO Bridgeware considers more discrete components such as girders, joints, piers, and the deck itself. Subjective ratings applied to these elements during visual inspections are the primary data available to bridge managers.

Although national standards are implemented for bridge inspection, management decisions are ultimately deferred to individual state transportation departments. One advantage of making management decisions at the state level is the ability to tailor bridge management practices to the specific needs of bridges in different regions. These bridges may be experiencing varying degrees of deterioration over time, especially those with different environmental conditions or traffic volumes. Deterioration modeling can improve the efficiency of maintenance funding allocations by predicting the rate at which certain bridge components will deteriorate, and, with better models, the localized factors can be included in predicted levels of degradation. By forecasting how and when a bridge will degrade, bridge maintenance can be planned in advance, and unnecessary maintenance can be avoided.

To assist bridge managers with decisions regarding bridge maintenance and repair, two general approaches to deterioration modeling have been developed: statistical models that are based on visual inspection rating history, and mechanistic models that are based on physical deterioration mechanisms. Although both model types share the goal of predicting bridge deterioration in advance, they operate under different assumptions and require different inputs. Statistical models such as a Markov chain or Weibull distribution rely on past data from biannual visual inspections to predict future deterioration. Alternatively, mechanistic models attempt to predict the condition of a bridge by analytically describing the physical mechanisms causing deterioration. They use environmental and other physical data such as concrete mix parameters as inputs to predict how a bridge element will degrade over time. The complicated nature of multiple deterioration mechanisms presents a challenge for creating accurate mechanistic models.

In the absence of accurate mechanistic models, many state departments of transportation choose to implement a statistical model that uses historical bridge data to predict future conditions. However, this approach is very dependent on the quality and availability of data, and it can be very difficult to collect enough data to develop accurate deterioration models for different conditions. For example, to collect enough data to develop a full deterioration model, bridges of similar type (e.g. steel girder with a concrete deck) might be lumped together in a single set even though individual bridges might have very different service environments in terms of traffic, weather, and maintenance. This generalized model has reduced accuracy for any individual bridge. Statistical modeling methods may also be unreliable for newer bridges built with current design standards

because there is little or no history of inspection data available for these bridge types. One example is reinforced concrete (RC) bridge decks that contain epoxy coated rebar (ECR). The lack of deterioration history on bridges with ECR means that any statistical model of deterioration would need to be based on older bridge decks with uncoated rebar for which data is available.

Accurate mechanistic models would be a significant improvement over statistical methods, due to their ability to model physical deterioration at the individual bridge or element level as a function of environmental and design parameters. They could also be used as a supplement to statistical methods, filling in gaps where not enough empirical data is available. A variety of mechanistic approaches currently exist as analytical models in research literature as well as commercial software packages. The purpose of this report is to investigate the application of currently available mechanistic deterioration models to CDOT bridge management and design practice.

In particular, this report focuses on models of reinforced concrete bridge deck cracking. This deterioration mechanism has been the subject of extensive past research and is important for management applications due to its immediate and severe effects on deck service life. Cracking, both vertical (surface) and horizontal (delamination), affects the strength and serviceability of RC decks throughout the entire service life. Once cracking has propagated through multiple sections of a deck, repair options are limited and deck replacement is often necessary for a bridge to remain in service. By applying mechanistic deterioration modeling techniques to RC decks, deterioration may be predicted ahead of time, and preventive maintenance may extend service life and avert costly repairs in late years of the bridge's service life.

1.2 Objectives

The ultimate goal of this research is to provide ways to apply mechanistic models to the management of existing bridges and design of new bridges in Colorado. To move towards this goal, this report addresses the following objectives:

1) Investigate deterioration mechanisms that are most useful in predicting bridge condition.
2) Locate and update mechanistic models for important deterioration mechanisms to reflect modern bridge design practices.

3) Identify limitations in available models and data that limit the applicability of mechanistic deterioration models, and make recommendations about future research and data collection to enhance the applicability of mechanistic models to bridge management.

4) Demonstrate how mechanistic models can include the effect of environmental conditions, design parameters, and maintenance actions in predicting bridge performance.

5) Suggest ways that analytical models may be used in the future to improve new designs or develop preventive maintenance schemes through lifecycle cost analysis.

1.3 Research Approach

In order to achieve these objectives, several existing analytical models which represent the individual stages of deterioration of reinforced concrete bridge decks are combined, and then modified to reflect current design practices such as epoxy coated rebar, waterproofing membranes, and asphalt wearing surfaces. Interactive effects between decks and joints are also considered to demonstrate the ability of mechanistic models to predict deterioration of multiple elements simultaneously. Then the effects of maintenance actions on model outputs are examined. Finally, model application is discussed, and the types of data necessary to implement the model are highlighted. If these objectives are met, an improved understanding of bridge deterioration will aid in predicting condition states of bridge elements and assist bridge managers in making informed decisions about maintenance strategies.

1.4 Report Organization

This report is arranged to demonstrate how the project objectives can be achieved through specific application of the process outlined in Section 1.3. Chapter 2 presents a literature review of current deterioration modeling techniques and their limitations. Service life factors are identified and their influence on the deterioration models is discussed. Chapter 3 presents a proposed assemblage of existing localized deterioration models (denoted "sub-models") for bridge decks. Based on the assembled baseline model, Chapter 4 presents modifications made to the model to reflect modern bridge design, including protective systems and the interactive effect of joint deterioration on a specified failure mode in RC decks. Chapter 5 discusses the influence of maintenance actions on the modified deterioration models in Chapter 4 and timing of maintenance.

Chapter 6 presents the modified deterioration model at the global deck level and results of a probabilistic approach to mechanistic modeling. Chapter 7 discusses model application and disparities between inspection ratings and model outputs. Finally, a project summary, conclusion, and recommendation for future research are presented in Chapter 8.

2. LITERATURE REVIEW

2.1 Introduction

Current bridge asset management is centered on the dynamic between inspection, maintenance, and available funds. Often, available funds do not allow for preventive maintenance, and thus inspection is conducted to identify the extent of deterioration. As a result, maintenance is performed to correct serious issues identified during inspection. This "worst first" approach is not the most effective way to preserve assets, and models that predict deterioration in advance could be used by bridge managers to more efficiently allocate resources.

In considering the application of mechanistic models to bridge management, this report focuses specifically on reinforced concrete bridge decks because they are very common elements, they often deteriorate at a more rapid pace than other elements, and there are existing deterioration models in the literature relevant to reinforced concrete. This review begins with a discussion of current bridge inspection and maintenance practices; then covers existing literature regarding deterioration modeling of bridge decks. Inspection plays an important role in statistical deterioration models since its results are used as inputs to various statistical methods of predicting deterioration. Inspection results are also useful for validating the effectiveness and accuracy of physics-based mechanistic models. Maintenance is conducted as a result of low inspection ratings; it also contributes towards a long-term understanding of bridge deterioration.

2.2 Bridge Inspection

Although bridge inspection is conducted at the state level, the nationwide Federal Highway Administration (FHWA) maintains inspection consistency throughout the United States through implementation of the National Bridge Inspection Standards (NBIS). State departments of transportation are required to submit the basic results of their inspections to the National Bridge Inventory (NBI). The NBI uses a numerical scale to represent bridge condition that ranges from 0 to 9, where a rating of 9 represents a brand new bridge in "excellent" condition, and 0 represents a bridge in "failed" condition (FHWA 1995). Bridge inspectors rate individual bridge elements during visual inspection, and report ratings for the three primary elements (deck, superstructure, and substructure) to their department of transportation and the FHWA. For purposes of bridge asset management, state departments of transportation (DOTs) will often divide bridges into

smaller elements and record ratings for items such as girders, joints, etc. using a system such as the Commonly Recognized Structural Elements created by AASHTO (AASHTO 1994). Ratings for these smaller bridge elements can then be mapped to the NBI scale, but criteria for rating each element is not always consistent among rating systems. This is one example of subjectivity present in the current inspection rating system.

Bridge inspectors have multiple resources available to them for conducting inspections, such as the Bridge Inspector's Reference Manual (2012). However, inspection guides often include limited quantitative support for determining ratings, especially for inspection methods that are entirely visual. Ultimately, decisions made about the rating of a bridge element during inspection are left to the discretion of the individual inspector. Phares et al. (2004) investigated variability in inspection ratings by comparing inspection results from 49 state DOT inspectors on one group of seven bridges. In general, there was significant variation in assigned bridge element ratings among inspectors, as demonstrated in Figure 1. This subjectivity is difficult to overcome in visual inspection with limited tools available for measuring bridge condition.

	Primary Component		
	Deck	Superstructure	Substructure
Reference	4	4	4
Average	4.9	4.2	4.3
Standard Deviation	0.94	0.77	0.76
COV	0.19	0.18	0.18
Minimum	2	2	3
Maximum	7	6	6
Mode	5	4	4
N	48	49	49
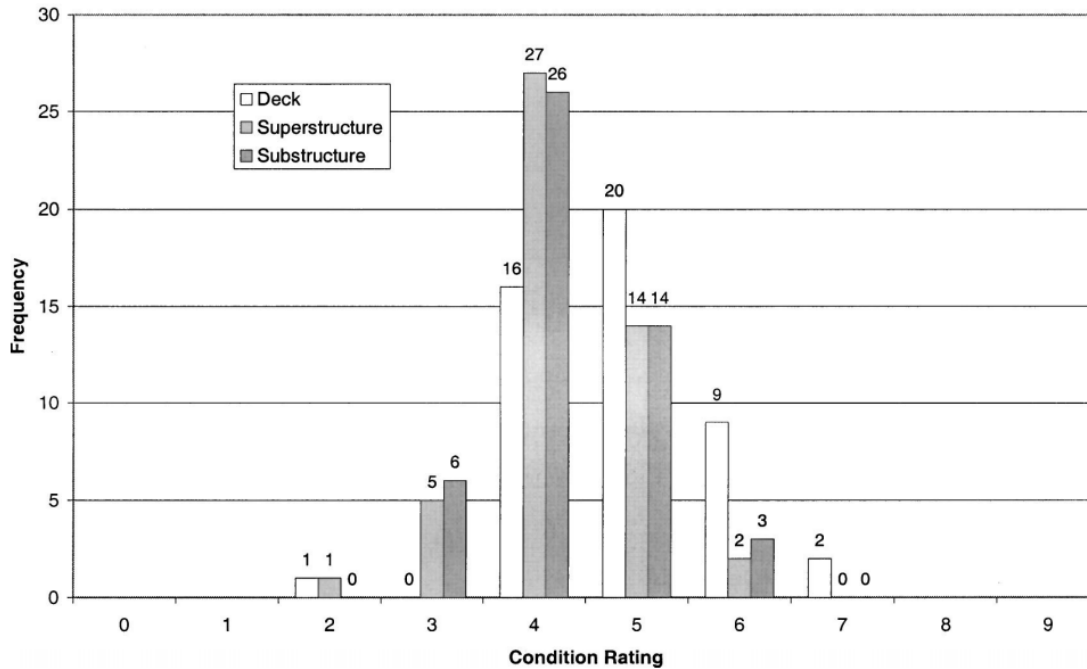
Figure 1. Variability in inspection ratings for primary bridge elements (Phares et al. 2004)

Another limitation of visual inspection is the inability to see imminent yet inactive deterioration. Visual examination of a deck may not provide enough insight into developing corrosion or other interior damage if surface cracking has not already begun. Non-visual techniques such as chain drag can identify active deterioration, but do not give good estimations of when future deterioration will occur. This system often lends itself to a "worst first" maintenance philosophy, where bridges with imminent but inactive deterioration are often neglected. Thus, maintenance is typically reactive rather than preventive. As a result, maintenance funds may be used inefficiently.

NBIS mandated inspections are most often conducted on a biannual basis, with some exceptions. This system allows for insight into bridge condition at each interval, but tells little about the condition of the bridge between inspections. Additionally, Washer et al. (2014) noted

that biannual inspection is simple for bridge administrators, but restricts bridge managers from allocating inspection resources efficiently. Washer et al. (2014) proposed a new system for bridge inspection that uses reliability to dictate inspection timing and thoroughness. With reliability-based inspection, more thorough attention would be given to bridges with higher risk of deterioration and failure. However, irregular inspection intervals would make it more difficult to use current statistical methods to predict deterioration. Mechanistic deterioration models may be better able to accommodate inspection data with varying frequency.

Additionally, inspection data contributes little towards understanding which deterioration mechanisms are causing condition-state ratings to change (Washer et al. 2014). If the mechanisms affecting deterioration are not well understood through inspection, maintenance cannot be conducted efficiently to combat these mechanisms in the future. Additional limitations of inspection data and its applicability to deterioration modeling are discussed in Section 2.4.

2.3 Bridge Maintenance

The purpose of bridge maintenance is to extend service life by repairing or replacing damaged bridge elements. Inspection ratings and reports dictate the timing and extent to which bridge managers allocate maintenance resources. Yehia et al. (2008) listed several important factors that influence maintenance decisions:

1. Nature, extent, and severity of the defect
2. Effect of the repair method on bridge service life
3. Extent to which the repair process will disrupt traffic flow
4. Availability of funds

Yehia et al. (2008) also categorized bridge deck repair methods in two ways: by depth of damage and by presence or absence of a waterproofing mechanism. The latter categorization assigned maintenance actions as either protective or non-protective repairs, where protective repairs provide the deck with some form of waterproofing intended to delay deterioration mechanisms dependent on water.

Optimization of bridge maintenance using statistical deterioration modeling has been previously studied and applied as a means to assist bridge managers with maintenance decisions. Robelin and Madanat (2007) used bridge histories to optimize maintenance based on a Markovian

deterioration model (see Section 2.4) for a single facility, but noted that further research is needed to optimize maintenance at the system level. Frangopol et al. (2001) discussed the benefits of transitioning bridge management from current statistical approaches to a reliability-based system. Rather than allocating maintenance to bridges with high probability of a condition state change, changes in reliability dictate resource allocation. Neves et al. (2006) utilized multi-objective optimization to combine condition state, safety, and cost when considering maintenance types and timing. In this manner, maintenance decisions are not driven by a single factor. Work is still necessary to demonstrate how these detailed analytical approaches could be applied to real bridges with limited available data.

Huang et al. (2004) used probabilistic analysis to compare estimated service lives of bridge deck treatments subject to early, on-time, and late maintenance. In general, the estimated service life of a deck treatment increased if early maintenance was conducted, and decreased or stayed the same with on-time and/or late maintenance. For maintenance of a deck with an asphaltic concrete (AC) overlay and waterproofing membrane, the estimated service life increased when maintenance was conducted earlier than is typical. Since conducting effective and cost-efficient maintenance is a primary objective of bridge management, bridge deterioration modeling should be accurate and informative enough to support these decisions. Deterioration models should also be capable of factoring in effects of maintenance before and after repairs have been conducted. In this manner, effective maintenance can be proactively applied to bridge decks.

2.4 Statistical Modeling

In current bridge management practice, many DOTs employ probability-based statistical models to predict bridge element deterioration. These models are popular because they are relatively cheap and do not require an understanding of the complex mechanistic deterioration behavior of a particular element (in this case, reinforced concrete elements). Visual inspection of existing bridges allocates condition-state ratings to individual elements, from which transition probabilities to lower condition states can be estimated. A common stochastic approach is the Markov chain model, which has seen application in various software packages including PONTIS/AASHTOWare (AASHTO 2016) and BRIDGIT (NCHRP 1996). Equation 1 demonstrates the matrix format of a Markov chain.

$$
\begin{array}{l}
CS1: \\
CS2: \\
CS3: \\
CS4: \\
CS5:
\end{array}
\begin{pmatrix} x_1 \\ x_2 \\ x_3 \\ x_4 \\ x_5 \end{pmatrix}_{t+1}
=
\begin{bmatrix}
a_{11} & a_{12} & a_{13} & a_{14} & a_{15} \\
0 & a_{22} & a_{23} & a_{24} & a_{25} \\
0 & 0 & a_{33} & a_{34} & a_{35} \\
0 & 0 & 0 & a_{44} & a_{45} \\
0 & 0 & 0 & 0 & a_{55}
\end{bmatrix}^{T}
\ \text{X}\
\begin{pmatrix} x_1 \\ x_2 \\ x_3 \\ x_4 \\ x_5 \end{pmatrix}_{t}
\qquad (1)
$$

In Equation 1, CS is defined as the condition state. 1 represents an element in "good" condition, and 5 represents an element in "alarming" condition. However, a Markov chain may be applied to any number of condition states, rather than just five. Roelfstra et al. (2004) noted that the coefficients of matrix a_{ij} can be represented in two ways:

1. As the percentage of an element that changed from state i to state j after one inspection period, or

2. The probability of a unit quantity of an element to pass from condition state i to condition state j after one inspection period.

Although the Markov chain model is simple and efficient at the network level, several limitations of the approach are highlighted by Agrawal et al. (2010):

- Assumption of discrete transition time intervals, constant bridge population, and stationary transition probabilities.

- Assumption of duration independence, which ignores the effects of facility condition history in predicting future states.

- Inability of transition probabilities to predict a condition state increase, which is unrealistic, especially in the event of bridge maintenance.

- Inability to efficiently consider the interactive effects between deterioration mechanisms of different bridge elements, such as the interaction between deteriorating joints and the surrounding deck area.

The impact of constant state duration in the Markov model was investigated by Morcous (2006). Because transition probabilities are calculated for a constant period, inspection records should reflect this time period to be accurate. However, inspections from the data used by Morcous (2006) were noted to occur every 2.85 years on average, with a standard deviation of 0.787 years. Because

22

the inspection intervals varied, the assumption of constant duration was violated (Morcous 2006). Roelfstra et al. (2004) compared Markov chain models to numerical simulations of corrosion damage. They noted that a lack of inspection data for the worst and second-worst condition states can lead to unreliability in the predictions made by Markov chains. Since bridge elements are often fixed before reaching states close to failure, this unreliability is difficult to overcome without jeopardizing safety. However, Markov chains provide an easier solution to optimization of bridge preservation actions when compared to numerical simulation.

Agrawal et al. (2010) proposed an alternative statistical approach to deterioration modeling using the Weibull distribution. The Weibull distribution is designed to consider duration dependence characteristics when developing transition probabilities. While more conservative, the Weibull approach appeared to perform closer to actual condition ratings than the Markov chains approach.

Although purely stochastic deterioration modeling is cheap and somewhat efficient on the network level, it does a poor job of representing deterioration at the project level, and a worse job of representing deterioration at the element level. The benefits of mechanistic modeling become apparent when discussing the deterioration of bridges at a local scale.

2.5 Mechanistic Modeling

As an alternative to purely statistical models, which use previous observations of service life to predict future condition, mechanistic models offer the potential of a more accurate and precise solution that may be able to overcome some of the shortcomings of statistical models listed above. Urs et al. (2015) defined mechanistic models as those that provide prediction of service life based on mathematical descriptions of the phenomenon involved in concrete degradation, such as understanding microstructure of concrete before and during degradation. Although concrete is used as an example here, mechanistic models could theoretically be applied to each element of any bridge type, if the deterioration mechanisms affecting those elements are described mathematically.

Before mechanistic models can be developed, the underlying causes of deterioration must be identified. In RC bridge decks, concrete cracking is the primary result of deterioration. Cracking may occur as a result of many deterioration mechanisms. Early sources of cracking include plastic

settlement, plastic and drying shrinkage, and thermal displacement. Later throughout the service life, sources of cracking transition to freeze/thaw, corrosion, and alkali-aggregate reactions (TRB 2006). Although many mechanisms may act at once, most causes of cracking occur within the first few months or years of service life. To make long-term projections of bridge condition, it may be more beneficial to study deterioration that occurs throughout the life of the bridge as opposed to just those that occur very early on. Rebar corrosion is an example of a deterioration mode that affects the condition of RC decks throughout most of the deck's service life.

Mechanistic models of RC deterioration exist both in the literature as mathematical solutions to deterioration phenomena, as well as in commercial software available to bridge managers. Hu et al. (2013) provided a comprehensive review of three commercial software packages: STADIUM, Life-365, and CONCLIFE. Each of these is designed to predict deterioration of concrete structures, but they use different approaches and even consider separate mechanisms. While STADIUM and Life-365 are focused on chloride-induced corrosion, CONCLIFE seeks to predict damage from sulfate attack and freeze-thaw cycles. Advantages and limitations of the commercial models are described by Hu et al. (2013).

Analytical models also exist in the literature for predicting deterioration of RC decks. Models exist for predicting freeze-thaw damage (Bazant et al. 1988) and carbonation damage (Isgor and Razaqpur 2004) as well as creep and shrinkage (Bazant et al. 1995). However, most analytical models focus on one or more stages of steel reinforcement corrosion and its damage to surrounding concrete. This deterioration mechanism is explored in detail in Section 2.5.2.

2.5.1 Service Life Factors

To understand the complex mechanisms causing bridge deck deterioration, a comprehensive analysis of the underlying factors affecting service life should be conducted. Then, factors with the greatest impact can be used as inputs for mechanistic models. These factors may be categorized as environmental or physical. Environmental factors may include humidity, temperature, and other weather conditions that affect durability of concrete. Physical factors may include the design parameters of the concrete and reinforcement, such as the water-cement ratio and rebar diameter. Kim and Yoon (2010) investigated a variety of bridge factors and their association with deterioration for bridges in cold regions. These factors are listed in Table 1. By applying Pearson's

24

correlation to each combination of factors, it was determined that age, traffic volume, and presence of water were most strongly correlated with structural deficiency. Age is a factor that can be considered in mechanistic models through the use of time-dependent variables. Traffic volume, while not a physical parameter of the bridge itself, may be considered by applying its effect on one or more bridge parameters. For example, high traffic volumes could reduce the effectiveness of protective overlays. In this manner, factors that are known to increase the rate of deterioration can be included in mathematical models. Finally, water presence can be included as an input to many mechanistic models, especially those that consider corrosion to be the primary deterioration mechanism. A complete list of factors included in the proposed mechanistic model is included in Chapter 3.

Table 1. Service life factors affecting bridge condition (Kim and Yoon 2010)

Factor	Variable	Description	Data source
Physical	Design load	Design load	NBI, Item 31
	Number of spans	Number of spans in main unit	NBI, Item 45
	Width	Deck width	NBI, Item 52
	Year built	Year built	NBI, Item 27
	ADT	Average daily traffic	NBI, Item 29
	Truck ADT	Average daily truck traffic	NBI, Item 109
	Replacement	Replacement, widening, and rehabilitation of bridge	NBI, Item 75
	Replaced length	Length of structure improvement	NBI, Item 76
	Deck status	Deck condition ratings	NBI, Items 58
Material	Concrete	Concrete bridge	NBI, Item 43A
	Preconcrete	Prestressed concrete bridge	NBI, Item 43A
	Steel	Steel bridge	NBI, Item 43A
Structural system	Slab	Slab bridge	NBI, Item 43B
	Girder/beam	Girder bridge	NBI, Item 43B
	Truss	Truss bridge	NBI, Item 43B
Environment/weather	Precipitation	Annual mean precipitation in inches (1971–2000)	NDSCO[a]
	Snow fall	Average mean annual snowfall (1930–1960)	USGS[b]
	Below 32	Annual number of days 32°F or below (1961–1990)	USGS[b]
	Above 90	Annual number of days 90°F or above (1961–1990)	USGS[b]
	Average temperature	Average temperature (1961–1990)	USGS[b]
	Over water	Bridge over waterway	NBI, Item 42
Service	Highway	Bridge service on highway	NBI, Item 42
	Railroad	Bridge service on railroad	NBI, Item 42
	Toll	Toll bridge	NBI, Item 20
	Average farm size	Average farm size of census track where bridge locates	Census Bureau
	Population	Population of census track where bridge locates	Census Bureau

[a]North Dakota State Climate Office.
[b]Northern Prairie Wildlife Research Center.

2.5.2 Chloride-induced Corrosion Modeling

Corrosion in RC bridge decks is a commonly observed deterioration mechanism that represents roughly 15 percent of concrete deterioration, a higher fraction than any other single mechanism affecting durability (Basheer et al. 1996). Due to its prevalence in concrete deterioration, chloride-induced corrosion is a popular subject of mechanistic modeling. Corrosion of reinforcement and subsequent expansion of rust products induces expansive hoop stresses on the surrounding concrete, producing vertical cracking (surface cracking) and horizontal cracking (delamination). These cracks can cause significant reduction in bridge safety due to loss of strength, as well as reduction in serviceability due to driver discomfort. A basic diagram of the rebar corrosion process is shown in Figure 2. Chlorides from de-icing and anti-icing salts are necessary to depassivate the steel rebar, and water and oxygen are required to sustain the corrosion reaction and develop rust products.
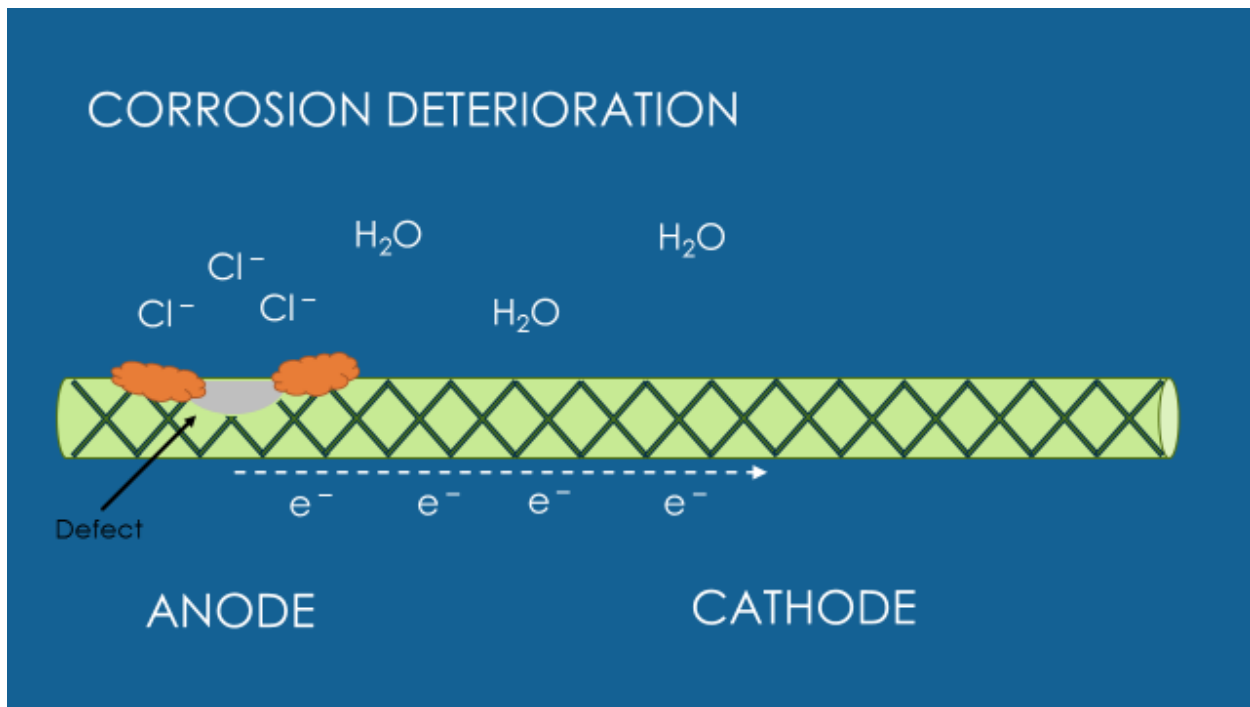
Figure 2. Micro-corrosion process on epoxy-coated steel rebar

Many corrosion models consider deterioration in three stages. The first is corrosion initiation, which includes the time taken for chlorides to infiltrate the concrete surface and reach the depth of steel reinforcement. The second stage is crack initiation, where corrosion products (rust) build up on the surface of the steel rebar and exert pressure on the surrounding concrete until cracking

begins. The final stage is crack propagation, wherein sustained pressure from rust products widens the existing crack(s) until the surrounding concrete is no longer serviceable. A graphic of this process is presented in Figure 3.
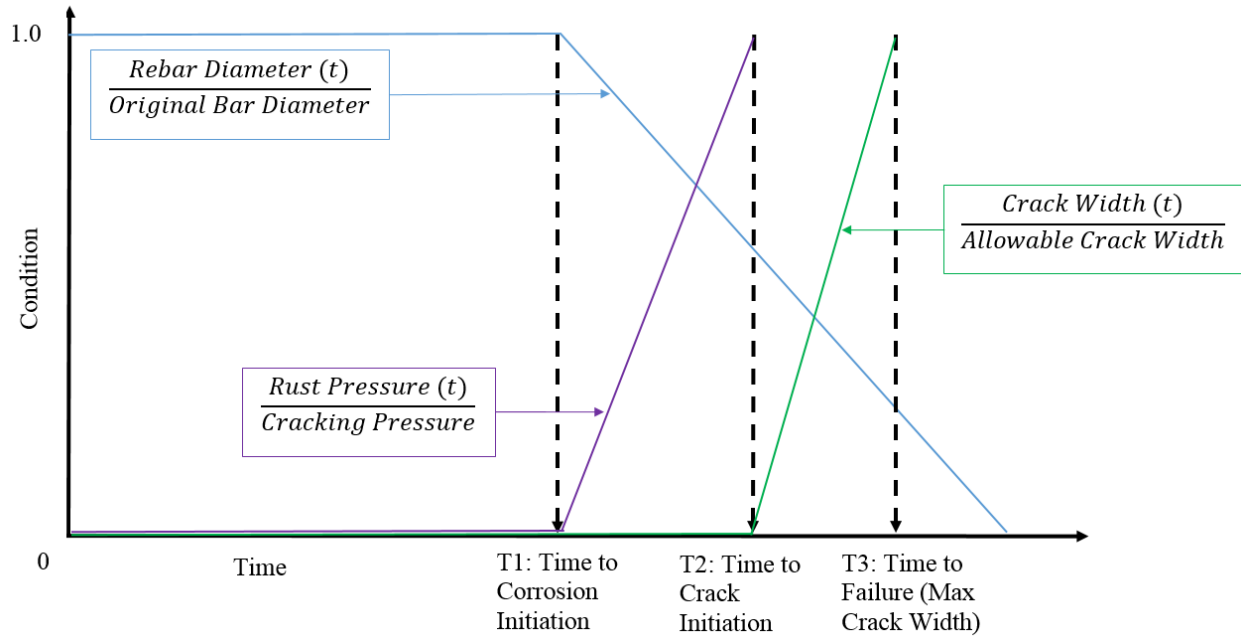
Figure 3. Stages of corrosion-induced concrete cracking in bridge decks

A landmark study conducted by Liu and Weyers (1998) has served as the basis for many corrosion-damage-based models. The study used experimental results to predict the rate of corrosion of reinforcing steel as a function of temperature, ohmic resistance of concrete, chloride content, and time since corrosion initiation. Balafas and Burgoyne (2011) presented a mathematical model for predicting pressure build up due to corrosion and ultimately the time for concrete cover failure. These sub-models were both implemented in a comprehensive time-to-failure model proposed by Hu et al. (2013). This comprehensive model serves as a useful starting point for the implementation of mechanistic models in bridge asset management. A diagram of a single rebar experiencing corrosion is displayed in Figure 4 (Hu et al. 2013).
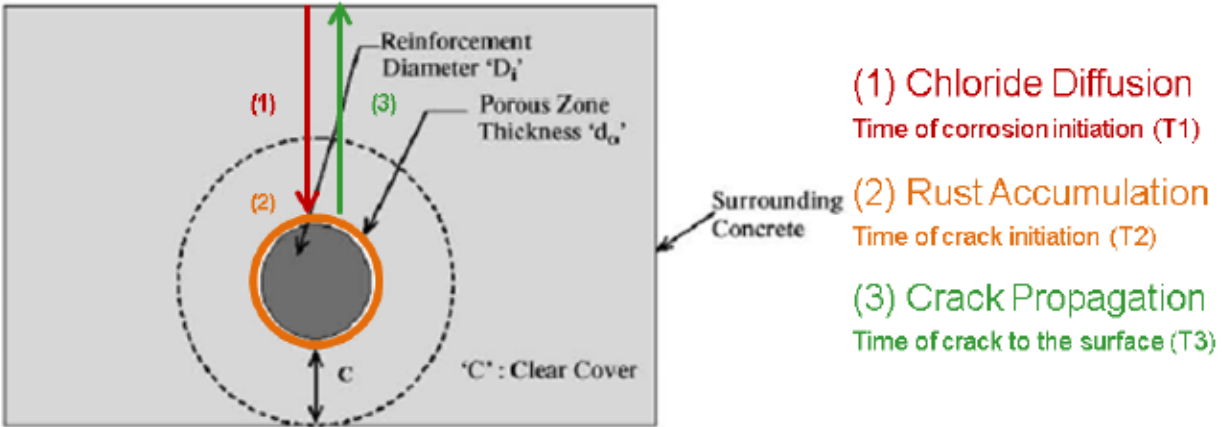
Figure 4. Stages of corrosion-induced cracking on steel rebar (Hu et al. 2013)

Each stage of the time-to-failure model is governed by a separate mathematical model, which each require a set of physical and environmental inputs. A review of each sub-model and their inputs is presented in the following sections.

2.5.2.1 Chloride Diffusion and Concentration

In the first stage, chloride ions from de-icing salts infiltrate the concrete surface and diffuse to the level of rebar. The purpose of modeling chloride diffusion is to determine the time for surface chlorides to reach the depth of rebar and initiate corrosion. Fick's second law is the most computationally convenient way to model the diffusion process. However, it is only a linear approximation and assumes homogeneity of the concrete (Hu et al. 2013). The diffusion coefficient, which governs the rate of chloride ingress for a given material, has been shown to be time dependent (Song et al. 2009). The coefficient can be estimated from the w/c ratio of the concrete mix. To address some simplifications of Fick's second law, Pan and Wang (2011) developed a finite element transport model for chloride ingress that considers the heterogeneous properties of concrete. The Arrhenius equation was used to determine the diffusion coefficient as a function of temperature and thermal properties of concrete. Djerbi et al. (2008) compared the effect of concrete type, specifically ordinary and high performance concretes, on the diffusion coefficient. It was noted that the diffusion coefficient for ordinary concrete was, on average, 2.44 times that of high performance concrete, indicating faster chloride infiltration for ordinary concrete.

28

Luping and Gulikers (2007) studied the accuracy of the simplified solution to Fick's second law and possible errors in predicting chloride diffusion. Despite its simple nature, the original mathematical model was found to predict chloride ingress fairly well for long-term diffusion, with some error leaning on the conservative side. However, it was noted that chloride ingress was significantly underestimated in concrete with fly ash.

The solution to Fick's second law considers surface chloride concentration, commonly measured in kg/m^3, as a primary input. Hu et al. (2013) provided a comprehensive review of typical surface chloride concentrations and their probabilistic distributions used in previous modeling attempts. The mean concentration values ranged between 2.85 kg/m^3 and 4.56 kg/m^3, and were most often described by lognormal distributions. Kassir and Ghosn (2002) examined the surface chloride concentration as a function of bridge age. Although the initial surface chloride concentration of a newly constructed deck was zero, the surface content increased exponentially within the first 5-10 years of service life before stabilizing. As shown in Figure 5, the surface concentration leveled off at approximately 7 lbs./yd^3 (4.15 kg/m^3) after 15 years, which is in agreement with the typical values presented by Hu et al. (2013). However, many mechanistic deterioration models assume a constant, nonzero surface concentration, even for new decks.

Surface chloride concentration may not necessarily be considered constant after 15 years. If no maintenance is performed, the surface chloride concentration will be expected to increase more linearly as deicing salts are applied each year. The effect of a non-uniform increase in surface chloride concentration and the effect of maintenance on the concentration should be considered in order to represent actual bridge conditions.

Once a certain chloride concentration is reached at the rebar surface, corrosion will initiate. The concentration required to cause initiation is referred to as the chloride threshold level. Similar to the surface chloride concentration, the chloride threshold level has been debated in the literature. Hu et al. (2013) conducted a review of threshold chloride levels observed in the literature. The mean concentration ranged from 0.4 kg/m^3 to 5.5 kg/m^3 with coefficients of variation between 0.1 and 0.2. Each observed concentration was described probabilistically by a normal, lognormal, or uniform distribution. In their predictive model, Hu et al. (2013) used 1.2 kg/m^3 as the chloride threshold for black steel rebar. Ann and Song (2007) conducted an extensive study on the accuracy of different representations of chloride threshold concentration. The accuracy of the chloride

29

threshold level was found to be dependent on whether the value was expressed as a mole ratio, free chloride, or total chloride. Total chlorides by percent weight of cement yielded the narrowest range of threshold levels when compared to molecular ratios.
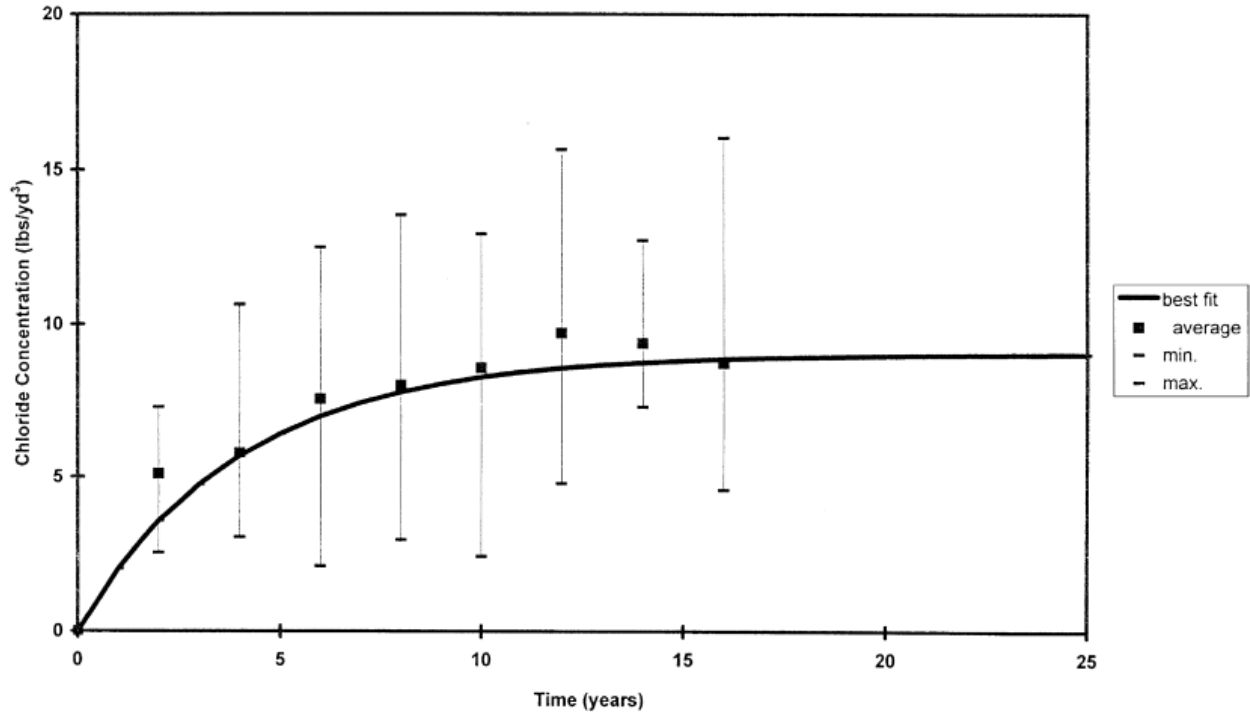
Figure 5. Chloride concentration at the concrete surface (Kassir and Ghosn 2002)

2.5.2.2 Crack Initiation and Propagation

After the chloride threshold is reached, the corrosion process will begin and rust will accumulate at the rebar surface. Rust products, which are less dense than plain steel, expand and exert pressure on the surrounding concrete. The magnitude of pressure is governed by the rate of corrosion. Hu et al. (2013) noted that the rate of corrosion can be determined empirically from

experimental data or mathematically from electrochemical principles. Corrosion may exist in RC decks in micro-cells or macro-cells, as shown in Figure 6.

(a) Micro-cell Corrosion   (b) Macro-cell Corrosion
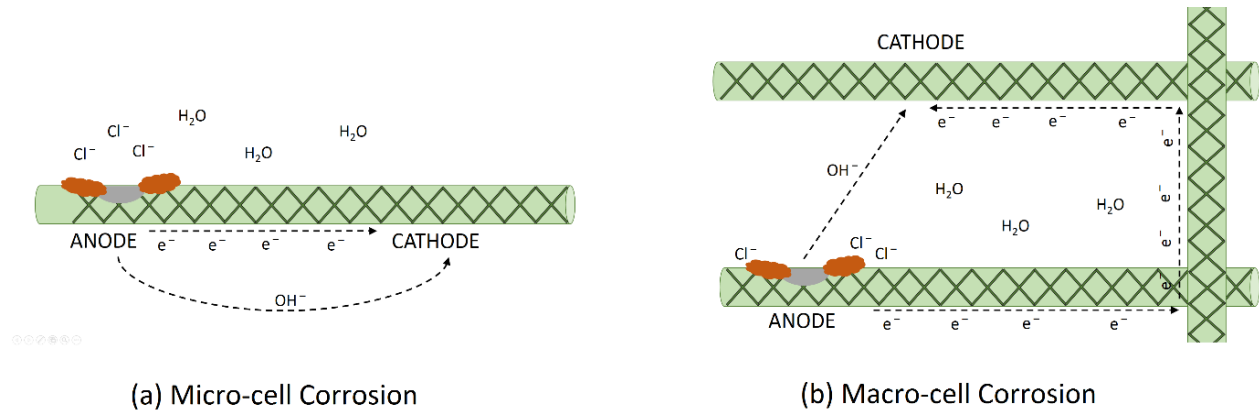
Figure 6. Micro- and macro-cell corrosion processes in rebar mesh in concrete

A relationship between rate of corrosion and pressure build-up can be estimated from the mechanical properties of steel, rust, and concrete. A linear relationship between corrosion rate and loss of rebar diameter was proposed by Andrade et al. (1993). Šavija et al. (2013) summarized the process for determining pressure exerted on surrounding concrete. First, a free expansion phase occurs, wherein rust accumulates in the pores adjacent to the rebar. These pores are accounted for by the inclusion of an oxide layer, often assumed to be in the range of 10-100 µm. Then, a uniform pressure is applied to the surrounding concrete from the free-expansion strain and an average stiffness of the corroded system. The average stiffness is estimated using the volumetric fraction of steel and rust.

Once the calculated pressure exceeds the cracking pressure of concrete, cracks will initiate. The crack propagation phase can be modeled as a one-dimensional problem of cracks to the concrete surface (Balafas and Burgoyne 2011) or to the edge of a concrete cell (Chen and Leung 2015). However, crack propagation is likely to occur in two or three dimensions, as cracks may propagate at an angle, causing spalls. The finite element model proposed by Pan and Wang (2011) used fracture mechanics to predict cracking in two directions as cracks propagate away from the rebar

surface. Surface crack width and delamination can then be used to estimate the condition of a bridge.

2.5.3 Considerations for New Models

Corrosion-induced cracking models in the literature often aim to predict cracking for a simple scenario of bare concrete with unprotected steel rebar and no protective deck overlays. This scenario is rarely observed in newer bridge decks. In modern bridge construction practice, decks often contain epoxy-coated rebar (ECR) and other forms of corrosion and moisture protection, such as deck sealers and waterproofing membranes. Asphaltic or concrete overlays are also often applied to protect the sealers and membranes and increase cover. These factors are often unaccounted for in current mechanistic deterioration models, which can make modeling efforts inapplicable or highly inaccurate for newer decks. In addition to using environmental factors and concrete properties as inputs, mechanistic models should be able to represent in situ conditions for bridges with current design standards.

For the purpose of demonstration, a common bridge design used by the Colorado Department of Transportation (CDOT) can be examined for suitability in mechanistic modeling. Factors that do not appear in many current time-to-failure models such as ECR, non-uniform corrosion, joint deterioration, and protective membranes/overlays are reviewed in the following sections.

2.5.3.1 Epoxy Coated Rebar

Epoxy coatings were developed in the early 1970s to combat significant corrosion damage observed in bridge decks constructed in the 1960s and earlier (Manning 1996). Coatings delay the onset of corrosion by providing a barrier between moisture, chlorides, and steel reinforcement. However, their effectiveness has been debated, since the coating can be significantly affected by damage during construction and adhesion loss from water infiltration.

Experimental studies have suggested that ECR can extend bridge deck service life by anywhere from 5 to 40 or more years (Hu et al. 2013, Fanous and Wu 2005). This wide range of estimated service lives lends to the idea that the effectiveness of ECR varies significantly under different conditions. Epoxy coatings may impact various inputs of mechanistic models, especially the chloride threshold level and rate of corrosion. Keßler et al. (2015) conducted experiments on epoxy coated rebar specimens that suggested that the coating may increase the chloride threshold level

from 0.6% by cement weight for black steel to 0.9% for ECR. Fanous and Wu (2005) noted that corrosion became noticeable on epoxy-coated rebar at a threshold of approximately 4.56 kg/m^3, which is significantly higher than many values observed for black steel. Once corrosion has initiated, the rate of corrosion may also be different from that of black steel. However, whether the rate of corrosion is greater or less than black steel is debated. Keßler et al. (2015) suggested that the limited available corrosion sites in ECR makes propagation slow, while others (Hu et al. 2013) suggest that a higher threshold chloride concentration accelerates corrosion once it begins.

One complicating factor for mechanistic modeling of ECR is the presence of coating defects. Xi et al. (2004) noted that the number of defects in a deck has significant influence on the performance of ECR. Defects may negate the corrosion-inhibiting properties of the coating by providing anodic and cathodic sites for corrosion and prompting adhesion loss. ASTM Standard A775/A775M (ASTM 2016) limits the number of allowable defects in rebar to no more than one per foot. A study conducted by Sohanghpurwala and Scannell (1998) examined the condition of epoxy-coated reinforcement in existing bridge decks in Pennsylvania and New York. A total of 240 cores from 80 bridge deck spans were analyzed, and the results of the analysis are shown in Tables 2 and 3. The average length of rebar in each core was specified as 3.7 inches. Although none of the bridge decks in this study was older than 19 years, the extracted cells provide insight into the expected number of defects within a bridge deck. Most of the defects on epoxy coating are likely to have occurred during installation of the deck, with the remaining defects occurring during the service life of the bridge due to deterioration.

Table 2. Age and deck ratings of 80 bridges (Adapted from Sohanghpurwala and Scannell 1998)

	N	Min.	Max.	Avg.	Median	Std. Dev.
Age, years	80	3	19	10	10	4
Deck Rating	79	6	7	7	7	1.1

Table 3. Epoxy coating defects in concrete cores (Sohanghpurwala and Scannell 1998)

	N	Min.	Max.	Avg.	Median	Std. Dev.
No. Mashed Areas	473	0	20	2.1	2.0	2.2
No. Bare Areas	473	0	21	2.4	2.0	2.6
No. Holidays	473	0	156	7.7	3.0	15.8
Coating Thickness, mils	473	2.4	21.9	11.2	11.1	2.8
Pencil Hardness	473	6 (3B)	10 (F)	9.0 (HB)	9.0 (HB)	0.18
Corrosion Condition Rating	473	1	4	1.1	1.0	0.4
Adhesion Rating	473	1	5	2.2	2.0	1.4

In mechanistic modeling, defects can be considered as sites of accelerated corrosion, either by applying a lower chloride threshold level or by increasing the rate of corrosion at the site of the defect. The size of the defect can also be considered, since larger defects provide more area for corrosion. Although the corrosion density (rate of corrosion per area) does not change, the larger area will increase the corrosion current and accelerate corrosion damage. Keßler et al. (2015) accounted for anode and cathode sizes in a corrosion rate model for ECR.

In addition to initial coating defects, disbondment of the epoxy coating may also occur during the service life of a bridge deck. In this event, the entire disbonded area may act as a site for corrosion, increasing the rate of corrosion and likelihood for cracking at that location. Brown (2002) conducted a comprehensive review of adhesion loss studies, and noted that long-term exposure to moisture (not chlorides) causes loss of adhesion between the bar and epoxy coating. A study conducted by Pyć (1998) of the field performance of ECR showed that epoxy coatings in Virginia might only sustain adhesion to rebar for 15 or fewer years. In this case, adhesion loss occurred before the chloride threshold level was reached. If adhesion is maintained, corrosion may be prevented indefinitely. In current mechanistic modeling efforts, the timing and degree of adhesion loss for ECR is often neglected, despite its impact on corrosion damage. A proposed adhesion loss model is thus presented in Chapter 3.

2.5.3.2 Non-uniform Corrosion

More recent development of mechanistic deterioration modeling has considered corrosion geometry at the bar level. Uniform corrosion assumes that the steel rebar corrodes evenly around the circumference of the bar, and thus uniform pressure is exerted on the surrounding concrete. However, non-uniform corrosion is also common in natural environments (Cao and Cheung 2014). Non-uniform corrosion is likely to exist in conjunction with epoxy coating defects, since rust products may accumulate at the location of the defect, and not necessarily around the entire rebar surface area. In mechanistic models, non-uniform cracking pressure can be implemented to represent more realistic conditions of deterioration.

   The degree of non-uniform corrosion can be represented by a shape factor, α. Various corrosion geometries and their associated shape factors are shown in Figure 7 (Jang 2010). Pitting corrosion, which has a severely non-uniform geometry, indicates that both the anode and cathode may be inside the defect and thus the electrons do not travel far to create a current. As such, corrosion occurs very rapidly.
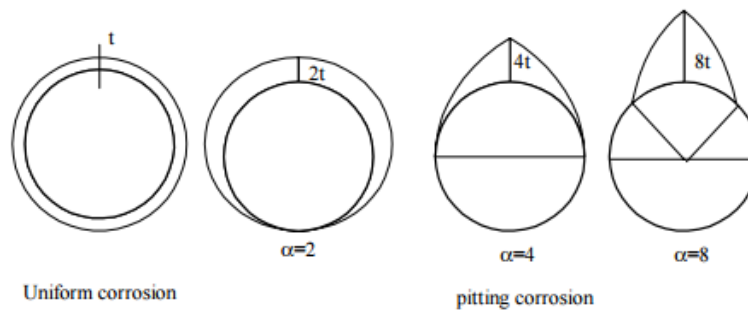
Figure 7. Uniform and non-uniform corrosion geometry on steel rebar (Jang 2010)

Jang et al. (2010) used finite element modeling to simulate the effect of non-uniform and pitting corrosion on concrete cracking pressure. Pressure required to crack concrete for α=8 was found to be at little as 40% of the pressure required for cracking in a uniform case. Therefore, if non-uniform corrosion is not considered, mechanistic models may significantly overestimate service life. Šavija et al. (2013) also presented cracking pressures for non-uniform corrosion using a two-dimensional lattice study. One example of cracking pressures for several cover depths and rebar orientations is shown in Figure 8. Cracking pressures for high shape factors were approximately

25% of those for uniform corrosion. Measurements on the graphic represent the crack widths immediately following crack initiation.
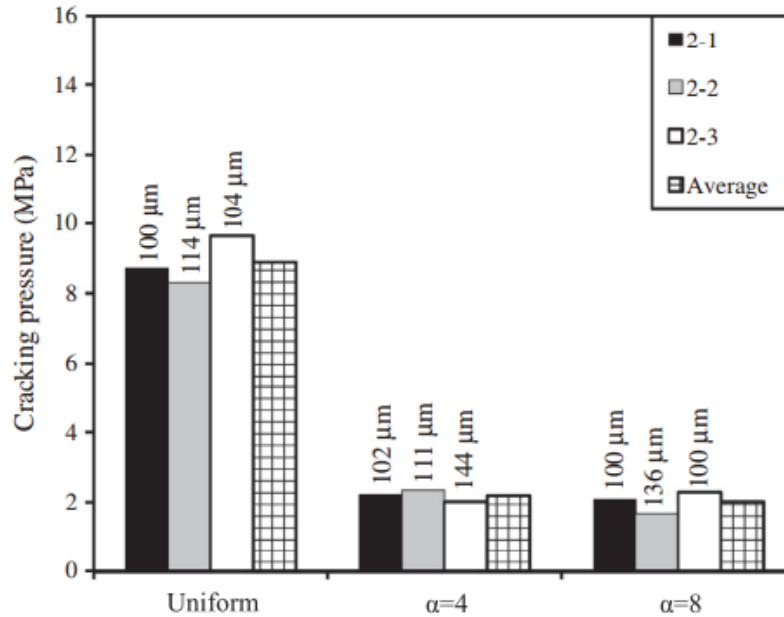
Figure 8. Concrete cracking pressure for various shape factors (Šavija et al. 2013)

2.5.3.3 Protective Systems

Data from the 2015 NBI record indicates that over 65% of national highway bridges have a wearing surface other than concrete (FHWA 2015). Asphaltic overlays account for over 30% of surfaces alone. In Colorado, asphaltic overlays are the dominant wearing surface, representing over 50% of highway bridges. Asphaltic overlays share some similar properties with the base concrete, but should not be modeled as concrete in the interest of an accurate mechanistic model. Specifically, asphalt may not share the same chloride diffusion properties as concrete. In addition, water may not permeate an asphalt cover in the same manner as concrete. This aspect of separate cover material is often neglected in current deterioration modeling.

Diffusion of chlorides in asphalt has not been thoroughly researched, despite the fact that chlorides are often applied directly to the asphalt surface and must diffuse through the asphalt

before reaching the base concrete. In theory, the principles of Fick's second law could be applied to asphalt in the same manner as concrete, but with a separate diffusion coefficient.

Additional protective layers are regularly applied to bridge decks, such as waterproofing membranes and sealers. These layers, which may exist in the form of preformed sheets or spray-on liquids, aid in preventing moisture and chlorides from penetrating the base concrete and inciting corrosion. They may be applied at the time of deck construction as preventive layers, or later in the deck service life to slow the rate of damage. Krauss et al. (2009) investigated the popularity of various overlays, membranes, and sealers on highway bridges. Asphaltic overlays without an underlying waterproofing membrane were found to be uncommon because asphalt can trap salt-laden water in the deck and promote corrosion. Additionally, waterproofing membranes without overlays are uncommon because a wearing surface is not available to protect the membrane from damage. A lack of field research on the effectiveness of membranes and sealers was also highlighted. Safiuddin and Soudki (2011) showed that limited studies have been conducted to examine the physical and chemical effects of de-icing salts when applied to protected concrete. The waterproofing and chloride-resistant properties of membranes and sealers should be further investigated in order to be applied to mechanistic deterioration models.

2.5.3.4 Joints

In documentation of bridge inspections, deck joints are considered to be a separate bridge element from decks, and the interactive effects of joint deterioration on deck deterioration are not reflected by existing mechanistic models. Pincheira et al. (2015) investigated active corrosion in bridge decks and found that corrosion most often coincided with proximity to joints and cracked or delaminated areas. Half-cell potential readings, which indicate the likelihood of corrosion, were taken at various locations along a bridge in Minnesota, and the results are shown in Figure 9. Sites with low half-cell potentials have much higher likelihood for active corrosion. Although cracking near joints may not necessarily be caused by corrosion, these cracks provide access for chlorides and moisture to exposed rebar, accelerating the corrosion process. As a result, corrosion damage

near joints can become a circular issue. Deterioration of joints can have a direct impact on inputs of deck deterioration models, such as the surface chloride content and crack width.
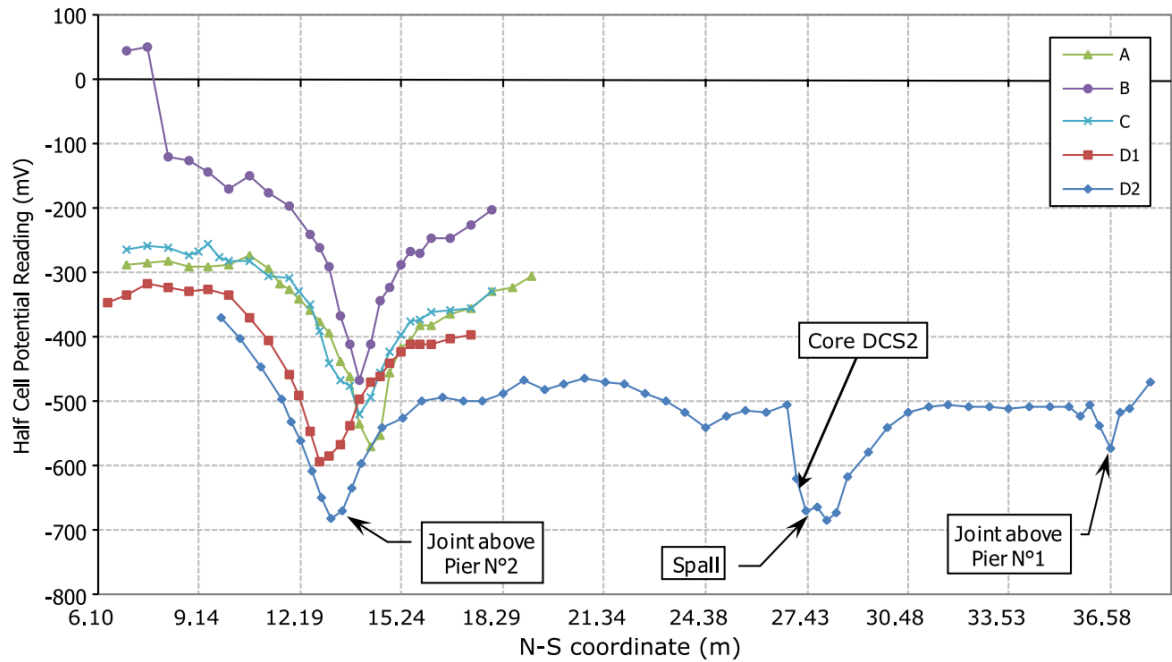
Figure 9. Half-cell potential readings of a bridge deck in Minnesota (Pincheira et al. 2015)

Caicedo et al. (2011) conducted a study on the effectiveness of various joint types and their degradation. In general, joint deterioration was best described as a linear process. However, the study only considered inspection results in forming a deterioration model, and did not analyze the physical mechanisms affecting deterioration. In order to create a more accurate deck deterioration model, the interactive effects of joint deterioration should be included, even at the most basic level.

2.5.3.5 Maintenance Implementation

Investigation of the effects of maintenance on mechanistic deterioration models has been limited. Morcous et al. (2010) highlighted the benefits of mechanistic models for optimizing maintenance timing. After bridge condition is estimated using predictive modeling, cost analysis can be conducted for several maintenance alternatives. However, application of maintenance

actions to mechanistic models can be difficult to validate due to a lack of detailed maintenance histories, as highlighted by Morcous (2006).

If mechanisms affecting deck deterioration are well understood, maintenance actions can be directly reflected by changes in deterioration model functions and inputs. For example, power washing a deck surface could reduce the surface chloride concentration. Milling and replacing the top layer of concrete or asphalt could reset the surface chloride concentration to zero. When a deteriorated joint is replaced, the likelihood for corrosion would become uniform again for the entire deck. In this manner, the effects of different maintenance strategies on bridge condition can be predicted throughout the bridge service life. Further investigation of maintenance strategies and their effects on mechanistic models would be valuable for asset management.

2.6 Discussion

Bridge deck deterioration modeling has been explored in two categories. Purely statistical models, such as the Markov chains method, are currently the preferred bridge management technique for many state departments of transportation due to their relative simplicity and ease of application at the network level. Mechanistic models, which mathematically describe the physical processes causing deterioration, are limited in use due to the complex nature of each mechanism and their interactive effects. However, mechanistic models have several advantages over statistical models, including accuracy at the project level and ability to predict deterioration at any time. Prediction results are not limited to constant-duration inspection intervals, and rely less heavily on subjective inspection results. Existing models are capable of describing deterioration for simple scenarios, but are inadequate for modern bridge design standards, and do a poor job of including the effect of maintenance.

While statistical models are purely probabilistic, it should be noted that mechanistic models are not necessarily deterministic. Mechanistic models may still benefit from the use of probabilistic inputs, due to the inherent random nature of deterioration. Morcous et al. (2010) noted that a bridge management system that integrates probabilistic deterioration models with reliability-based mechanistic models presents a balanced solution. If a baseline model with constant inputs is developed at the local level, the impact of probabilistic inputs can be applied at the global scale through Monte Carlo simulation (MCS) or other statistical approaches. Then, the impact of maintenance actions on a probabilistic deterioration model may be investigated. The following

chapters aim to implement this strategy. In Chapter 3, a localized corrosion cell model is proposed by combining sub-models from the literature to represent each phase of deterioration. In Chapter 4, the effects of protective systems and joint deterioration are considered. In Chapter 5, various maintenance actions are applied to the cell deterioration model and their effects on cell service life are evaluated. In Chapter 6, deterministic input variables are replaced with probability density functions and the localized corrosion model is applied to an entire deck. Finally, in Chapter 7, model application through condition-state mapping is discussed.

3. BASELINE DETERIORATION MODEL

3.1 Overview and Prototype Cell

The baseline model presented in this chapter aims to predict time-to-failure of a single section of reinforced concrete, denoted a "cell", due to chloride induced corrosion, considering environmental conditions representative of Colorado. At the local level, reinforced concrete deck deterioration due to corrosion consists of three stages. In this work, each stage is modeled using one or more analytical models from the literature. The goal of the selected sub-models is to estimate the time for corrosion initiation, the time for cracking initiation, and the time for cracking to extend to the surface of the concrete or a significant horizontal distance. These times are labeled as T1, T2, and T3, respectively. This method seeks to build and expand upon the techniques used by Hu et al. (2013). The primary additions are to include non-uniform and pitting corrosion mechanisms, which are common deterioration modes found in bridges constructed with ECR. Table 4 compares the methodology of the presented model and that of Hu et al. (2013).

Table 4. Sub-model selection for corrosion and crack width modeling

Model Stage	Selected Analytical Models	
	Hu at al. (2013)	Present Model
T1. Time to corrosion initiation	• Fick's second law of diffusion	• Fick's second law of diffusion • Proposed loss of epoxy adhesion model
T2. Time to cracking initiation	• Rate of uniform corrosion (Liu and Weyers 1998) • Thick walled cylinder model (Balafas and Burgoyne 2011)	• Rate of uniform corrosion (Liu and Weyers 1998) • Rate of non-uniform corrosion (Keßler et al. 2015) • Cracking pressure models (Šavija et al 2013, Jang et al. 2010)
T3. Time to cell failure	• Linear crack width model from exposure testing (Hu et al. 2013)	• Linear crack width model from finite element modeling (Chen and Leung 2014)

The chloride diffusion and rate of uniform corrosion are predicted using the same sub-models. However, investigation of non-uniform corrosion mechanisms dictated that different models be

used to represent the corrosion process, as discussed in Chapter 2. The details of these sub models are presented in subsequent sections. A flowchart summarizing the basic steps of the complete model is shown in Figure 10. As described subsequently, each bridge deck is divided into small sections referred to as cells, and the model is run to predict the performance of each cell. To determine if the cell experiences non-uniform or uniform corrosion, an input is available for whether or not a defect exists in the epoxy coating. If a defect is present, the model will conduct only those analyses that are applicable to non-uniform corrosion mechanisms. Alternatively, if no defect is present, the model will analyze the cell according to uniform corrosion mechanisms.

To act as a starting point and reference for comparison of baseline model parameters and inputs, a prototype deck cell representing typical design for a CDOT highway bridge (from the CDOT Bridge Rating Manual 2011 and associated memorandums) is presented in Figure 11. For the baseline model, only the top transverse layer of rebar is considered due to its proximity to the concrete surface and applied surface chlorides. Design parameters for this prototype cell are used throughout the chapter where results are presented, unless otherwise specified. In the present chapter, a baseline model is created using deterministic input variables, which will predict deterioration of the prototype cell. Model stages are described in Section 3.2, and inputs and predictions are presented in Section 3.3. Modifications to the cell which reflect current design practices and maintenance are addressed in Chapters 4 and 5, and the prototype cells are combined for a full-deck analysis in Chapter 6.
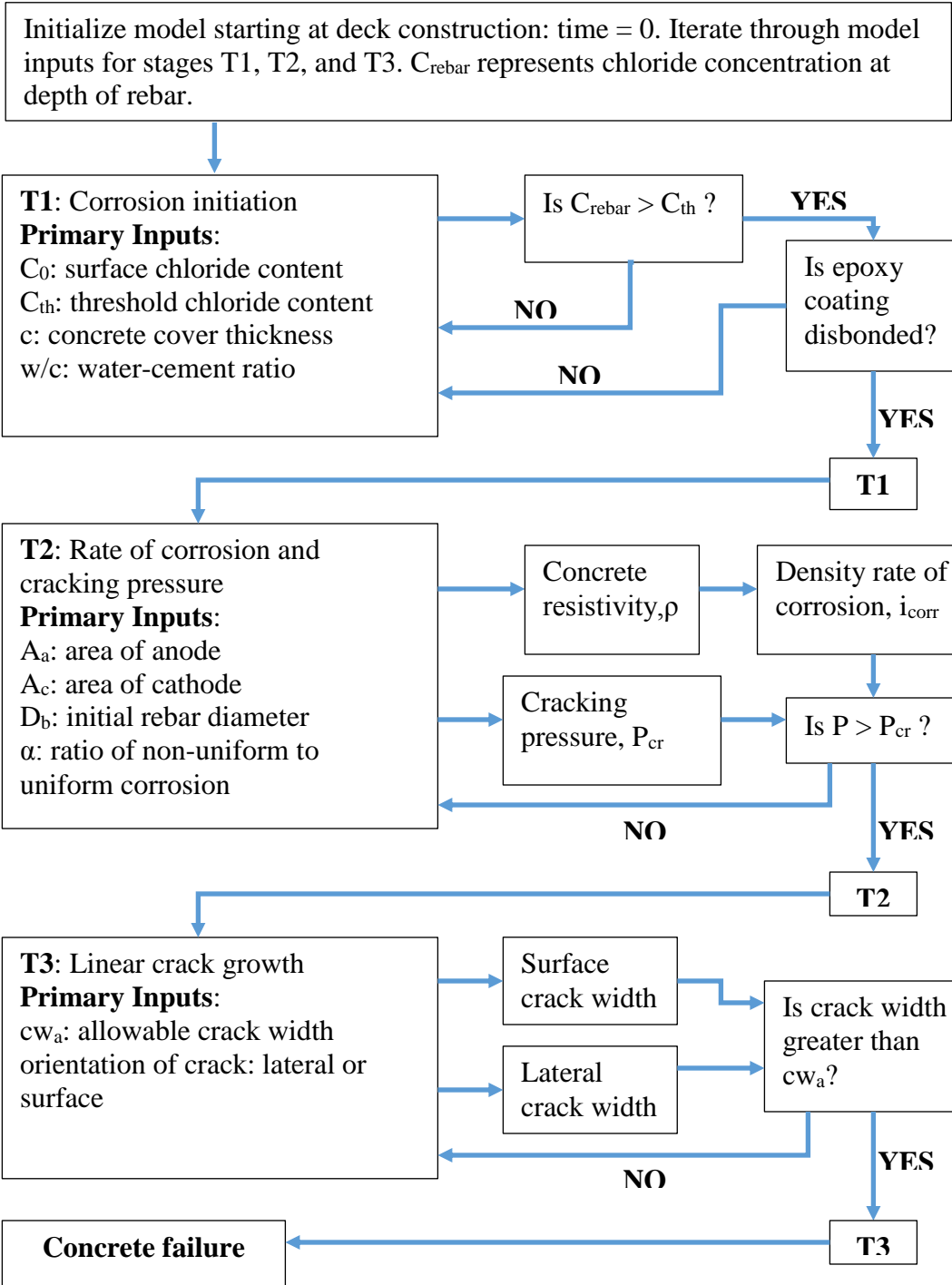
Figure 10. Model process for predicting concrete failure
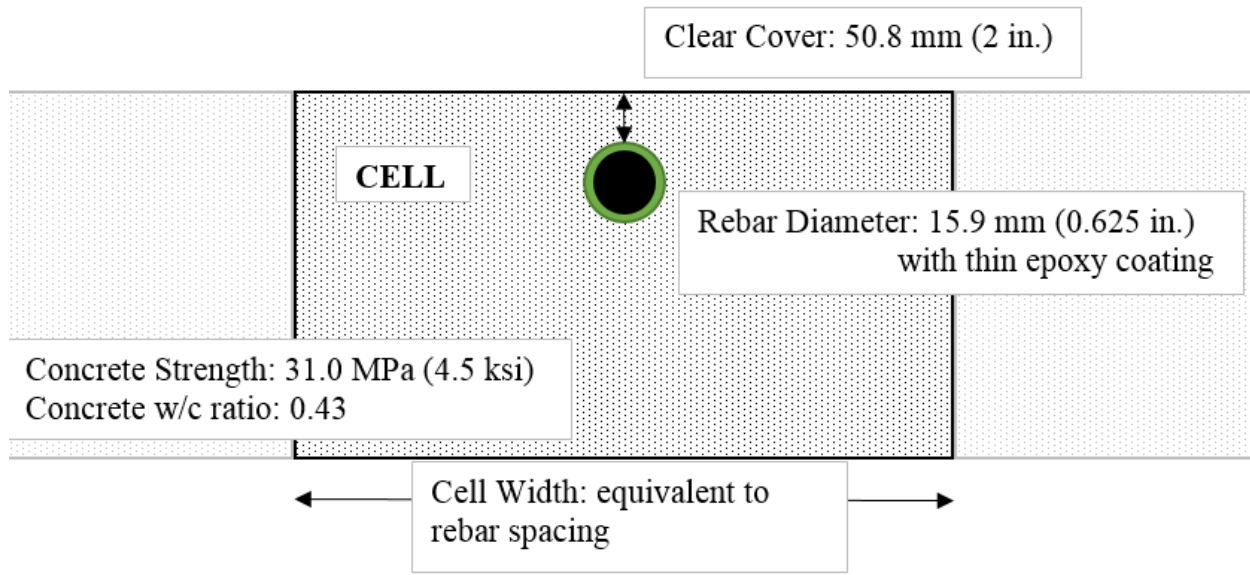
Figure 11. Prototype concrete deck cell with transverse rebar

3.2 Model Stages

3.2.1 Time to Corrosion Initiation (T1)

The time to corrosion initiation is commonly predicted as the time it takes for the concentration of chloride ions at the level of the rebar to reach a threshold value. Fick's second law is widely considered as the basis for modeling the diffusion of chloride ions in concrete (Andrade 1993, Thomas and Bamforth 1999), and is presented in Equation 2 below:

$$\frac{\partial C}{\partial t} = D \frac{\partial^2 C}{\partial x^2} \tag{2}$$

where C is the chloride concentration at depth x and time t, and D is the chloride diffusion coefficient. Solving Equation 2 yields the following:

$$C(x,t) = C_0 \left(1 - \text{erf}\left(\frac{x}{2\sqrt{Dt}}\right)\right) \tag{3}$$

where C_0 is the surface chloride concentration. This one-dimensional solution allows for estimation of the chloride concentration at the rebar level at any point in time, if the depth of cover and chloride diffusion coefficient are known.

The chloride diffusion coefficient in concrete, D, can be taken as constant or time-dependent. Thomas and Bamforth (1999) proposed a time-dependent relationship for determining the coefficient:

$$D_t = D_{28} * \left(\frac{t_{28}}{t}\right)^m \tag{4}$$

where D_{28} is the diffusion coefficient at t = 28 days, and *m* is a constant. D_{28} and *m* were selected by Thomas and Bamforth as those that best fit experimental data for concrete without fly ash or slag, resulting in values of 8e-12 (m^2/s) and 0.1, respectively. Song et al. (2009) presented two equations for estimating the diffusion coefficient as a function of $D_{w/c}$:

$$D_t = D_{\frac{w}{c}} * \left(\frac{t_{28}}{t}\right)^m \qquad when\ t \leq 30\ years \tag{5}$$

$$D_t = D_{\frac{w}{c}} * \left(\frac{t_{28}}{t_{lim}}\right)^m \qquad when\ t > 30\ years \tag{6}$$

where t_{lim} is 30 years and $D_{w/c}$ is an empirical function of the water-cement ratio of concrete:

$$D_{\frac{w}{c}} = 10^{-12.06 + 2.4 * \frac{w}{c}} \tag{7}$$

These equations predict that the diffusion coefficient decays over the first 30 years of deck service life due to cement hydration (Song et al. 2009), then remains constant.

In a cell with a defect, even epoxy-coated rebar is always exposed at the location of the defect. Therefore, when the chloride level reaches the threshold, non-uniform corrosion will initiate. In a cell without a defect, corrosion will not initiate while the epoxy coating is still intact. The adhesion of the coating depends on the availability of moisture. Therefore, if little or no water infiltrates the deck, corrosion will not initiate even if chloride levels at the rebar are well above the threshold level. When moisture is present, the epoxy coating will gradually be lost allowing corrosion to begin.

3.2.1.1 Adhesion

To predict the degree of adhesion between the rebar and epoxy coating, a new adhesion model is proposed. This model attempts to estimate the adhesion of the coating as a function of time and relative humidity. Similar to the way that corrosion will initiate after reaching a threshold,

disbondment will occur after reaching an "adhesion threshold". Pyć (1998) suggested a relative adhesion scale of 1 to 5, where 1 is a completely intact bond and 5 is complete loss of bond, and found that disbondment will begin to progress rapidly at a 3 rating until all adhesion is lost at a rating of 5. For the present model, it is assumed that corrosion will initiate when an adhesion rating of 5 is reached, indicating total adhesion loss between the rebar and coating. However, corrosion will likely initiate before this limit is achieved.

Geenen (1991) indicated that wet adhesion loss between rebar and its epoxy coating will initiate and progress nonlinearly when the relative humidity of the environment exceeds approximately 48%. After about 60% relative humidity, the bond strength will decrease approximately linearly with an increase in humidity. To determine the relationship between time and adhesion loss, a 1996 field study of epoxy coatings in Virginia bridge decks referenced by Pyć (1998) is used as a starting point. The author noted that epoxy coatings maintained adhesion to rebar for about 15 years in bridge decks subjected to an average relative humidity of about 80%. For an average relative humidity in Colorado of about 52%, adhesion can thus be expected for roughly 19.5 years if the assumed linear relationship from Geenen (1991) is applied. From this estimation, a relationship between daily average humidity and loss of adhesion can be defined for humidity over 48%, and is presented in Figure 12. This relationship is based off the estimation that for an average daily relative humidity of 52%, 100% cumulative adhesion loss will occur after 19.5 years. Although this model does not consider temperature at the rebar level, an increase in temperature is known to negatively affect the degree of adhesion. This aspect of disbondment should be investigated in future modeling efforts.
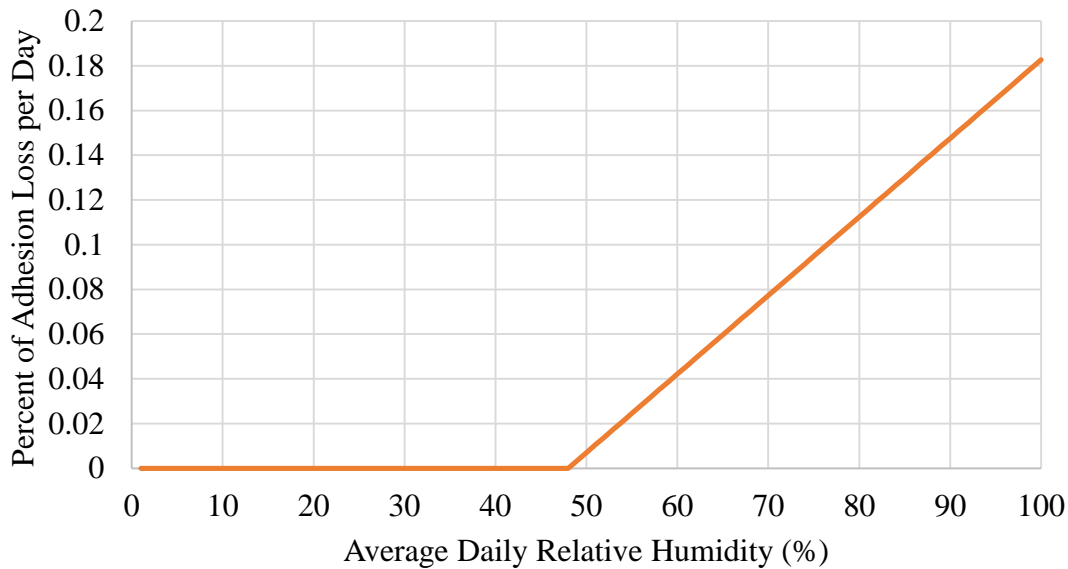
Figure 12. Loss of epoxy coating adhesion due to environmental relative humidity

Once the chloride concentration at the rebar level reaches the threshold, corrosion will begin if rebar is exposed (adhesion has been lost). The time taken for both of these conditions to be met is labeled T1.

3.2.1.2 Surface Chloride Concentration

In the baseline model, surface chloride concentration begins at zero and increases exponentially to 3.5 kg/m^3 during the first 15 years, as dictated by the median value from the literature review. As the bridge ages, the amount of chlorides on the deck will continue to increase as deicing salts are applied cyclically. The model assumes the surface concentration increases linearly at the rate of 0.045 kg/m^3 per year, such that after 100 years, the maximum surface concentration found in the literature of about 8.0 kg/m^3 would be reached. This rate assumes no cleaning or removal of chlorides.

3.2.1.3 Chloride Threshold Level

From the literature, a chloride threshold level which represents the minimum density of chlorides needed to initiation corrosion is selected as 1.2 kg/m^3, which is an intermediate value representing normal conditions. This number is constant for cells with and without defects, since corrosion only exists at exposed rebar. Once the chloride level at the depth of the rebar reaches the chloride threshold and adhesion has been lost (if epoxy is present), corrosion will initiate.

3.2.2 Time to Concrete Cracking (T2)

Two rate of corrosion models are used to represent the rate density of corrosion for non-uniform and uniform cases. First, the electrical resistance of the concrete is calculated. The concrete resistance is a function of relative humidity and is independent of the type of corrosion. Then, the rate of corrosion can be calculated based upon whether the corrosion is uniform or non-uniform. The rate of corrosion leads to a corresponding loss of rebar cross-sectional area, and a resulting pressure due to rust build-up on the surrounding concrete. The time required for the rust pressure to exceed the cracking pressure of the concrete is labeled T2.

3.2.2.1 Concrete Resistance

Concrete resistance is a property of the concrete that is dependent on relative humidity, according to the experimental relationship defined by Balafas and Burgoyne (2011), where resistance is measured in ohms:

$$R_{c,res} = 90.537 * h^{-7.2548}\left[1 + \exp\left(5 - 50(1 - h)\right)\right] \tag{8}$$

It is important to note that the relative humidity is an environmental factor, and may not necessarily represent the water available in concrete to cause corrosion, especially if moisture protection is applied to the concrete. This concept is explored in further detail in Chapter 4. For the baseline model, however, relative humidity and concrete resistance are assumed to be related by Equation 8.

3.2.2.2 Rate of Corrosion

The rate of rebar corrosion in concrete is dependent on the corrosion geometry. For uniform corrosion, an empirical relationship defined by Liu and Weyers (1998) is selected:

$$i_{corr} = 0.0092 * \exp(8.37 + 0.618 * \ln(1.69 * C) - \frac{3034}{T} - 0.000105 * R_{c,res} + 2.35 * t^{-0.215} \tag{9}$$

where i_{corr} is the corrosion density measured in A/m^2. C is the free chloride content (kg/m^3), T is the temperature at the rebar surface (K), and t is the time since corrosion initiation (T1).

For non-uniform geometries, especially at defects in epoxy coatings, the rate of corrosion may not be represented by the same empirical function as uniform corrosion. The shape of corrosion, especially pitting, should be considered. The area of the defect(s) is also a significant factor in the

rate of corrosion, which is not represented by Equation 9. To accommodate these differences, a rate of corrosion model for non-uniform corrosion proposed by Keßler et al. (2015) is selected:

$$I_{corr} = \frac{\Delta E}{\frac{r_{P,A}}{A_A} + \frac{r_{P,C}}{A_C} + \frac{\rho_e}{k_e}}$$

(10)

where I_{corr} is the corrosion current measured in amps. A_A and A_C are the anode and cathode areas in m^2, respectively, and $r_{P,A}$ and $r_{P,C}$ are the anode and cathode resistances in Ωm^2. ΔE is the driving potential [V], and k_e is the cell factor in meters. Unlike the rate of corrosion model for the uniform case, this model uses concrete resistivity (ρ_e) to calculate corrosion current, rather than using concrete resistance ($R_{c,res}$) to calculate corrosion density. However, by calculating the concrete resistance from Equation 8, and by using the cell factor k_e, concrete resistivity of the bar can be estimated as:

$$\rho_e = k_e * R_{c,res}$$

(11)

The cell factor is dependent upon the size of the corroding anode as well as the ratio of cathode and anode areas. Figure 13 shows the relationship between the anode and cathode sizes and corresponding cell factor, from the numerical results reported by Keßler et al. (2015). Once the corrosion current is known, the corrosion density is calculated by dividing the current by the area of the defect. Thus, the corrosion density can be calculated for uniform and non-uniform cases and directly compared.

$$i_{corr} = \frac{I_{corr}}{A_A}$$

(12)
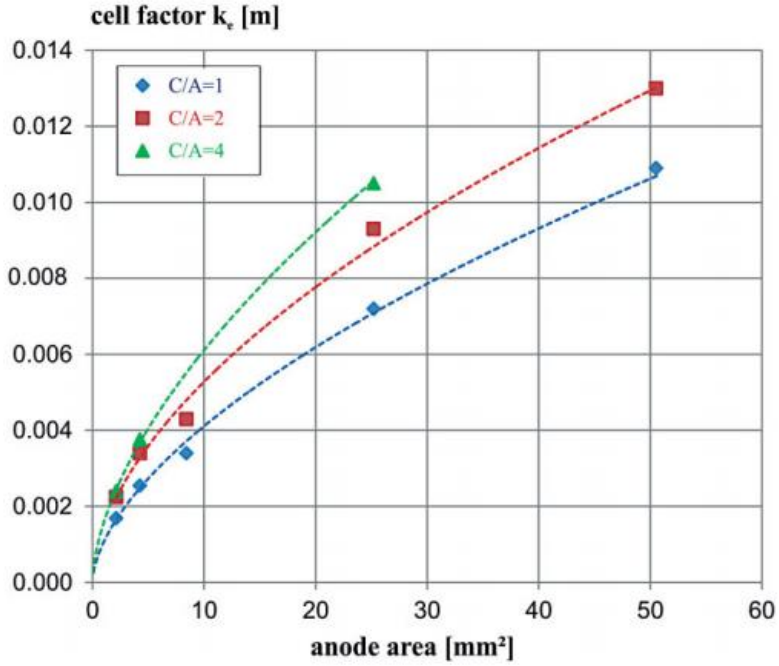
Figure 13. Cell factors as a function of anode and cathode area (Keßler et al. 2015)

3.2.2.3 Concrete Pressure

To calculate the relationship between rate of corrosion and internal pressure created by the buildup of corrosion products, the model by Šavija et al. (2013) is adopted in the present work. A linear relationship between rate of corrosion and loss of rebar diameter is defined as:

$$D_{rb} = D_b - 0.023 i_{corr} \Delta t \tag{13}$$

where D_{rb} is the reduced bar diameter (mm), D_b is the original bar diameter (mm), and Δt is the time since T1, in years. The volume of consumed steel is then:

$$\Delta V_s = \frac{0.023}{2} \pi D_b i_{corr} \Delta t \tag{14}$$

where ΔV_s is measured in mm^3/mm. The reduced diameter of the bar is:

$$R_{rb} = \sqrt{\left(R_b^2 - \frac{\Delta V_s}{\pi} \right)} \tag{15}$$

50

where R_{rb} is the reduced bar radius (mm). The total radius of the rebar can then be calculated as the sum of the reduced bar and thickness of the rust layer, t_r. The thickness of the rust layer can be calculated as:

$$t_r = \sqrt{R_{rb}^2 + \frac{\Delta V_r}{\pi}} - R_{rb} \tag{16}$$

where ΔV_r is the volume of accumulated rust, which can be calculated from the volume of consumed steel (ΔV_s) and properties of the steel and rust:

$$\Delta V_r = \Delta V_s * \frac{\beta}{r_m} \tag{17}$$

β is the ratio of densities of steel to rust, and r_m is the ratio of molecular weights of steel to rust. However, Šavija et al. notes that the thickness of the rust layer should not include the thickness of the small porous zone that surrounds the rebar. Thus, not all of the rust that is produced will exert pressure on the surrounding concrete. The inclusion of a porous layer is accounted for by modifying Equation 16:

$$t_r = \sqrt{R_{rb}^2 + \frac{\Delta V_r}{\pi}} - R_{rb} - t_f \tag{18}$$

where t_f is the thickness of the porous layer. Šavija et al. modifies this relationship once more by including the volume of existing cracks as a location where rust is deposited before exerting pressure on the concrete. However, in the present study, it is assumed that no cracks exist prior to the cracking pressure being reached. Therefore, Equation 18 is used to calculate the thickness of the rust layer.

To calculate pressure exerted by the rust layer on the surrounding concrete, a non-dimensional effective mass loss is calculated by:

$$\gamma = \frac{\frac{(D_b + 2t_r)^2}{D_b^2} - 1}{\beta - 1} \tag{19}$$

This allows the mean strain of the corroded system to be calculated as:

$$\varepsilon_{s,free} = \sqrt{1 + \gamma(\beta - 1)} - 1 \qquad (20)$$

To calculate the average stiffness of the rust and remaining steel, the volume fraction of each material is used:

$$E_{s,eq} = \frac{1 + \gamma(\beta - 1)}{\left(1 - \frac{\gamma}{E_s}\right) + \left(\frac{\gamma\beta}{E_r}\right)} \qquad (21)$$

where E_s and E_r are the elastic moduli of the steel and rust, respectively. Finally, once the average strain and stiffness of the rebar and rust are known, the internal pressure can be calculated:

$$P = E_{s,eq} * \varepsilon_{s,free} \qquad (22)$$

For additional details on how internal pressure is calculated, see Šavija et al. (2013).

3.2.2.4 Cracking Pressure

Internal pressure required to crack concrete surrounding rebar is dependent upon the corrosion geometry, and should consider the effects of non-uniform and pitting corrosion. Jang et al. (2010) studied the effects of various cover depths and rebar diameters against cracking pressure. They noted that the pressure was almost linearly proportional to the cover-to-rebar diameter (c/d) ratio. For example, Figure 14 presents the cracking pressure for a concrete strength of 44 MPa (6.38 ksi) and cover of 32 mm (1.26 inches).

The corrosion geometry, represented by α, has direct influence on the pressure required to crack the concrete cover. As shown in Figure 7 (see Section 2.5.3.2), a corrosion distribution factor $\alpha = 1$ represents uniform corrosion, whereas factors between 4 and 8 represent pitting corrosion.
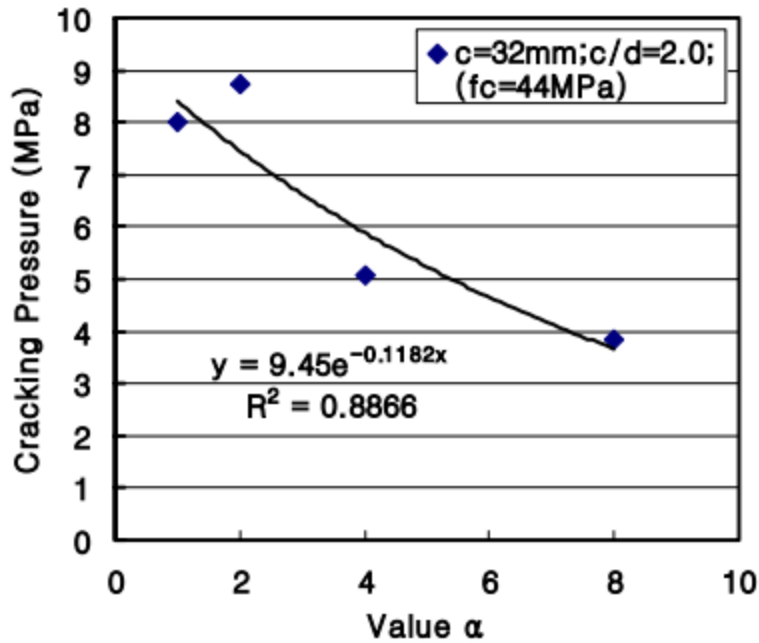
Figure 14. Concrete cracking pressure vs. shape factor (Jang et al. 2010)

For the baseline model, concrete with lower compressive strength and a larger cover is being considered. Therefore, linear interpolation of the data in Jang et al. (2010) is used to determine the relationship between corrosion geometry and cracking pressure. Equation 23 estimates the cracking pressure for concrete with compressive strength 31 MPa (4.5 ksi) and c/d ratio 3.2, for a concrete cover of 50.8 mm (2 inches) and bar diameter of 15.9 mm (0.625 inches).

$$P_{cr} = 10.5 * \exp(-0.09 * \alpha) \tag{23}$$

The time required for P to exceed P_{cr} is labeled as T2. After this point, the concrete crack will grow from an initial width to an allowable "failure" width, to be determined in the propagation period.

3.2.3 Time to Concrete Failure (T3)

For uniform corrosion, chloride concentration is assumed to be greatest on top of the rebar and nearest the concrete surface. As a result, the initial crack will propagate upwards. However, in the case of non-uniform corrosion, a defect in the epoxy coating may exist on the side of the rebar. In this situation, corrosion products are likely to build up at the location of the defect and not necessarily at the top of the rebar. Additionally, cracks may not propagate radially in all directions as is the case with uniform corrosion. For these reasons, the concrete cylinder model proposed by

53

Balafas and Burgoyne (2011) and utilized in a cell deterioration model by Hu et al. (2013) is not applied in the present model. Instead, results from a finite element analysis of cover cracking conducted by Chen and Leung (2014) are considered. This sub-model represents crack propagation for both uniform and non-uniform corrosion. It is also able to consider the location of the crack and whether the crack is lateral, or propagates towards the surface. As shown in Figure 15, the relationship between degree of corrosion and width of crack is approximately linear.

The model presented by Chen and Leung (2014) has several limitations when applied to the prototype cell. Figure 15 only considers two concrete covers, 20 mm (0.79 in.) and 40 mm (1.6 in.). In addition, different concrete and steel properties are used in the finite element modeling. Table 5 lists the properties used by Chen and Leung (2014). Concrete strength is approximately 57.9 MPa (8400 psi), as opposed to 31.0 MPa (4500 psi) used in the baseline model. The bar diameter is 20 mm, whereas the baseline model considers a diameter of 15.9 mm. As a result, the crack width estimations in the baseline model are only approximations, and cannot be considered accurate predictions of crack width.

Table 5. Material properties used for crack propagation modeling (Chen and Leung 2014)

Material constants in the finite element model.

Material	Parameters	Values
Elastic concrete	Young's modulus	36 GPa
	Poisson's ratio	0.2
Rust	Young's modulus	500 MPa
	Poisson's ratio	0.3
	Volumetric ratio	3
Steel	Young's modulus	200 GPa
	Poisson's ratio	0.3
	Yield strength	350 MPa
	Steel diameter	20 mm
Discrete crack	Tensile strength f_t	3.2 MPa
	Fracture energy	0.082 N/mm
	σ_s	$0.15f_t$
	w_s	0.024 mm
	w_c	0.18 mm
Interface of concrete/rust or concrete/steel	Tensile strength	2 MPa
	Friction coefficient	0.2
	Cohesion	1 MPa
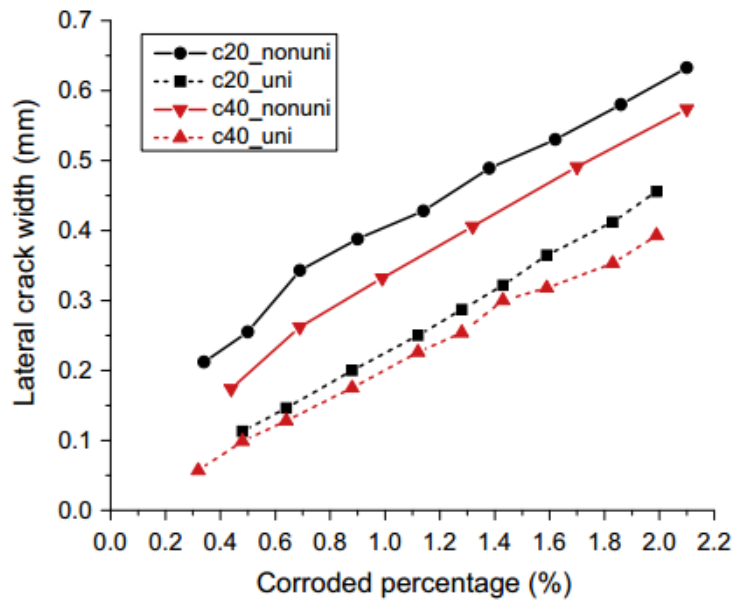
Figure 15. Crack width vs. rebar corrosion for uniform and non-uniform corrosion (Chen and Leung 2014)

To be able to apply the relationships observed by Chen and Leung, corroded percentage is first calculated from the reduced bar diameter calculated during the crack initiation phase. The corroded steel area is determined from the reduced bar diameter, and then the corroded percentage is calculated as the ratio of corroded steel area to original rebar area. Finally, the corroded percentage is related to the lateral or surface crack width by linear approximation from the results of Chen and Leung (2014).

Time to cell failure is dependent upon the allowable crack width. AASHTO recommends that the maximum allowable crack width be no more than 0.3 mm (AASHTO 2002 [Standard Specifications for Highway Bridges]), and as reported by Hu at al. (2013), sometimes this limit is smaller. For the baseline model, the time to cell failure (T3) is defined as the time until the lateral or surface crack width exceeds 0.3 mm.

In some cases, the calculated crack width at a given corroded percentage will indicate that a crack is present, even if the cracking pressure calculated in the previous phase has not yet been reached. When this occurs, it is assumed that the crack will not appear until the cracking pressure is achieved. As a result, it is possible that times T2 and T3 are the same. This situation suggests

that the pressure required to crack the concrete was great enough to generate an initial crack width of greater than 0.3 mm, without subsequent rust or pressure build-up.

3.3 Baseline Model Predictions

3.3.1 Selected Inputs

To complete a baseline cell model for deck deterioration due to corrosion cracking, deterministic values for input variables are selected as a starting point. Most model inputs for each stage are selected based on commonly used values from the literature. Some physical inputs such as concrete strength and concrete cover, as well as environmental inputs such as temperature and relative humidity, were selected to represent CDOT's current practice for new deck construction (see Section 3.1) and the average weather conditions in Colorado. Table 6 displays selected model inputs. Rate of corrosion inputs for the T2 stage were adopted from Keßler et al. (2015), and steel/rust properties and porous layer thickness were adopted from Šavija et al. (2013). These inputs were selected to match those used in their respective sources, since some relationships such as cracking pressure are based on specific inputs selected by the source authors and the specific properties are not often documented by other researchers.

Table 6. Selected baseline model inputs

Model Stage	Variable	Value	Source
Deck Construction	Concrete compressive strength, f'_c	31 Mpa (4.5 ksi)	Prototype Deck (CDOT Bridge Rating Manual 2014)
	Concrete cover, c	50.8 mm (2 in.)	
	Rebar diameter, d	15.9 mm (0.625 in.)	
	Water/cement ratio, wc	0.43	
	Elastic modulus of steel, E_s	200 GPa (29,000 ksi)	
T1: Corrosion initiation	Surface chloride concentration, C_0	3.5 kg/m^3	Stewart and Rosowsky (1998)
	Chloride threshold level, C_{th}	2.19 kg/m^3	Fanous and Wu (2005)

	Driving potential, ΔE	0.225 V	Keßler et al. (2015)
	Polarization resistance of anode, $r_{P,A}$	2.5 Ωm^2	
	Polarization resistance of cathode, $r_{P,C}$	25.0 Ωm^2	
	Area of anode, A_A	50.37 mm^2	
	Area of cathode, A_C	54.29 mm^2	
	Cell factor, k_e	0.0107 m	
T2: Crack initiation	Steel/rust density ratio, β	2.2	Šavija et al. (2013)
	Steel/rust molecular weight ratio, r_m	0.622	
	Porous layer thickness, t_f	0.01 mm	
	Elastic modulus of rust, E_o	7 GPa (1015 ksi)	
	Corrosion distribution factor, α	6	Jang et al. (2010)
	Average relative humidity, rh	52 %	Current Results (2016)
	Average temperature, T	50.15 °F (283.2 K)	US Climate Data (2016)
T3: Crack propagation	Allowable crack width, cw_a	0.3 mm	AASHTO (2002)

3.3.2 Baseline Model Predictions

Table 7 summarizes the results of the baseline model for uniform and non-uniform corrosion for three cases. The first uniform corrosion model represents a plain, uncoated rebar. The second uniform corrosion model suggests an initially intact epoxy coating with no defects. The non-

uniform corrosion model is indicative of a single defect in the epoxy coating with an area of 50.37 mm^2.

Table 7. Baseline cell model results

Model Stage	Time from Deck Construction to End of Stage (years)		
	Black Steel Uniform Corrosion	Intact Epoxy Coating Uniform Corrosion	Epoxy Coating w/ Defect Non-uniform Corrosion
T1: Corrosion Initiation	11.0	19.5	11.0
T2: Crack Initiation	14.8	23.7	12.6
T3: Crack Growth	16.7	25.8	12.6

Baseline model results suggest that a bridge deck cell with damaged, epoxy-coated rebar may deteriorate faster than a bridge deck cell with black steel rebar. Although there is less exposed steel, corrosion geometry at a defect dictates a faster rate of corrosion and loss of cross section. In the case of non-uniform corrosion, the times to crack initiation and cell failure are equal, because the pressure required to crack the concrete is also sufficient to generate an initial crack width greater than 0.3 mm. The cell with the longest service life contains a clean, intact epoxy coating. In this case, the time to corrosion initiation is driven by disbondment of the coating, rather than the chloride threshold level.

As indicated by the chloride diffusion model, chloride levels at the level of rebar reach the threshold of 1.2 kg/m^3 at 11 years. The relationship between time and chloride level at the rebar is shown in Figure 16. Figure 17 shows the linear relationship between cell age and cumulative loss of adhesion, for a constant relative humidity of 52%. If the relative humidity varies throughout the year, as is the case for bridge decks in situ, then the relationship will not necessarily be linear. This situation is explored in Chapter 6.
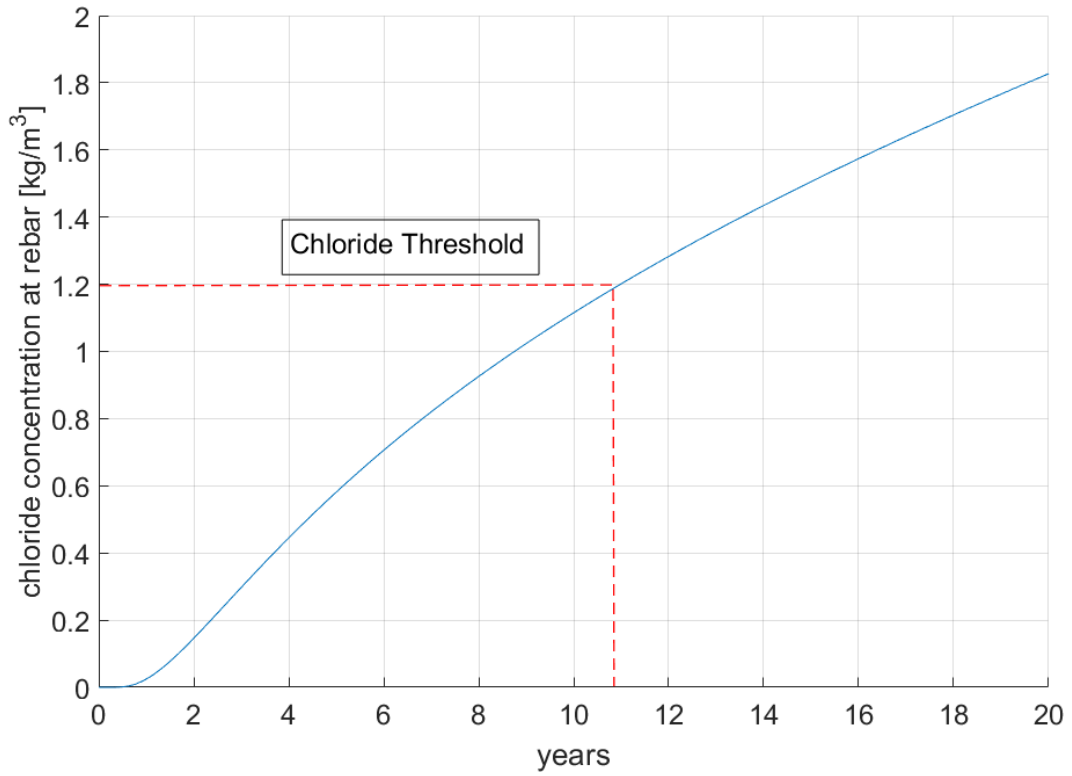
Figure 16. Chloride concentration at level of rebar
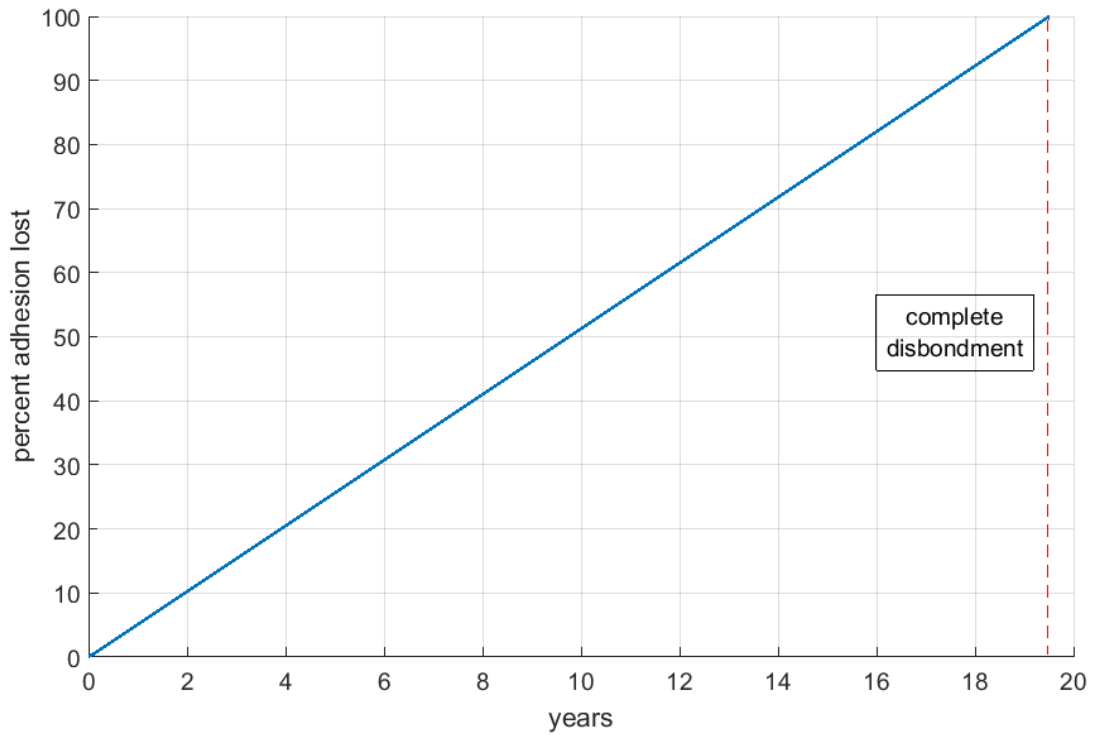
Figure 17. Loss of epoxy coating adhesion

After corrosion initiates, the rate of corrosion is dictated by a uniform or non-uniform model. The uniform model proposed by Liu and Weyers (1998) includes time and other time-dependent variables, so the rate of corrosion is inversely related to age of the structure. The non-uniform model proposed by Keßler et al. (2015) only includes one variable which may or may not be time dependent (concrete resistivity). Because resistivity is assumed constant in the baseline model, the non-uniform rate of corrosion does not vary with time. Figures 18 and 19 compare corrosion rates for epoxy coated rebar. In the case of uniform corrosion, disbondment delays the onset of corrosion to almost 20 years, and the rate at which corrosion progresses is slower than that of pitting corrosion. For the non-uniform case, corrosion begins as soon as the chloride threshold level is reached, and continues at a higher rate than the uniform case.
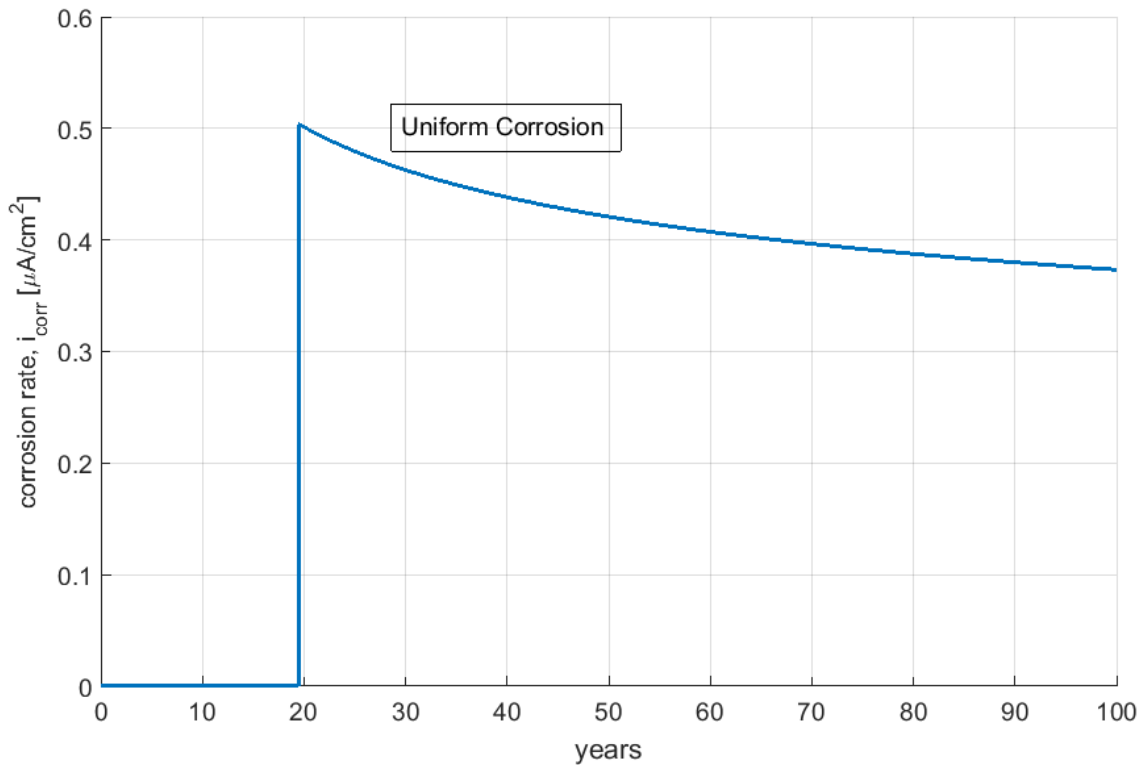
Figure 18. Uniform rebar corrosion
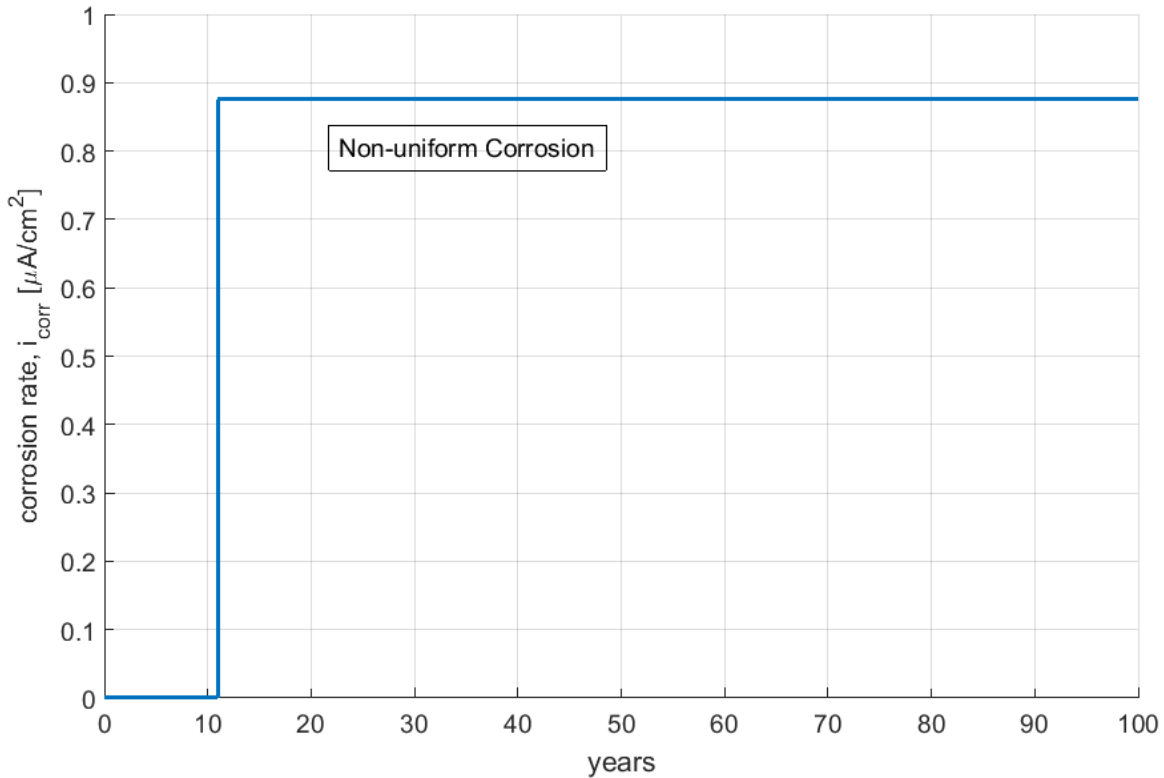
Figure 19. Non-uniform rebar corrosion

As corrosion products build up, accumulated rust fills the pores at the concrete rebar interface, and then pressure from the additional rust products exerts pressure on the surrounding concrete. Figures 20-22 demonstrate pressure over time for each baseline scenario. For uniform corrosion, Equation 23 and a corrosion distribution factor of 1 estimate a cracking pressure of 9.60 MPa. Using Equation 23 and a corrosion distribution factor of 6 for non-uniform corrosion, the cracking pressure is estimated as 6.12 MPa. This cracking pressure is reached at different times for all three cases.

Finally, Figures 23-25 show the linear progression of crack growth for the black steel and epoxy coated cases.
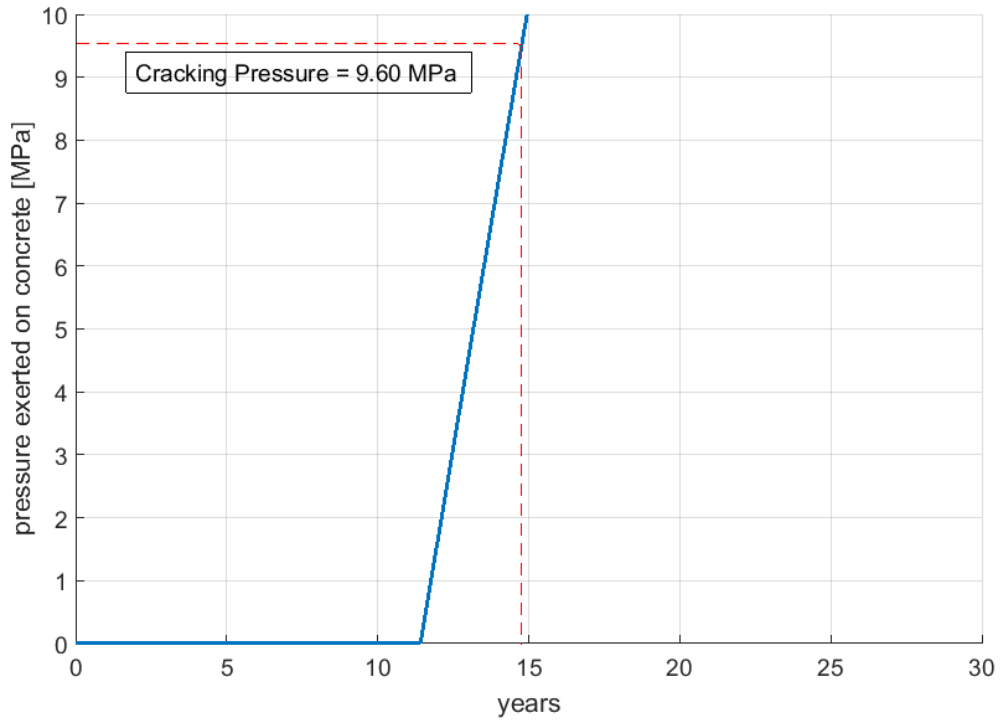
Figure 20. Pressure at the concrete-rebar interface for uniform corrosion on black steel
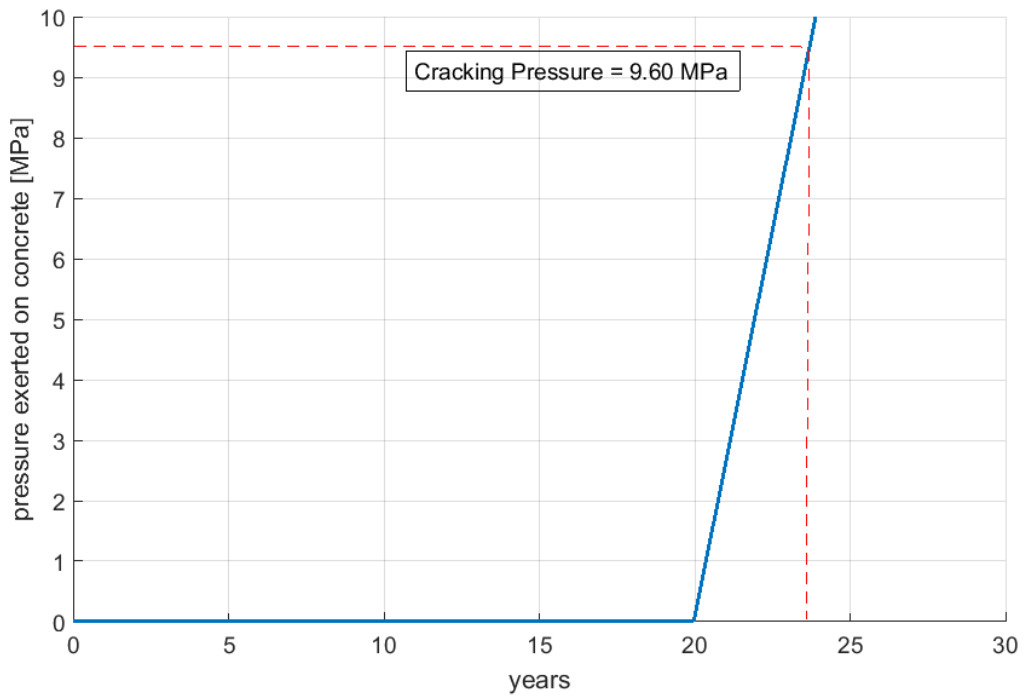
Figure 21. Pressure at the concrete-rebar interface for uniform corrosion on epoxy-coated rebar
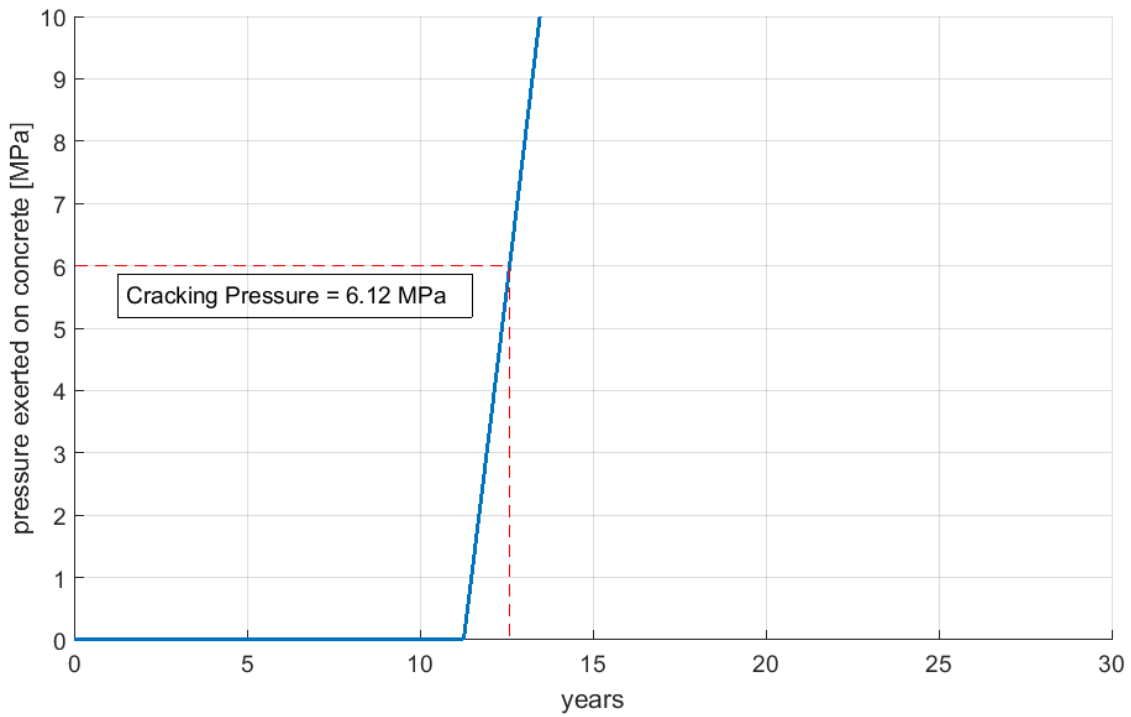
Figure 22. Pressure at the concrete-rebar interface for non-uniform corrosion on epoxy-coated rebar
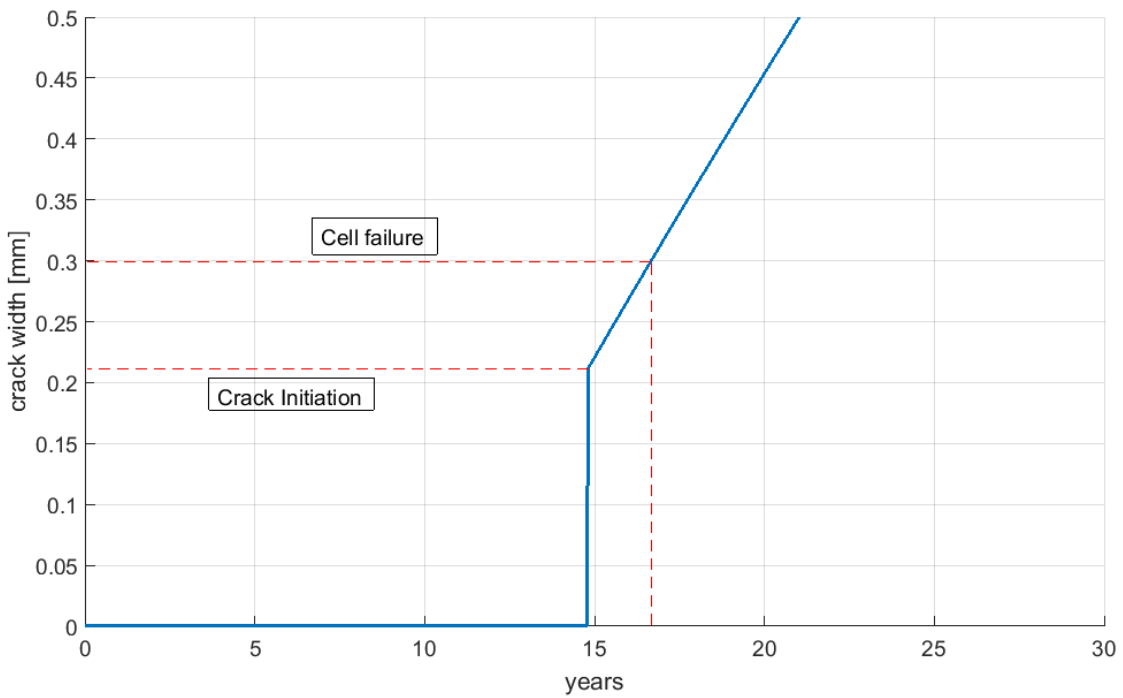
Figure 23. Surface crack growth for uniform corrosion on black steel
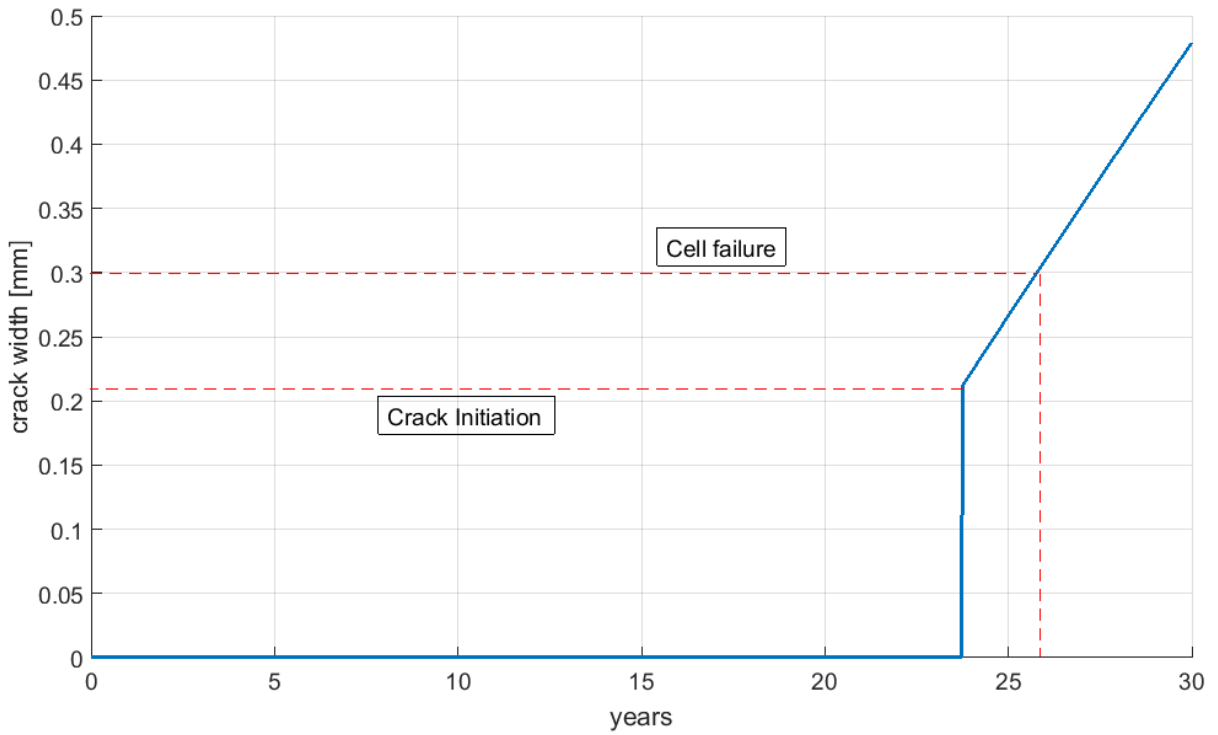
Figure 24. Surface crack growth for uniform corrosion on epoxy-coated rebar
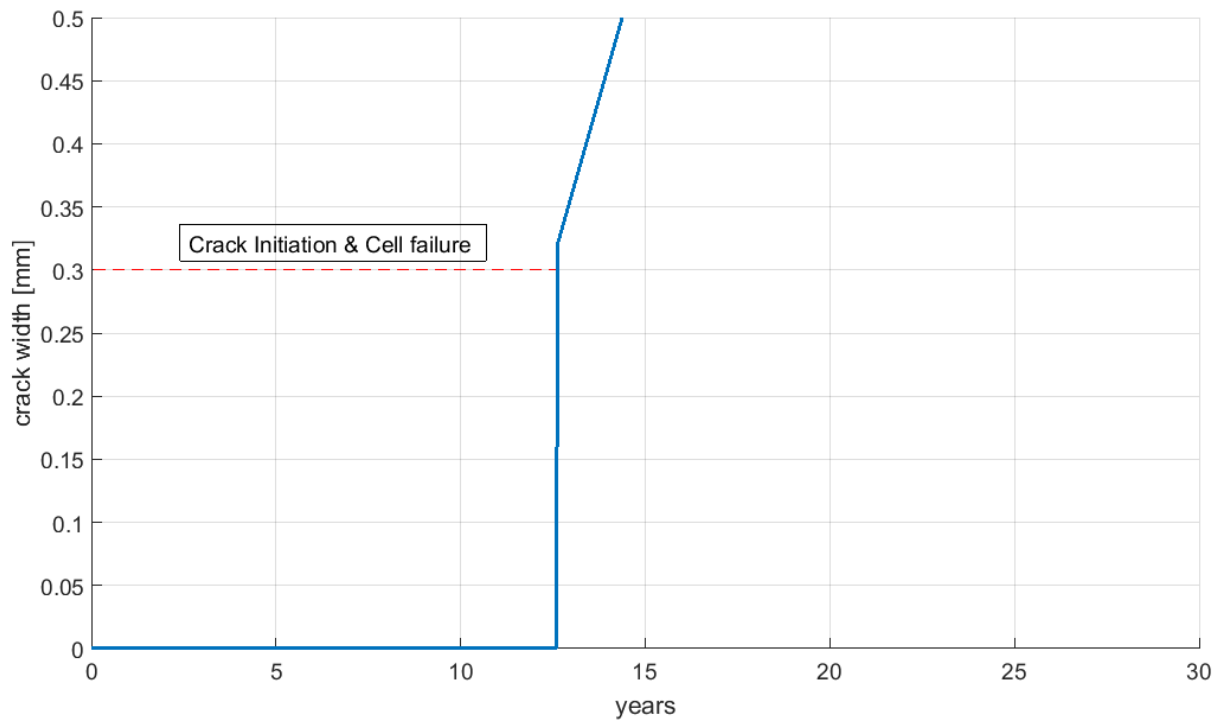
Figure 25. Surface crack growth for non-uniform corrosion on epoxy-coated rebar

3.4 Baseline Model Limitations

Development of the baseline model to predict the failure of a single concrete cell demonstrated limitations present in the state of the art for mechanistic deterioration models for reinforced concrete. Each stage of deterioration was represented by a separate analytical model(s) from the literature. As a result, certain assumptions made for one stage did not necessarily carry over to the next. Effort was made to best represent the actual conditions of Colorado bridge decks in each stage of the model, but ultimately some assumptions about in situ deck conditions had to be made.

One major assumption of the model is the presence of non-uniform corrosion. The impact of non-uniform corrosion on cell service life is significant, with more than 13 years separating the time to failure for an intact epoxy coating and one with defects. It is unrealistic to assume that non-uniform corrosion is exclusive to rebar with epoxy defects, or that rebar without epoxy defects only experiences uniform corrosion mechanisms. However, for the purposes of an analytical model, the presence of an epoxy defect remains the best indicator that non-uniform corrosion will exist.

Two of the most significant inputs in determining time to failure exist in stage T1, where time to corrosion initiation is estimated. The model is highly sensitive to both surface chloride concentration and chloride threshold level. For example, changing the chloride threshold level from 1.2 kg/m^3 to 2.2 kg/m^3 changes the time to corrosion initiation from 11 years to nearly 27 years. Both values for chloride threshold were observed in the literature, as noted by Hu et al. (2013). This variability demonstrates the need for probabilistic inputs and physical data collection in the region where the model is to be applied, especially in the case of corrosion initiation. In addition, the adhesion threshold model contains many assumptions. The state of adhesion loss at which corrosion will begin is not necessarily representative of field conditions, as very little research has been conducted in the area. The field study analyzed by Pyć (1998) only considered bridge decks in Virginia, and the observed loss of adhesion did not have a strong observed relationship with the age or environmental conditions of the structure.

In addition, the baseline model is only able to represent basic deterioration for a bare concrete deck. Condition of other bridge elements and their effects on corrosion mechanisms is not considered. In particular, the condition of a joint adjacent to a cell will likely have an impact on the time to failure of the cell. Other realistic bridge deck conditions, such as asphaltic overlays and

waterproofing membranes, are not included in the baseline model. Finally, the baseline model is only able to represent pure deterioration, and does not include the impact of repair or maintenance. In the interest of creating a more practical model for bridge management, the effects of bridge rehabilitation and care should be considered. Many of these topics are addressed in the following chapters.

4. MODIFIED DETERIORATION MODEL

4.1 Overview

In Chapter 3, a baseline model for deterioration of a prototype reinforced concrete deck cell was proposed by combining existing sub-models from the literature, as well as a proposed adhesion loss model for epoxy coated rebar. The baseline model is useful for estimating the service life of a section of bridge deck that is bare and unprotected, and isolated from adjacent cells. Non-probabilistic inputs provide only a single time-to-failure for all cells, and thus the entire deck has the same predicted life, as opposed to the gradual deterioration observed in the field. Location dependence (e.g. proximity to joints) is also not considered. In the present chapter, the baseline model is modified to include the effects of factors that represent more realistic conditions for a newly constructed deck in Colorado.

The modified deterioration model seeks to improve upon the baseline model in the following ways:

- Consider the effect of a waterproofing membrane on corrosion rate
- Consider the effect of an asphaltic overlay on time to corrosion initiation
- Consider the effect of joint deterioration on corrosion mechanisms in surrounding cells

Figure 26 demonstrates the basic schematic differences between a local cell (baseline), local cell (modified), and global deck model with multiple cells and two joints. To begin, the effects of the waterproofing membrane are examined to estimate concrete saturation as a function of membrane condition and environmental relative humidity. Then, the diffusion of chlorides through asphalt is discussed. The impact of joint deterioration on corrosion in nearby deck cells is also investigated. Explanations of cell modifications are given in Section 4.2, joint deterioration is discussed in Section 4.3, and results of the modified cell model are given in Section 4.4.
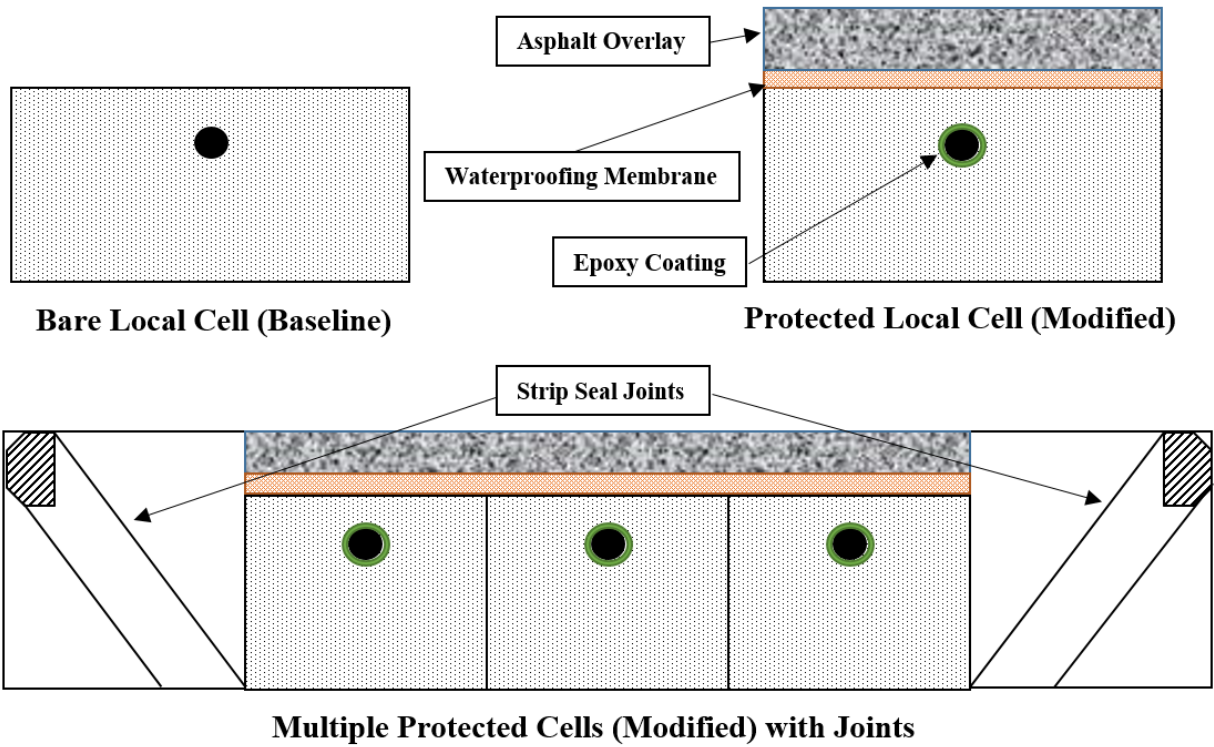
Figure 26. Baseline and modified prototype concrete cells

4.2 Baseline Model Modifications

4.2.1 Waterproofing Membrane

When exposed to the environment, corrosion resistivity of concrete will change based upon water saturation. In the empirical model for corrosion rate proposed by Liu and Weyers (1998), the effect of concrete saturation is represented by relative humidity of the environment. For bare concrete with no protective system, a direct relationship between relative humidity and rate of corrosion can be determined. However, when a protective layer such as a waterproofing membrane is added, concrete saturation and rebar corrosion may no longer be dependent on relative humidity alone, and should consider saturation in the concrete and the waterproofing effects of the membrane. Chloride infiltration may also be impeded by a waterproofing membrane, but this effect is not considered in the present model. A chloride diffusion model that considers an interruption due to a waterproofing barrier is not available in the literature and may significantly increase the time to corrosion as predicted by the baseline model.

The condition of the waterproofing membrane should dictate the concrete saturation providing a link between the condition of the membrane and the rate of rebar corrosion. Jiang and Yuan (2013) studied the relationship between concrete saturation and relative humidity as a function of temperature and w/c ratio. As shown in Figure 27, concrete saturation can be described as a nonlinear function of humidity in three phases. By applying multi-layer molecular-level adsorption theory to the specific case of concrete saturation, a basic physical model was developed by Jiang and Yuan (2013):

$$S = \frac{\lambda_1 * h}{(1 - \lambda_2 * h)(1 + \lambda_3 * h)} \tag{24}$$

where S is concrete saturation and h is relative humidity of the environment. λ_1, λ_2, and λ_3 represent coefficients determined through non-linear regression analysis of experimental data. Each coefficient can be determined as a function of temperature and w/c ratio:

$$\lambda_1 = (2.9142 * w/c - 2.5849) * (T * 10^{-3}) - 0.1994 * w/c + 0.1647 \tag{25}$$

$$\lambda_2 = (2.907 * w/c - 1.1446 * (T * 10^{-3}) + 1.5594 * (T^3 * 10^{-5}) + 4.4465) * 10^{-3} \tag{26}$$

$$\lambda_3 = (2.158 * w/c - 3.2774) * (T * 10^{-3}) - 0.3272 * w/c + 0.3154 \tag{27}$$

where w/c is the water-cement ratio and T is the temperature in degrees Celsius. It should be noted that these relationships were developed for w/c ratios between 0.48 and 0.62, and temperatures between 10° C and 45°C.
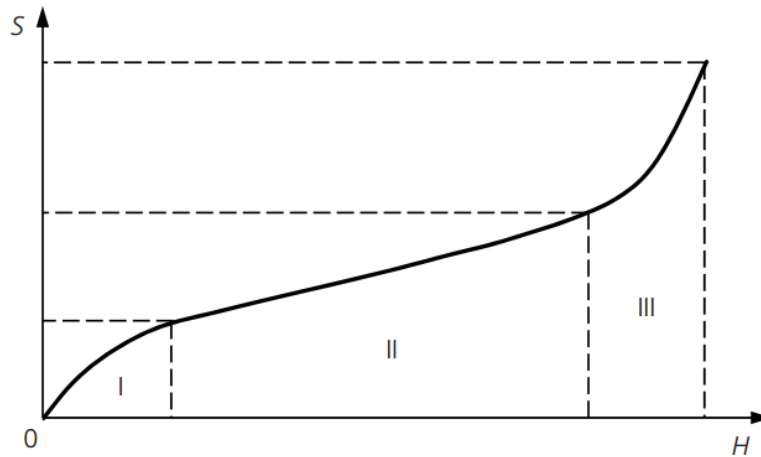
Figure 27. Concrete saturation vs. environmental relative humidity (Jiang and Yuan 2013)

Once a basic relationship between concrete saturation and relative humidity has been determined, the effect of waterproofing integrity of the membrane on concrete saturation should be examined. When a waterproofing membrane is first applied and has complete adhesion with the deck, the concrete saturation will be low regardless of environmental relative humidity, because moisture is not able to enter the deck through the top surface. Alternatively, when the waterproofing membrane has deteriorated and has defects, it will do little to prevent the concrete from being saturated at high relative humidity. This aspect of waterproofing integrity has seen little development within bridge deterioration research, as highlighted by the literature review.

In the present study, a very basic physical relationship between waterproofing membrane condition and concrete saturation is proposed. The purpose of the proposed relationship is not to accurately predict concrete saturation, but rather to demonstrate the necessity and applicability of such a relationship, which should be investigated via experimental study. The proposed relationship suggests a linear deterioration of the waterproofing membrane over its service life. When the waterproofing membrane is first applied, 0% of the concrete saturation predicted by the Jiang and Yuan sub-model (2013) is applied to the baseline corrosion model. At membrane failure, or if no membrane is applied, 100% of predicted concrete saturation is applied. For example, if a concrete saturation of 70% is predicted by the Jiang and Yuan sub-model, but the waterproofing membrane is 50% deteriorated, an effective concrete saturation of 35% is used in the corrosion model. Once an effective concrete saturation has been determined, an effective relative humidity can be calculated and applied directly to the rate-of-corrosion equations discussed in Chapter 3. This process is demonstrated in Figure 28.

Service life of waterproofing membranes is not well established among bridge managers, and may depend on bridge designs and environmental conditions. Sohanghpurwala (2006) noted that the service life of the waterproofing membrane is dependent on the service life of the asphaltic overlay, since a deteriorated overlay cannot protect the membrane from damage. As a result, the membrane should be replaced in conjunction with the overlay. Irfan et al. (2009) found that the service life of a thin asphalt overlay may vary from 7 to 11 years. Therefore, for the present study, the waterproofing integrity of the membrane is assumed to decrease linearly over the service life of the asphaltic overlay. This assumption may need to be adjusted for different asphalt maintenance schemes, especially if only part of an asphalt layer is milled and repaved.
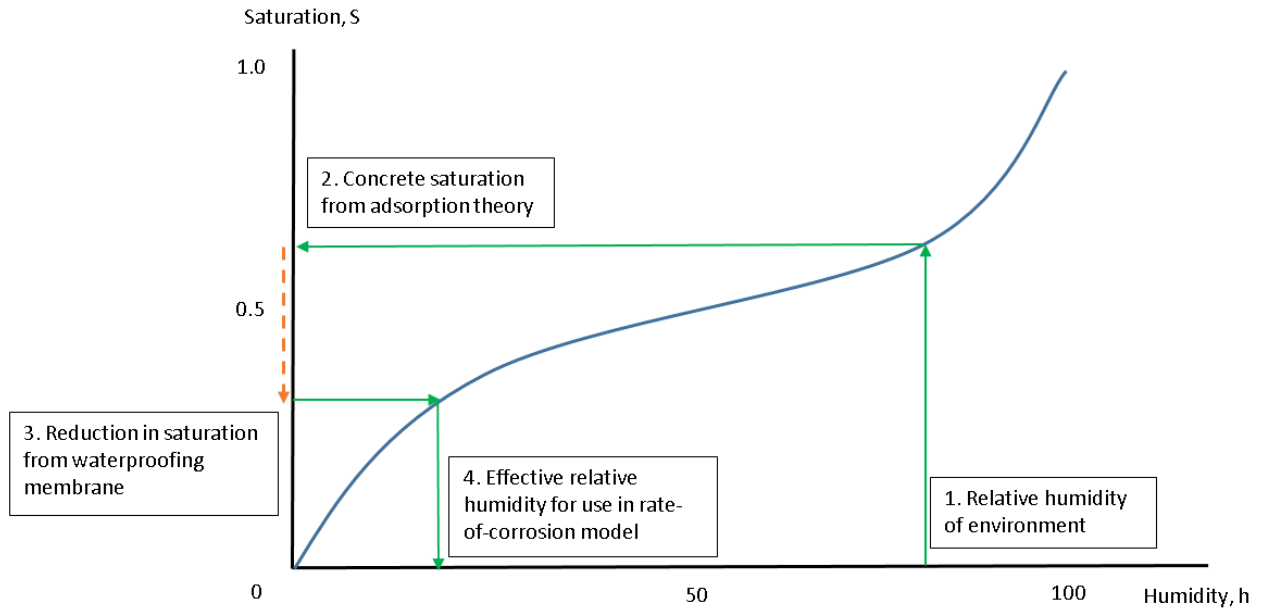
Figure 28. Process for estimating effective relative humidity

4.2.2 Asphaltic Overlay

Asphalt overlays add a layer of protection to the bare concrete deck, preventing damage to the waterproofing membrane and increasing the distance between steel reinforcement and applied de-icing salts. In order to apply the effects of an overlay to the baseline model, the diffusion characteristics of asphalt should be examined. However, very few works found during the literature review yielded information about chloride diffusion through asphalt as an independent material. Czarnecki and Day (2008) calculated diffusion coefficients for composite concrete and asphalt materials with various maintenance histories. Diffusion rate was dependent upon the type of surface material, and was generally found to be higher for asphaltic materials than concrete.

Rather than modeling the asphalt and concrete covers as a composite material of a single depth, asphalt should be treated as a separate material through which chlorides diffuse. Fick's second law can be applied to asphalt in the same manner as concrete. In the present model, chloride concentration at the full depth of the asphalt is input as the surface chloride concentration of the concrete. In the absence of experimental diffusion coefficients for asphalt, the same diffusion coefficient calculated for the concrete is used for asphalt, despite the coefficient likely being

higher. As a result, the time to corrosion initiation may be overestimated. For demonstration, the predicted time to corrosion initiation for black steel as a function of various chloride diffusion coefficients in asphalt is displayed in Figure 29. If the asphalt diffusion coefficient is twice that of concrete, the time to corrosion initiation decreases from 44 years to 32 years, assuming that the concrete is 2 inches thick and the asphalt is 3 inches thick.
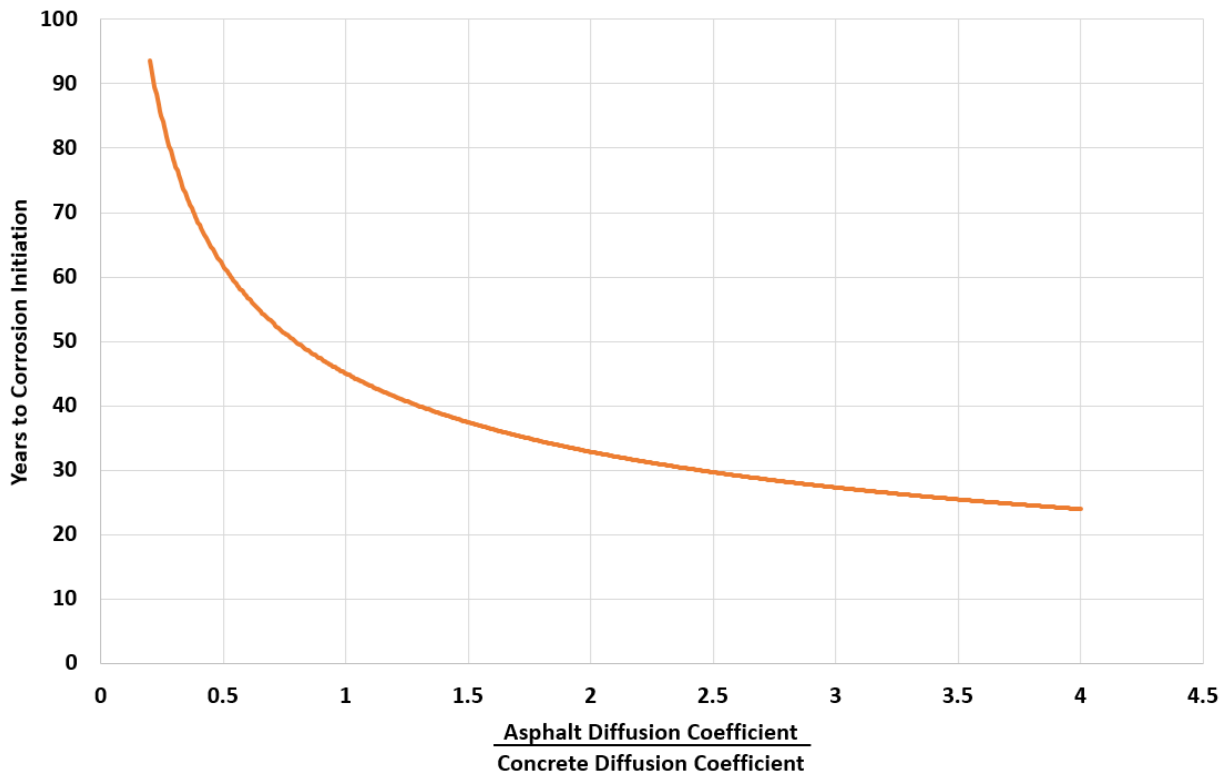
Figure 29. Time to corrosion initiation for various asphalt diffusion coefficients

4.3 Joint Deterioration

As discussed in Chapter 2, bridge joint deterioration has a direct impact on corrosion mechanisms in nearby cells. Half-cell potential readings, lower values of which dictate the likelihood of active corrosion, were shown to decrease non-linearly when approaching joint locations along the length of a deck (see Figure 9). Cells that exist near leaky or failing joints will not experience the same time to corrosion initiation or rate of corrosion as those near mid span.

Physical mechanisms that describe joint degradation are not well modeled mathematically in the literature. However, as mentioned in Chapter 2, joints often deteriorate linearly with time.

Information provided by CDOT bridge staff stated that joints have a typical service life of seven years, but factors such as location, design type, and snowplow usage have an important effect on the life of a specific joint. For the present deterioration model, it is assumed that joints deteriorate linearly over a seven-year service life.

Figure 30 demonstrates the associations between joint and deck conditions that must be made in order to factor joint deterioration into predictions made by the present model. Each numbered relationship must be addressed separately to create a numerical connection between joint condition and cell condition. Joint condition is modeled here as a function of time since installation. Location of the cell within the deck relative to a joint (proximity) is also known for each cell. The connection between joint condition, cell proximity, and half-cell potential is the critical relationship addressed in Section 4.3.2. Referring to Figure 30, some research is available to define relationship R3. Ahmad (2003) and ASTM Standard C876 suggest an association between half-cell potentials and probability of corrosion, where readings below -350 mV indicate a 90% chance of active corrosion. And research conducted by Dhir et al. (1993) produced a relationship between half-cell potential readings and rate of corrosion, as shown in Figure 31. The data provided by Pincheira et al. (2015) gives a preliminary indication for relationship R1, but provides a snapshot of half-cell potentials within the deck at a single time, rather than throughout bridge life. No data was found to address relationship R2, and thus not enough experimental data is available to predict half-cell potentials in bridge decks as a function of time and joint condition.

Due to these complications and lack of experimental data, it is difficult to accurately describe deck deterioration as a function of joint condition. However, a demonstration of how such a function would exist in mechanistic models can still be provided by examining the relationship between half-cell potential and proximity to joints.
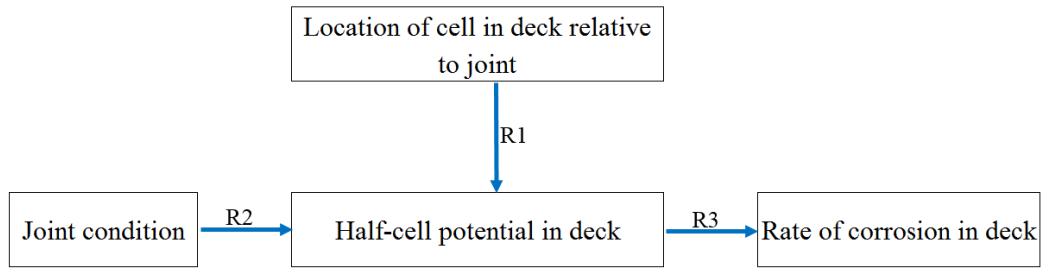
Joint condition: *estimated; function of time*   Location of cell in deck relative to joint: *known; function of cell row*
Relationship R1: *unknown*   **Relationship R2: *unknown***
Half-cell potential in deck: *unknown ; function of joint condition, cell location*
Relationship R3: *estimated from experimental data*
Rate of corrosion in deck: *estimated; function of HCP*

Figure 30. Relationships between deck joint deterioration and rate of rebar corrosion
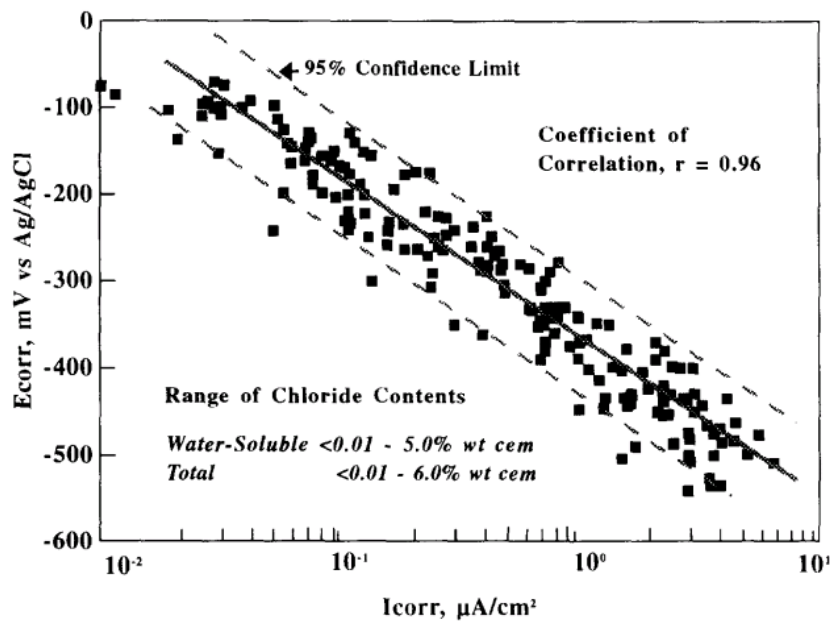
Figure 31. Rate of corrosion vs. half-cell potential readings (Dhir et al. 1993)

4.3.1 Cell Proximity to Joint

To determine the degree to which each cell is affected by joint deterioration, physical distance to the nearest joint is calculated. Proximity is then used to calculate the percent affected for each cell. The percent affected is an indicator of how much the half-cell potential in a cell will change

74

as a function of joint condition (relationship R1). For a cell adjacent to a joint, the percent affected is nearly 100%, whereas a cell near mid span will be zero percent affected. The maximum distance throughout which cells are affected by joint deterioration is assumed to be 8 meters, based on the findings by Pincheira et al. (2015) (See Figure 9). At more than 8 meters away from a joint, the half-cell potential is assumed to be unaffected by joint condition. Figure 32 demonstrates the proposed relationship between cell proximity to joint and percent affected.
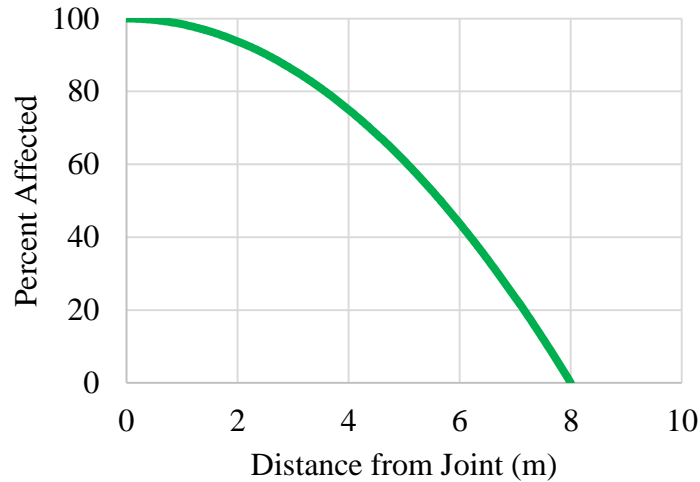
Figure 32. Concrete cell location vs. influence of joint deterioration

The percent affected is assumed to be related to distance from the joint by a quadratic of the form:

$$\% \, Affected = 100 - 1.5625 * (distance)^2 \tag{28}$$

Where distance is input in meters. Once the percent affected of a cell is calculated, the rate of corrosion can be changed to reflect deterioration of the nearest joint.

4.3.2 Rate of Corrosion for Affected Cells

Because a direct relationship between joint condition and rate of rebar corrosion is unknown, half-cell potential readings presented by Pincheira et al. (2015) can be used in conjunction with the data from Dhir et al. (1993) to estimate changes in rate of corrosion (relationship R3). Measurements for half-cell potentials discussed by Pincheira et al. (2015) were taken long after joints in the sample bridge had time to deteriorate. By assuming linearity in joint deterioration and a quadratic relationship between distance to joint and half-cell potential for a fully deteriorated joint, the half-cell potential of any cell within a deck can be predicted. In this manner, the

deteriorated condition of a joint can directly impact the rate of corrosion as estimated by the baseline model from Chapter 3.

Although only a rough estimate of rate of corrosion changes can be obtained, such a relationship will demonstrate an ability to consider the effects of multiple element deterioration in predictions of bridge condition. Similar to how an effective relative humidity was calculated in Section 4.2.1, the rate of corrosion of any cell can be increased as a function of joint condition and percent affected. As shown by Pincheira et al. (2015), the half-cell potential within a deck may decrease by roughly 300 mV near a joint (indicating a higher tendency for corrosion), when compared to a reference location 8 or more meters away. 300 mV is used as the maximum possible HCP reduction in the proposed function:

$$HCP_{reduced} = HCP_{initial} - 300 * \left[\frac{\%Affected * (100 - joint\ condition)}{10,000}\right] \qquad (29)$$

Where $HCP_{initial}$ is the half-cell potential (mV) associated with the rate of corrosion as calculated previously (see Section 3.2.2.2) and $HCP_{reduced}$ is the half-cell potential associated with a higher rate of corrosion. Joint condition, as mentioned above, deteriorates linearly over a seven-year period:

$$joint\ condition = 100 * \left(1 - \frac{joint\ age}{7}\right) \qquad (30)$$

Where joint age is the time since the latest joint was installed, in years.

The function for relating rate of corrosion and half-cell potential (relationship R3) is estimated from the data provided by Dhir et al. (1993):

$$HCP = -79.48 * \ln(i_{corr}) - 374 \qquad (31)$$

Where i_{corr} is the corrosion rate in $\mu A/cm^2$. Once a new half-cell potential is estimated, the actual rate of corrosion can be calculated and used throughout the remainder of the model in the same manner as before. A graphic summary of the process for calculating rate of corrosion is shown in Figure 33.
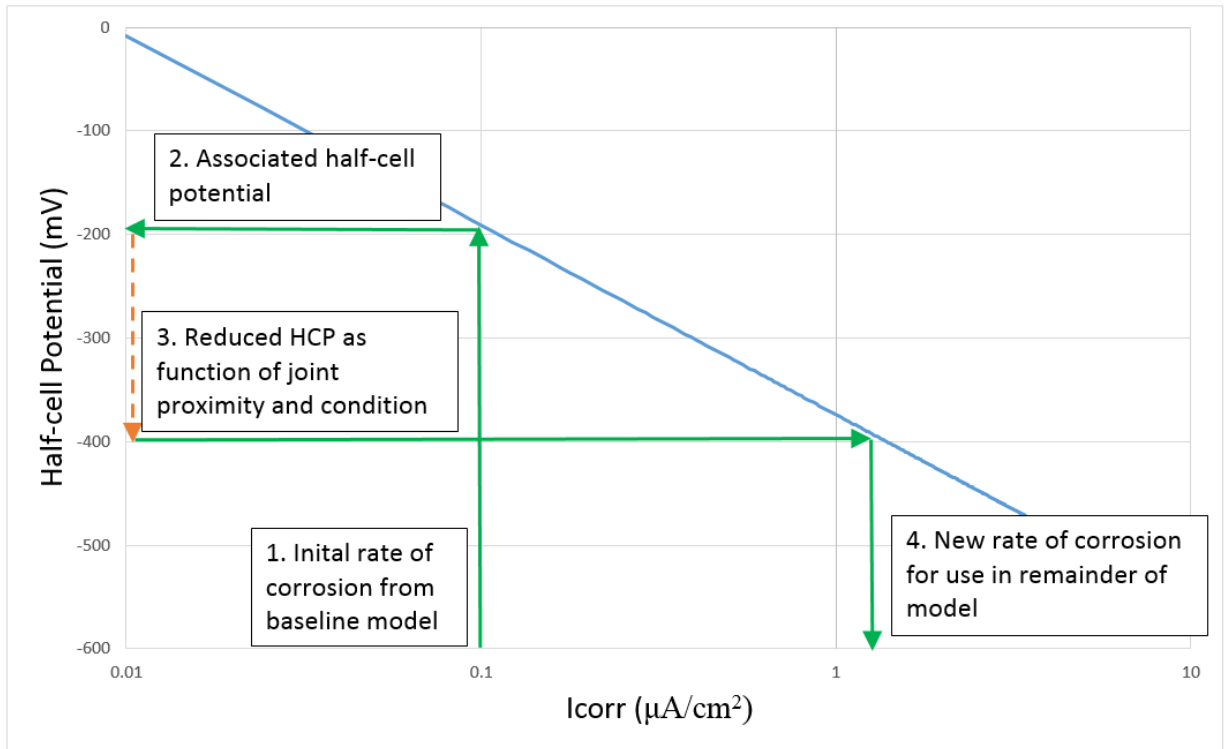
Figure 33. Process for calculating effective rate of corrosion

4.3.3 Factors Affected by Joint Condition

Although a new rate of corrosion can be estimated via the methods in Section 4.3.2, factors that alter the rate of corrosion are not individually identified. The change in rate of corrosion is a function of many model inputs, including temperature, moisture, and chloride concentration. Ideally, a joint deterioration model would lend itself to changes in the individual inputs of corrosion rate, rather than directly changing the output. Leaking joints may provide direct access for moisture in adjacent deck cells, and may cause more rapid disbondment and accelerated corrosion. Premature cracking due to non-corrosive mechanisms may occur in cells near joints, and prompt additional defects in the epoxy coating. The effects of joint deterioration on individual factors such as moisture, epoxy-coating, and chloride diffusion are not considered in the present model, but should be investigated in future efforts.

4.4 Modified Cell Results

Investigating time-to-failure for a single cell under various conditions and with constant inputs is valuable for comparing design alternatives and maintenance strategies. Relative changes in

model parameters can be easily compared. Table 8 presents model results for various cell conditions including modifications described in Section 4.2. Inputs for the model are consistent with those from Chapter 3 (See Table 6). The results of joint condition on time to cell failure are presented in Chapter 6, when cells are evaluated as a group at the global (deck) scale.

Table 8. Modified cell model results

Time from Deck Construction to End of Stage (years)				
Rebar Protection / Cell Protection		Black Steel	Intact Epoxy Coating	Epoxy Coating with Defect
None (Baseline)	T1	11.0	19.5	11.0
	T2	23.0	32.6	12.7
	T3	29.1	39.1	12.7
Membrane Only	T1	11.0	29.3	11.0
	T2	23.0	43.3	12.7
	T3	29.1	50.2	12.7
Overlay Only	T1	43.6	43.6	43.6
	T2	58.5	58.5	45.3
	T3	65.7	65.7	45.3
Membrane + Overlay	T1	43.6	43.6	43.6
	T2	58.5	58.5	45.3
	T3	65.7	65.7	45.3

Results from Table 8 represent times to corrosion initiation, crack initiation, and cell failure. Both protective layers (membrane and overlay) are assumed to be applied at deck construction where t=0. The membrane is assumed to deteriorate over a service life of 10 years and a second membrane is not installed thereafter. The effects of membrane application later in deck service life are explored in Chapter 5. The asphaltic overlay is assumed to exist throughout deck service life without replacement.

Table 8 suggests that the addition of a waterproofing membrane to a new deck will extend service life for a cell with intact epoxy coated rebar, but not for black steel or a cell containing a defect. In all three cases, the time for the chloride threshold to be reached is a constant 11 years, which is assumed to be unaffected by the addition of a membrane. If the membrane lasts 10 years, then it will have no impact on the times to crack initiation and cell failure, because it will be fully deteriorated by the time it would affect the rate of corrosion and crack growth. However, in the case of an intact epoxy coating, time to corrosion initiation is controlled by disbondment of the coating rather than the chloride threshold level. Because the membrane is actively protecting the deck from moisture penetration during the disbondment phase, it can extend service life by delaying disbondment from 19.5 years to 29.3 years. As a result, waterproofing membranes installed at deck construction may be more effective when epoxy coated rebar is also in use.

When an asphaltic overlay is applied to the deck at construction, service life is extended by nearly 37 years in the case of black steel and nearly 33 years for epoxy coated rebar with a defect. This large extension of service life is due to the significant increase in rebar cover. If the chloride diffusion properties of asphalt are assumed to be the same as concrete, rebar cover increases by 150% from a 2-inch concrete cover to a 5-inch cover of concrete and asphalt. This additional cover provided by asphalt significantly delays the time for chlorides at the rebar level to exceed the threshold. Realistically, chlorides will likely diffuse through the asphalt faster than predicted due to deterioration of the wearing surface and a higher permeability.

As discussed in Chapter 3, the model assumption of non-uniform corrosion when a defect in the epoxy coating is present has a clear impact on time to cell failure. Higher corrosion rate and lower pressure required to initiate cracking accelerates the cracking process, and thus a cell with a defect may see reduction in service life by as much as 38 years. The maximum service life predicted by the modified model is 65.7 years when an asphalt overlay is applied to a deck with black steel or intact epoxy. The minimum service life predicted is 12.7 years when a bare concrete cell contains rebar with a defect in the epoxy coating. This disparity in service lives can be expected when considering the corrosion-inhibitive effects of epoxy coatings, waterproofing membranes, and additional concrete cover.

4.5 Discussion

A baseline model for predicting time-to-failure of bridge decks cells was developed in Chapter 3 and subsequently expanded upon to include the effects of protective layering and expansion joint deterioration. Inclusion of protective systems in corrosion prediction is imperative due to their significant impact on model results. As demonstrated, the three primary protection systems (epoxy, asphalt layer, and membrane) can add more than 30 years to the expected life of the structure without any maintenance or replacement.

The presence of an epoxy coating defect within a cell was shown in Chapter 3 to reduce the time-to-cracking by increasing the rate of corrosion and lowering the cracking pressure due to a concentration of forces at the rebar-concrete interface. However, as the range of inputs for surface chloride concentration and chloride threshold found in the literature are large, the correlation between time-to-failure and presence of a defect becomes small if the full range of values is considered. A change in surface chloride concentration from $3 \, kg/m^3$ to $6 \, kg/m^3$ or more outweighs the influence of an increased rate of corrosion due to a bare area in the epoxy coating. This is especially true since the time to corrosion initiation (T1) is much longer than the interval between subsequent phases. To address the influence of uncertainty in model inputs on the predicted time to failure, constant input values should be replaced by probabilistic distributions (see Chapter 6).

In addition to modifying the baseline model, the impact of joint deterioration on cell deterioration was examined. By considering joint deterioration as an independent mechanism, changes in rate of corrosion within nearby deck cells can be quantified as a function of joint condition. Whereas previous research efforts have investigated the coupled effects of multiple deterioration mechanisms within the bridge deck (Hu et al. 2013), few models have considered the interactive effects of deterioration between multiple bridge elements. In future studies, additional bridge elements may be included. For example, leaking joints may influence the condition of piers and other substructure elements. The purpose of joint deterioration in the present study is to demonstrate how deterioration of one element may influence another, and how this effect can be modeled mathematically. Due to the reduction impact on bridge deck service life, joint deterioration mechanisms are worthwhile of future investigation, and their influence on deck deterioration should be further examined.

So far, a model has been developed to predict time-to-failure of a prototype cell by assembling previously existing and newly proposed sub-models that represent various stages of deterioration. A timeline of deterioration not impacted by maintenance or replacement can be estimated for a variety of bridge conditions, including environmental effects and design parameters. In Chapter 5, various maintenance and replacement actions are explored and implemented into the existing cell model. Then, probabilistic inputs are applied to the cell model and the deterioration rate of an entire deck is examined in Chapter 6.

5. DECK MAINTENANCE

5.1 Overview

As discussed in Chapter 1, an important reason for creating a predictive bridge deterioration model is to be able to analyze the efficacy of different maintenance strategies for both new and existing bridges, including the timing and type of maintenance. With the non-probabilistic, mechanistic deterioration model developed in Chapters 3 and 4, the groundwork has been laid for demonstrating how service life predictions can be made based on various maintenance strategies. First, maintenance actions can be implemented into the existing baseline model developed in Chapters 3 and 4 by changing sub-model inputs and/or outputs to reflect changes due to maintenance. Then, maintenance actions may be applied to an entire deck to demonstrate and compare the impact of several maintenance actions and their effectiveness at different times throughout bridge service life.

While depth of deterioration and presence of a waterproofing mechanism are two main categories used to classify maintenance actions (Yehia et al. 2008), in order to incorporate the effect of maintenance into the predictive model the maintenance needs to be classified by when it occurs. In order to distinguish maintenance actions between deterioration stages of the proposed model from Chapter 4, maintenance may be characterized by the current state of corrosion deterioration within the bridge:

1. *Preventive maintenance:* conducted before rebar corrosion has initiated (during stage T1).
2. *Intermediate maintenance*: conducted after rebar corrosion has initiated, but before concrete cracking has begun (during stage T2).
3. *Reactive maintenance*: conducted after concrete cracking has initiated (during stage T3).

In this manner, maintenance actions are categorized by the times they are applied to the bridge deck. The same maintenance action could be preventive in one stage, but reactive in another. For example, replacing a waterproofing membrane may act as a preventive action if disbondment of the epoxy coating has not occurred during stage T1. However, if the waterproofing membrane is applied after corrosion has initiated during stage T2, it may act as an intermediate action to reduce concrete resistivity and slow the rate of corrosion. Alternatively, certain maintenance actions may only be effective in one category. Power washing a deck to reduce the surface chloride

concentration will delay the onset of corrosion. If conducted after corrosion initiation, however, power washing may have little impact on the rate of corrosion or crack growth. Table 9 shows several deck maintenance actions within the context of the predictive model and shows when they may be effective in extending deck service life. It should be noted that this categorization does not fully represent realistic conditions, since each maintenance action is likely to cause at least some extension on service life regardless of the time applied, especially if deterioration mechanisms besides corrosion are considered. However, assuming that each maintenance action only acts to reduce corrosive damage during the specified period(s) provides a conservative estimate of deck condition.

Table 9. Maintenance categorization for corrosion modeling

Maintenance Type / Maintenance Action	Preventive (Stage T1)	Intermediate (Stage T2)	Reactive (Stage T3)
Deck Washing	Yes	No	No
Waterproofing Membrane	Yes	Yes	Yes
Asphalt Overlay	Yes	No	No
Joint Replacement	No	Yes	Yes
Crack Sealing/Patching	No	No	Yes

In the following sections, the impacts of various maintenance actions on cell service life are examined within the context of the baseline cell deterioration model developed in Chapters 3 and 4. The expected changes in global deck service life are recorded using probabilistic inputs for the sample 8-meter by 24-meter deck and presented in Chapter 6 following a discussion of service life modeling.

5.2 Deck Washing

Although power washing and deck cleaning are often used to remove debris from the deck surface, leftover de-icing salts and some surface chlorides may also be removed. In the context of the present deterioration model, this type of maintenance may reduce the surface chloride concentration and delay the onset of corrosion. In the present model, the surface chloride

83

concentration at deck construction is assumed to be zero. Then, the surface concentration for the baseline model increases exponentially to 3.5 kg/m^3 over 15 years. Subsequently, the concentration increases linearly with time to simulate the cyclical application of de-icing salts. According to Kirkpatrick et al. (2002), the chloride concentration at roughly 0.5 inches below the deck surface is relatively constant when compared to the concentration less than 0.5 inches below the surface. As a result, maintenance actions such as power-washing may only remove the chlorides that have been cyclically applied in later years of the service life.

However, a study conducted by the Oregon Department of Transportation concluded that washing salt-laden concrete with a frequency of once per month had little impact on the surface chloride concentration or chloride concentration at the depth of rebar (ODOT 2005). Therefore, power washing a concrete deck with a frequency of once per month or less is unlikely to have any impact on the surface chloride concentration, and thus will not change the inputs or results of the present model.

5.3 Membrane and Overlay Replacement

Waterproofing membranes and a wearing surface overlay are often installed with the deck at construction, but will deteriorate over a period of approximately 10 years, depending on traffic and environmental conditions. In order to maintain the waterproofing effects of the membrane and increased cover and wearing surface provided by an overlay, they must be replaced regularly. CDOT bridge staff suggested an asphalt overlay replacement timing of 10 years, whereas membranes are typically replaced on a 20-year cycle. In Chapter 4, results for the modified prototype cell included a membrane and overlay at installation using the preliminary membrane model described in Section 4.2, but neither the membrane nor the overlay were replaced throughout the remainder of the projected life. The effect of various replacement timings of both the membrane and overlay, given the characteristics of the preliminary membrane model, are examined in the following sections.

5.3.1 Waterproofing Membrane Replacement

The waterproofing membrane can be considered a preventive, intermediate, or reactive maintenance action depending on the condition of the deck at the time of replacement. In order for a membrane to be preventive, it must delay disbondment of the epoxy coating and thus be installed

during stage T1. In a deck with black steel rebar, a waterproofing membrane will have little impact on the time to corrosion initiation, since it is assumed that water content does not dictate the chloride concentration at the rebar level in the present model. In the baseline model with epoxy coating, the expected time for complete epoxy coating disbondment to occur was about 20 years, assuming no use of a membrane. Figure 34 shows the impact of a membrane installed at deck construction and replaced at 20 years on the time to epoxy coating disbondment. By installing a new membrane at construction and again at 20 years, the time to disbondment increases from 20 years to 39 years. Consequently, the time to corrosion initiation T1 also increases to 39 years. This delay in adhesion loss relies on the assumptions that adhesion loss only occurs if the water content remains above the threshold as described in Chapter 4, and that the life of each waterproofing membrane is equivalent.
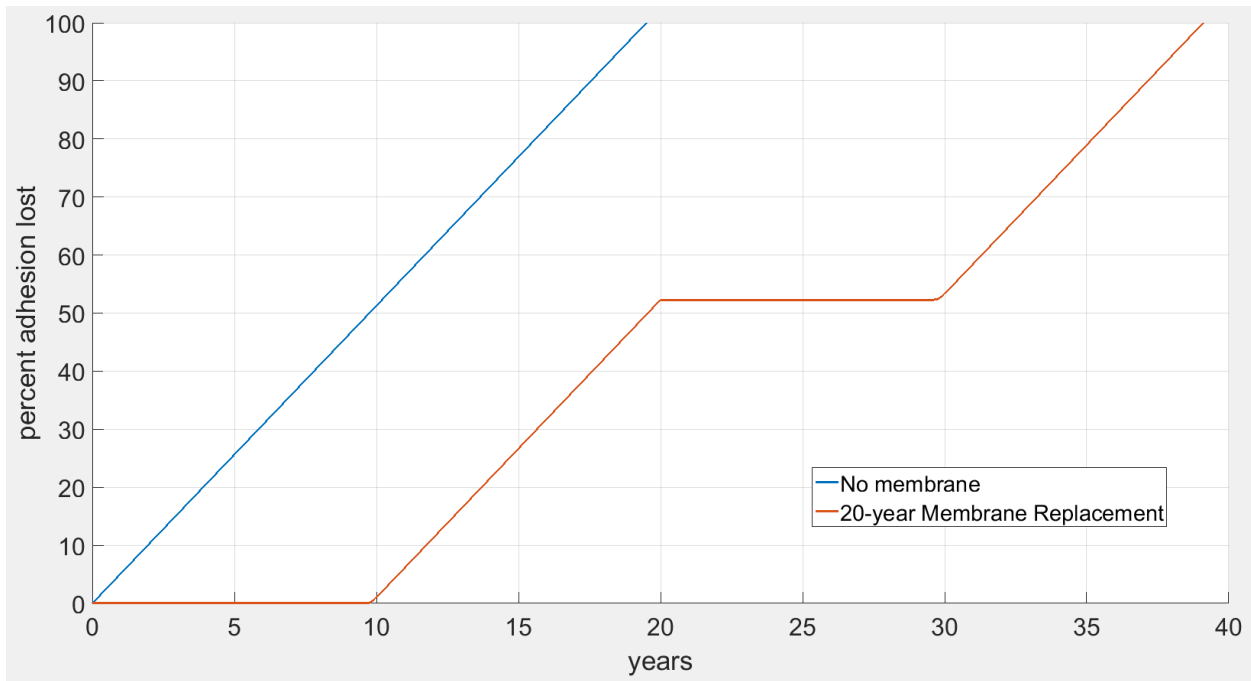
Figure 34. Delayed epoxy coating adhesion loss from membrane replacement

If the waterproofing membrane is replaced after corrosion initiation but before cracking, it may be considered an intermediate maintenance action. During this stage, the membrane will increase concrete resistivity and slow the rate of corrosion by reducing the effective relative humidity and concrete saturation. For the baseline model with an intact epoxy coating at construction, T1 = 20 years and T2 = 33 years. An intermediate waterproofing membrane may be installed between 20 years and 33 years, but not at construction. In the case of a membrane installed at 20 years, the

time to corrosion initiation is still 20 years, but the time to crack initiation is delayed from 33 years to 43 years. The effect of a waterproofing membrane as an intermediate maintenance action is shown in Figure 35, where the rate of corrosion is temporarily reduced to zero as a result of very low concrete saturation. Corrosive activity is unlikely to be stopped entirely during this period, but a significant drop in corrosion density should still be observed due to low water saturation of the concrete.

Finally, membrane replacement may act as a reactive maintenance action by slowing the rate of corrosion--and subsequent crack growth--after crack initiation. The behavior of the membrane will be similar to its proactive and intermediate counterparts, but may be more difficult to install properly due to the existence of cracks within the deck. Figure 36 shows the effect of a reactive waterproofing membrane on the rate of corrosion. For the baseline model, a reactive membrane must be installed between 33 years and 39 years, so an installation time of 35 years is selected for demonstration.
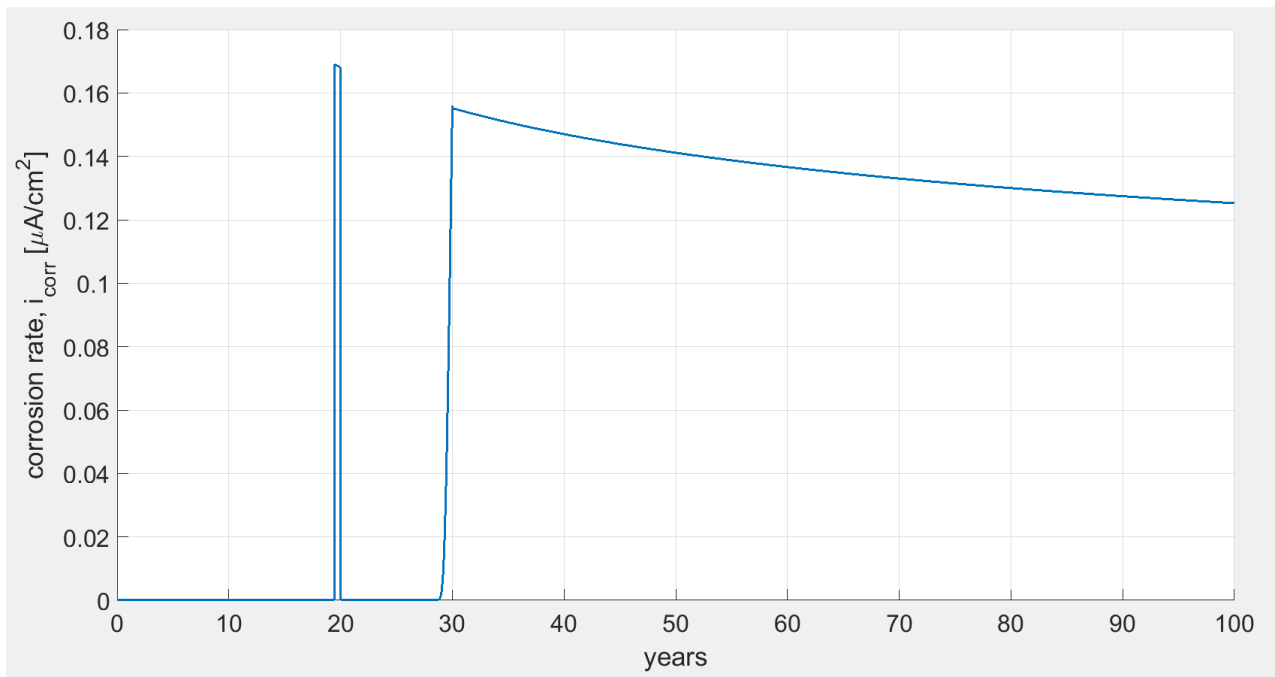
Figure 35. Temporary reduction of corrosion rate due to intermediate waterproofing membrane
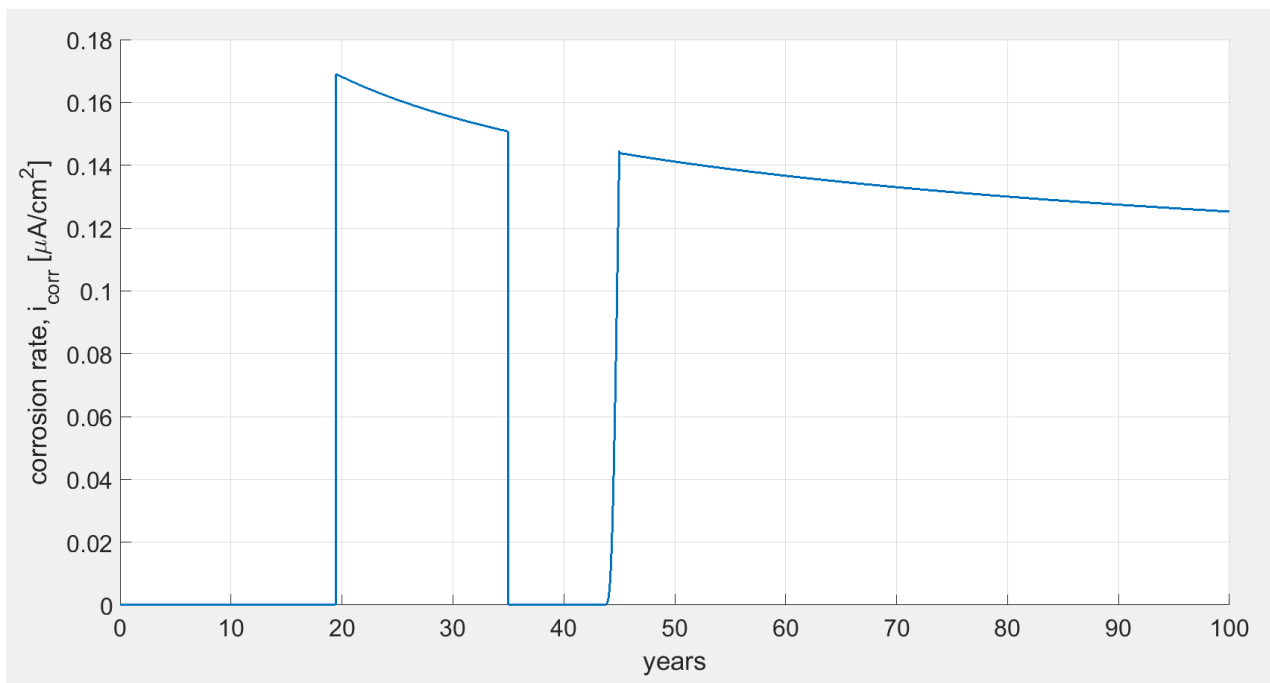
Figure 36. Temporary reduction of corrosion rate due to reactive waterproofing membrane

Table 10 summarizes the effect of membrane installation timing on times T1, T2, and T3 for the non-probabilistic baseline cell model. Times are provided for a cell with ECR (no defect) and the remaining inputs match those from Table 6.

Table 10. Extension of concrete cell service life from waterproofing membranes

	Time to End of Stage for Various Membrane Installation Timings (years)						
	Membrane Installation Time(s)						
	None	$t = 0$	$t = 20$	$t = 40$	$t = 60$	$t = 80$	$t = $ all (0,20,40,60,80)
T1	20	29	20	20	20	20	39
T2	33	43	43	33	33	33	74
T3	39	50	50	39	39	39	91

Results from various membrane installation timings show that service life extension is similar for a membrane installed at construction versus a membrane installed at 20 years; approximately ten years of additional service life can be expected from a single membrane. However, if a

87

waterproofing membrane is installed at construction and then replaced on a 20-year cycle, cell service life may extend up to more than 90 years. Although ECR adhesion is still lost at 39 years, the reduction in rate of corrosion from each membrane significantly slows crack initiation and growth. As expected, no service life extension is gained from installation of a single membrane after 39 years if no membrane is installed beforehand, since cell failure may have already occurred.

5.3.2 Asphalt Overlay Replacement

In the present model, the asphalt overlay affects the rate of deck deterioration by delaying the time taken for chlorides at the level of rebar to exceed the threshold. However, after corrosion initiates, the asphalt overlay does little to affect the corrosion or cracking variables and thus use of an overlay is considered a preventive maintenance action in the context of the deterioration model.

For an overlay installed at deck construction and not replaced, the surface chloride concentration will increase exponentially and then linearly as described in Chapter 3, but the overall thickness of the cover materials will be greater than that of a cell with bare concrete. However, if the asphalt overlay is replaced during the deck service life, the chlorides in the asphalt layer are removed and the chloride concentration throughout the asphalt depth will be reset to zero. The effect of the asphalt chloride concentration being reset with overlay replacement at a time $t = 10$ years is demonstrated in Figure 37.
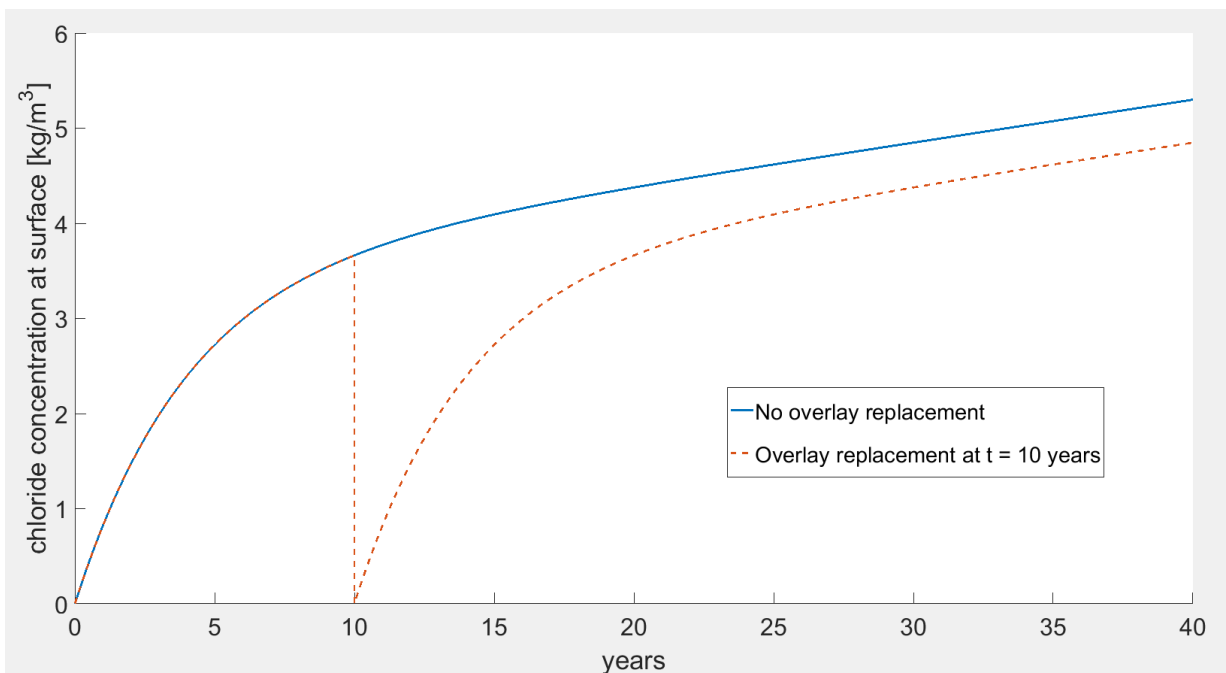
Figure 37. Chloride concentration at asphalt surface due to single asphalt replacement

While the chloride concentration at the asphalt surface and within the asphalt layer is reset to zero when an overlay is replaced, chlorides below the waterproofing membrane and within the concrete layer are not removed. As a result, the chloride concentration at the depth of the rebar never falls below its past maximum concentration. This effect is shown in Figure 38 for the same deck with an asphalt overlay being replaced at 10 years. The small discontinuity observed at 30 years is due to a change in the diffusion coefficient as discussed in Section 3.2.1. This incompatibility between existing mechanistic sub-models and the effect of maintenance actions is another limitation of mechanistic modeling that reinforces the preliminary and approximate nature of the present model.

For an overlay only replaced once at 10 years, the chloride concentration at the level of the rebar is only slightly affected, and leads to a service life extension of just 1.4 years. However, the benefits of replacing the asphalt overlay become evident when considering a regular, 10-year replacement cycle. Figure 39 shows the effect of replacing an overlay every 10 years on the chloride concentration at the depth of the rebar. The service life of a bridge deck with an overlay installed at construction but without replacement is 44 years. If the overlay is replaced every ten years, the service life extends to 83 years. By regularly replacing the chloride-laden asphalt, the service life of the bridge deck is nearly doubled.
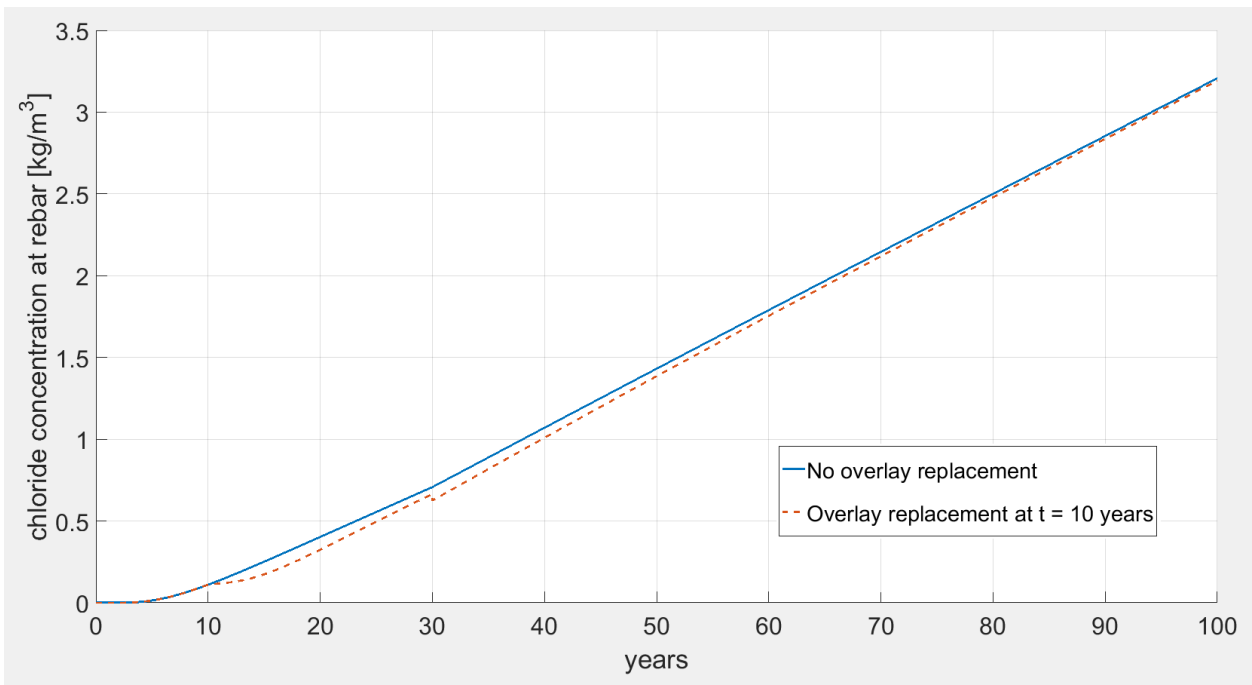
Figure 38. Chloride concentration at depth of rebar due to single asphalt replacement
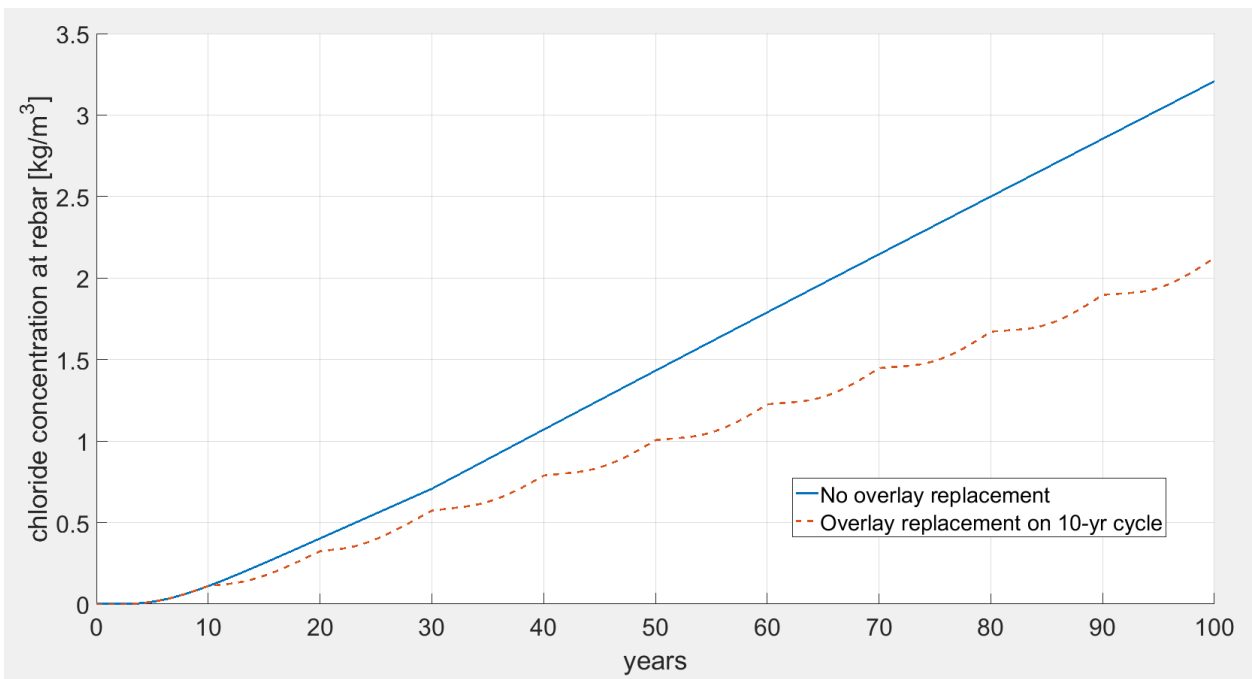
Figure 39. Chloride concentration at depth of rebar due to 10-year asphalt replacement cycle

Table 11 summarizes the effect of asphalt overlay installation timing on times T1, T2, and T3 for the baseline cell model. Times are provided for a cell with clean ECR (no defect) and the remaining inputs match those from Table 6. Aside from the column labeled "None", an overlay is installed at construction and then again at the specified time in each column. As expected, replacing the overlay prior to corrosion initiation extends the service life of the deck by delaying the onset of corrosion. However, if an overlay is replaced after corrosion initiation, it will have no expected impact on the service life. As shown by the highlighted green cells in Table 11, installing a new overlay at construction and again before 50 years may extend service life by between 50 and 57 years, primarily due to the added depth of cover. Installing and replacing the overlay on a 10-year cycle can extend the deck service life by as much as 43 years without the aid of a waterproofing membrane or other protective system, if the epoxy coating on the rebar is free of defects.

Table 11. Extension of concrete cell service life from asphalt overlays

Time to End of Stage for Various Overlay Installation Timings (years)							
	Overlay Installation Time(s)						
	None	t = 0	t = 0 & t = 10	t = 0 & t = 20	t = 0 & t = 30	t = 0 & t = 40	t = 0 & t = 50
T1	20	44	45	44	46	47	44
T2	33	59	60	59	61	62	59
T3	39	66	67	67	68	70	66
	t = 0 & t = 60	t = 0 & t = 70	t = 0 & t = 80	t = 0 & t = 90	t = all t = 0,10,20,30,40,50,60,70,80,90		
T1	44	44	44	44	59		
T2	59	59	59	59	75		
T3	66	66	66	66	83		

5.3.3 Combined Membrane and Asphalt Overlay Replacement

Although it is important to investigate the individual contributions of each surface protective system to deck service life, a combined membrane/overlay system is more representative of in situ deck conditions. By applying a membrane and overlay at construction and regularly replacing each

system, the service life of the deck may exceed the interest period of 100 years. Of particular interest to asset managers is the timing of replacement such that the fewest number of installations are necessary to reach the design life.

Figure 40 demonstrates a uniform maintenance strategy that allows the cell service life to exceed 100 years by using a constant-interval replacement schedule throughout the 100-year period. The asphalt overlay is replaced every 10 years, whereas waterproofing membranes are installed every 20 years. Figure 41 represents a front-loaded maintenance strategy that utilizes the proactive properties of the protective systems to exceed a 100-year service life. Both systems are replaced every 10 years until after the deck has been in service for 50 years. Finally, Figure 42 shows maintenance timings for a dispersed maintenance strategy, which achieves the 100-year service life using fewer waterproofing membranes and asphalt overlays than the uniform strategy. For this strategy to be viable, maintenance intervals may not be constant throughout service life.

Scenario 1 - Uniform Maintenance						
Installation						
Year	**Membrane?**	**AO?**				
0	Y	Y				
5				**Time to End of Stage (years)**		
10		Y		T1	T2	T3
15				59.4	94.8	100+
20	Y	Y				
25						
30		Y		**Number of Installations**		
35				Membrane		5
40	Y	Y		Asphalt Overlay		10
45						
50		Y				
55						
60	Y	Y				
65						
70		Y				
75						
80	Y	Y				
85						
90		Y				
95						

Advantages:	Simple; no irregular maintenance intervals.
Disadvantages:	Inefficient. Some maintenance not necessary to achieve design life.

Figure 40. Uniform maintenance strategy

	Scenario 2 - Front-loaded (Preventative) Maintenance		
	Installation		
Year	**Membrane?**	**AO?**	
0	Y	Y	
5			
10	Y	Y	
15			
20	Y	Y	
25			
30	Y	Y	
35			
40	Y	Y	
45			
50	Y	Y	
55			
60			
65			
70			
75			
80			
85			
90			
95			

Time to End of Stage (years)

T1	T2	T3
78.3	94.6	100+

Number of Installations

Membrane	6
Asphalt Overlay	6

Advantages: Simple; no irregular maintenance intervals. Very long T1; Corrosion is delayed significantly.

Disadvantages: No maintenance after 50 years.

Figure 41. Preventive maintenance strategy

Scenario 3 - Dispersed Maintenance		
Installation		
Year	Membrane?	AO?
0	Y	Y
5		
10		Y
15		
20		Y
25		
30	Y	Y
35		
40		Y
45		
50		Y
55		
60	Y	Y
65		
70		
75		
80		
85		
90	Y	Y
95		

Time to End of Stage (years)

T1	T2	T3
59.4	85.0	100+

Number of Installations

Membrane	4
Asphalt Overlay	8

Advantages:	Very few membrane installations. Avoids unnecessary asphalt installations.
Disadvantages:	Irregular asphalt installation. Earlier cracking due to high water content.

Figure 42. Dispersed maintenance strategy

Idealized installation timings would represent conditions in which either protective system may be replaced without affecting the condition of the other. In reality, a waterproofing membrane that underlies an asphalt overlay cannot be replaced without disturbing the overlay. As a result, the overlay must also be replaced at any time a new membrane is installed. Although replacement of the overlay may not be necessary to extend the service life by providing additional cover, it is still needed as a wearing surface when new membranes are installed near the end of the interest period. Additionally, the asphalt layer may not be removed entirely in favor of milling the asphalt to a

partial depth and repaving. This maintenance action would not reset the chloride concentration through the full asphalt depth to zero, which is an assumption made by the present model.

5.4 Joint Replacement

The present deterioration model assumes that any deck cell within 8 meters of a joint will experience an accelerated rate of corrosion damage due to deterioration of the local joint. However, this acceleration is dependent on the joint condition (See Section 4.3), which will change if the joint is removed and/or replaced. In the following sections, the effect of joint replacement on time to failure for a cell adjacent to a joint and on the average time to failure for the sample deck is examined using the non-probabilistic model.

5.4.1 Effect of Joint Replacement on an Adjacent Cell

Since deck cells closest to a deteriorating joint will experience the greatest change in rate of corrosion and corrosion damage, an adjacent cell is selected for examination of service life under joint replacement. The average time interval for joint replacement as noted by CDOT bridge management is approximately 7 or fewer years. To isolate the effect of joint replacement on cell service life, the waterproofing membrane and asphalt overlay are assumed absent in the present analysis. The cell is assumed to have clean, intact ECR at construction. Remaining non-probabilistic inputs are consistent with those in Section 3.3.1. Within the context of the deterioration model, replacing the joint resets the joint condition to 100%, and does not affect the rate of joint deterioration. Additionally, it is assumed that concrete in the deck near a joint is not replaced along with the joint, so chloride concentrations in adjacent cells are unaffected immediately following joint replacement.
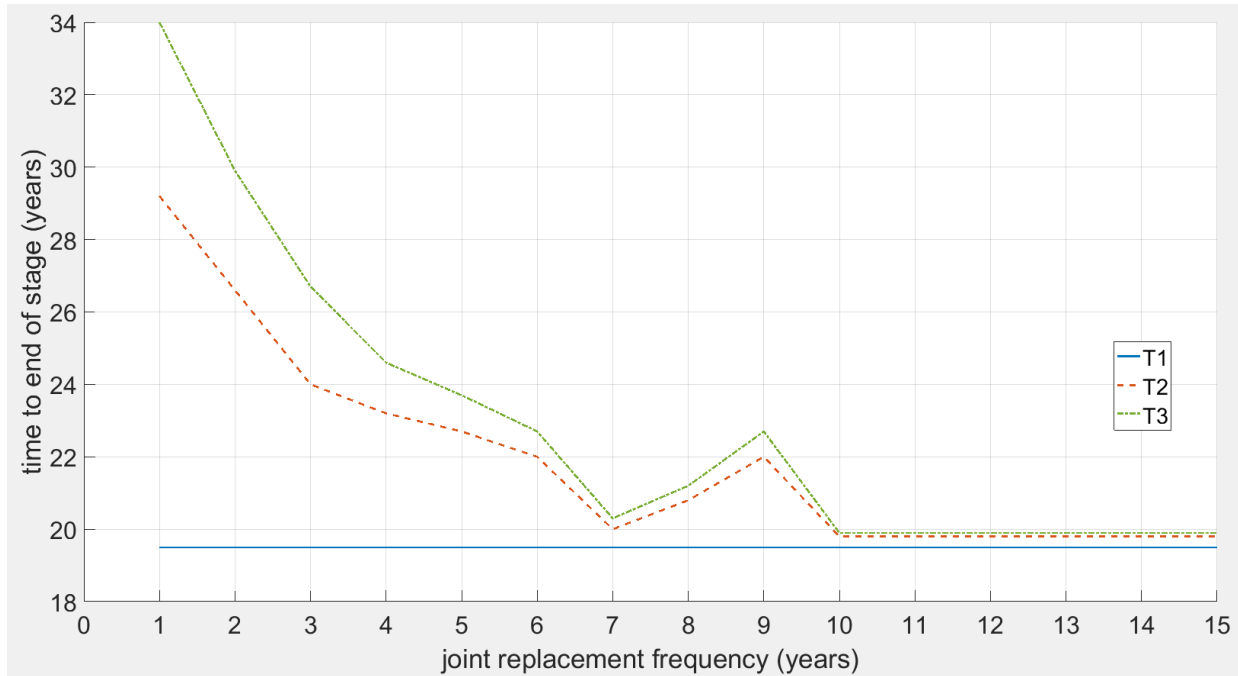
Figure 43. Joint replacement frequency vs. time to end of deterioration stage

Figure 43 shows the expected relationship between joint replacement frequency and adjacent cell service life within the 100-year interest period. Since joint condition is assumed not to affect the diffusion of chlorides into the deck, the time to corrosion initiation T1 is constant regardless of joint replacement frequency. In general, replacing the joint more often increases the time to cell failure by slowing the rate of corrosion immediately after T1. However, if the timing of joint replacement is such that a new joint is installed immediately before or after the initiation of corrosion, a lower replacement frequency may extend service life. Replacing the joint with a frequency of 7 years yields a lower cell service life than a frequency of 8 or 9 years, since a joint installation closer to T1 = 19.5 years will result in a higher joint condition and lower rate of corrosion during stages T2 and T3. The assumption that joint condition does not affect chloride diffusion should be examined in future research, since early cracking near joints may cause higher chloride concentrations at the level of rebar.

5.5 Crack Sealing

Crack sealing is a difficult maintenance technique to incorporate in mechanistic modeling. In the maintenance survey conducted by Krauss et al. (2009), the range of expected service life of bridge deck crack repair was between 2 and 75 years, and may depend on the type of crack sealant

used and timing of application. Rahim et al. (2007) recommended that a High Molecular Weight Methacrylate (HMWM) sealer be applied to bridge decks every 4-5 years.

In the context of the present mechanistic model, crack sealing may be considered by two different methods. Adding a sealant to the entire deck or sealing individual cracks may reset the width of any existing surface crack to zero, without any change in the pressure exerted on surrounding concrete by the corroded rebar. Alternatively, crack sealing may simply add 4-5 years to the total service life of any cell with an existing crack. The former solution may better represent the physical mechanisms in the deck following crack repair, whereas the latter solution is easier to implement. However, since the end of cell service life is represented by a crack width of 0.3 mm, larger cracks that are likely to exist in the deck are not considered in the present model. Defining the end of cell service life at a specific crack width is a limitation associated the baseline model. In the event of rapid, non-uniform corrosion, the window for applying a crack sealant between time T2 and T3 is very small. Due to the uncertainty associated with service life extension and difficulty of implementation, the effects of crack sealing are not applied to the current mechanistic model. Future efforts should incorporate the effects of surface repair when developing the crack propagation phase of the model.

6. GLOBAL DETERIORATION MODEL

In previous chapters, a baseline RC deck cell model was developed using non-probabilistic inputs and an assemblage of mechanistic sub-models that predict times to corrosion initiation, crack initiation, and ultimately cell failure. In the following sections, probabilistic inputs are applied to groups of prototype cells to represent an entire bridge deck, referred to as the "sample deck". Probabilistic inputs and their distributions are described in Section 6.1, and results of the global, probabilistic model are presented in Section 6.2.

6.1 Probabilistic Inputs

The baseline time-to-failure model for corrosion damage in bridge decks discussed in Chapter 3 provides a straightforward way to predict and compare service lives for various design alternatives. However, deterioration mechanisms contain inherent randomness that should be considered, especially at the scale of a full deck. At the local (cell) level, probabilistic inputs for factors such as cover thickness and surface chloride concentration can be applied to account for variability in construction and de-icing salt application. At the global (deck) level, probabilistic inputs include factors such as the number of epoxy coating defects and environmental conditions such as relative humidity. In this manner, a single deck can have failure occur at different times for each cell, and a percentage of deck failure can be calculated at any time. Deck condition will thus deteriorate gradually.

For corrosion initiation, primary probabilistic inputs include surface and threshold chloride concentrations. Per the literature review, surface chloride concentrations are typically represented by lognormal distributions with a mean of approximately 3.5 kg/m^3. Threshold chloride concentration can be considered a normal, lognormal, or uniform variable with mean values ranging from 0.4 kg/m^3 to 2.4 kg/m^3. In the present study, the threshold chloride concentration is modeled as a uniform random variable.

Deck design and construction parameters can also be modeled as probabilistic inputs. Concrete strength, cover thickness, and bar diameter may be random within a deck and among multiple decks. Hu et al. (2013) suggested a range of compressive strengths between 4.0 ksi and 5.0 ksi, and a variability of 15% in cover thickness due to construction. A variability of 10% for bar diameter was also used. In the present study, the mean design parameters are taken directly from

standard CDOT designs for highway bridges, and the variability in concrete strength, cover thickness, and bar diameter are adopted from Hu et al. (2013). These input values and their distributions are summarized in Table 12. Relative humidity, which is important for determining epoxy coating disbondment and rate of corrosion, is modeled as a normal random variable with a yearly mean of 52%, representing typical conditions for Colorado. Asphalt overlay and waterproofing membrane service lives vary between 7 and 11 years. However, rather than being considered a random input, overlay life is determined by average daily traffic. For a bridge in an urban, high traffic region, the service life is considered to be 7 years, whereas a bridge in a rural area with low traffic will have a service life of 11 years.

Finally, the location and size of epoxy coating defects should be considered as probabilistic inputs. Due to their high maximum and relatively low average, a lognormal distribution is used to determine the number of defects in each deck. From Table 3 (see Section 2.5.3.1), the average number of bare areas is 2.4 per 3.7 feet of rebar. This includes defects on both transverse and longitudinal rebar. Holidays are not considered because they may be too small to induce pitting or non-uniform corrosion. Additionally, the inclusion of holidays in the model would increase the average number of defects per foot to more than one, which is the construction limitation dictated by ASTM (ASTM775). It is assumed that, on average, the number of defects does not exceed the ASTM limit. Because transverse rebar is the primary subject of corrosion damage in this model, defects on the longitudinal rebar are neglected. This means that for an average of 2.4 defects per 3.7 feet, approximately 0.64 defects per foot of rebar would be expected. To determine the total number of defects in a deck, the total length of transverse rebar is multiplied by the per-foot average and rounded to the nearest whole number. Each defect is then randomly assigned to a location within the deck. To simplify the model, each cell may only contain one defect, for a maximum total possible number of defects equal to the total number of deck cells. Possible defect locations for a sample 8-meter by 24-meter deck with few and many defects are shown in Figure 45 and Figure 46, respectively.

Defects may be present at any point on the perimeter of each rebar. Location of a defect is assumed to dictate the direction of initial cracking, especially in the case of non-uniform corrosion. For simplicity, defects are assumed to exist only on top or on either vertical face of the rebar. A defect on top of the rebar represents surface cracking, whereas a defect on either side represents

lateral cracking. It is assumed that defect location is random and uniform, indicating a 50% probability of surface cracking and equivalent probability of lateral cracking for cells with defects. For cells experiencing uniform corrosion, lateral cracking does not control and thus only surface cracking is considered.

Table 12. Selected probabilistic inputs and distributions for global deck model

Input Variable	Distribution Type	Distribution Parameters
Surface Chloride Concentration C_0	Lognormal	μ: 3.5 kg/m^3 σ: 1.75 kg/m^3
Threshold Chloride Concentration C_{th}	Uniform	Min: 0.4 kg/m^3 Max: 2.4 kg/m^3
Concrete Strength f'_c	Uniform	Min: 27.6 MPa (4.0 ksi) Max: 34.5 MPa (5.0 ksi)
Concrete Cover Thickness x	Uniform	Min: 43.2 mm (1.7 inches) Max: 58.4 mm (2.3 inches)
Bar Diameter D_b	Uniform	Min: 14.3 mm Max: 17.5 mm
Relative Humidity rh	Normal	μ: 52% σ: 10%
Protective Layer Longevity	Dependent	7 years for high traffic 11 years for low traffic
Average Number of Defects	Lognormal	μ: 2.4 σ: 2.6

6.2 The Sample Deck and Probabilistic Results

6.2.1 The Sample Deck and Defect Locations

To demonstrate the results of the modified cell model at the global scale using both non-probabilistic and probabilistic inputs, a sample deck 8 meters wide and 24 meters long is utilized for comparison. Figure 44 demonstrates a plan view of the sample deck divided into cells for a bar spacing of 12 inches, which is representative of the prototype cell used in previous chapters.

Although in situ bar spacing is often closer to 8 or 9 inches, 12 inches is used to reduce computational time and provide clearer visuals. The sample deck contains 1,950 cells and is used throughout the remainder of the report to demonstrate model outputs. Figures 45 and 46 show possible locations of defects within the sample deck, with yellow cells representing defects, and green cells representing intact epoxy coating. In Figure 45, the mean number of defects is 0.631 per meter of rebar, whereas Figure 46 has a much higher average of 1.16 per meter of rebar.
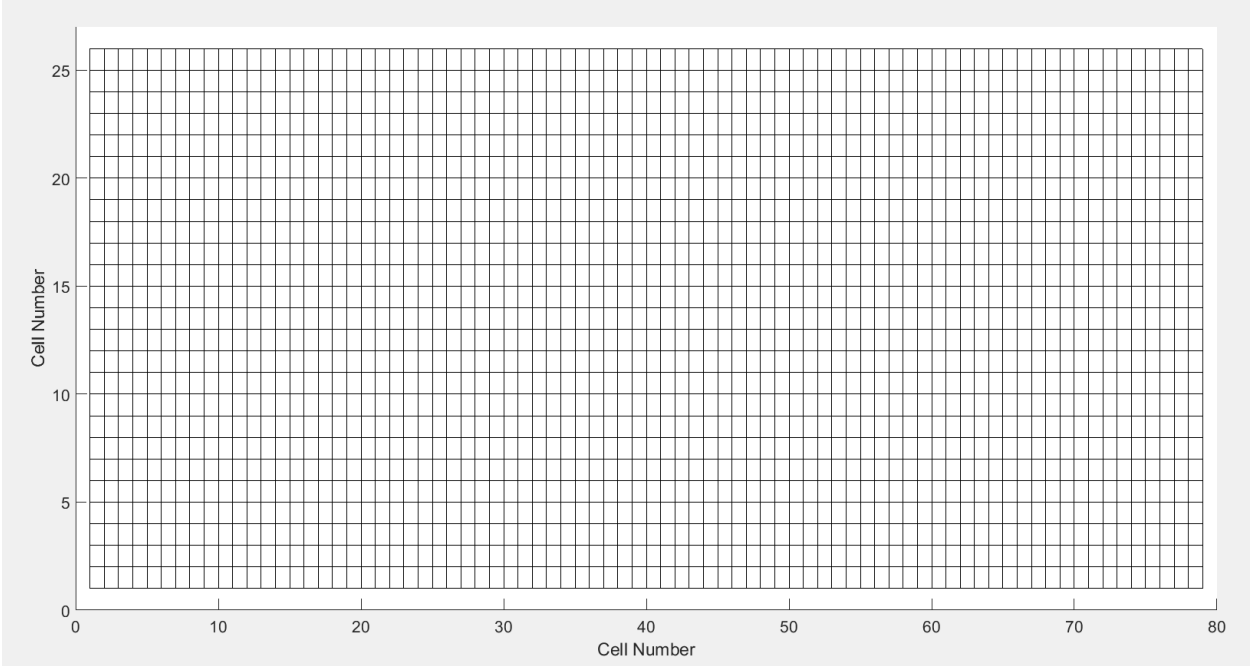
Figure 44. Sample 8-meter by 12-meter deck
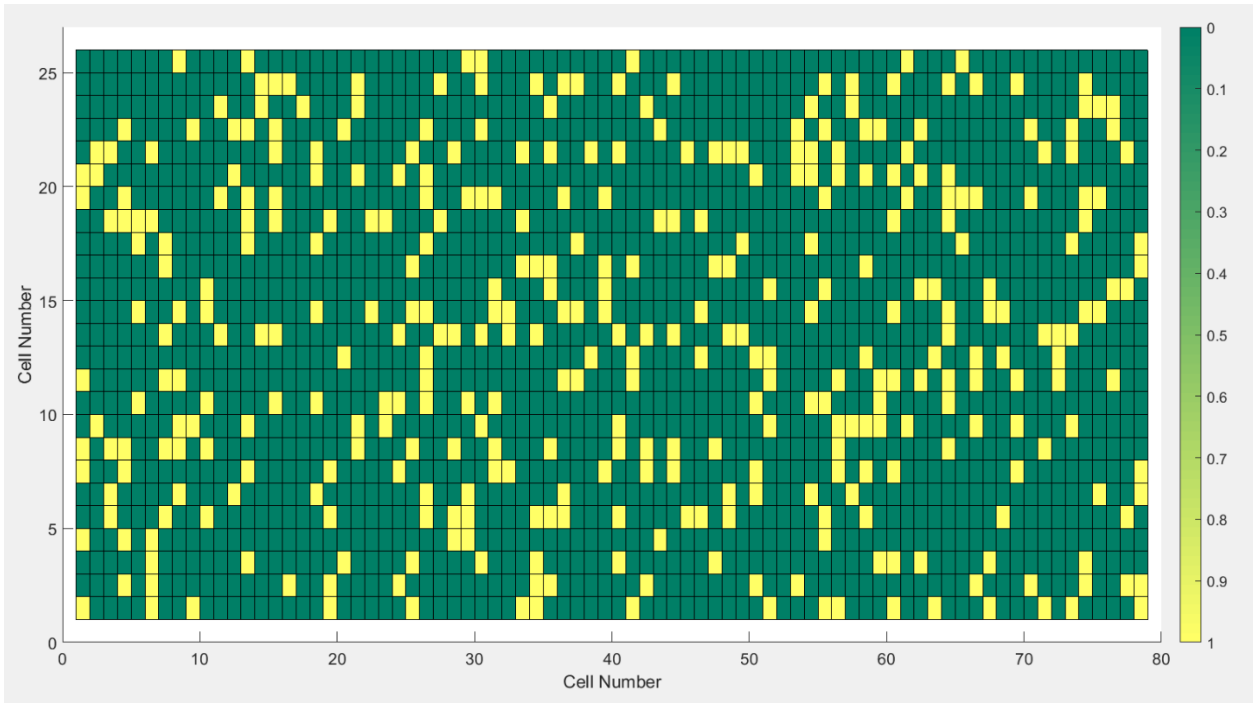
Figure 45. Possible random epoxy coating defect locations (sparse)
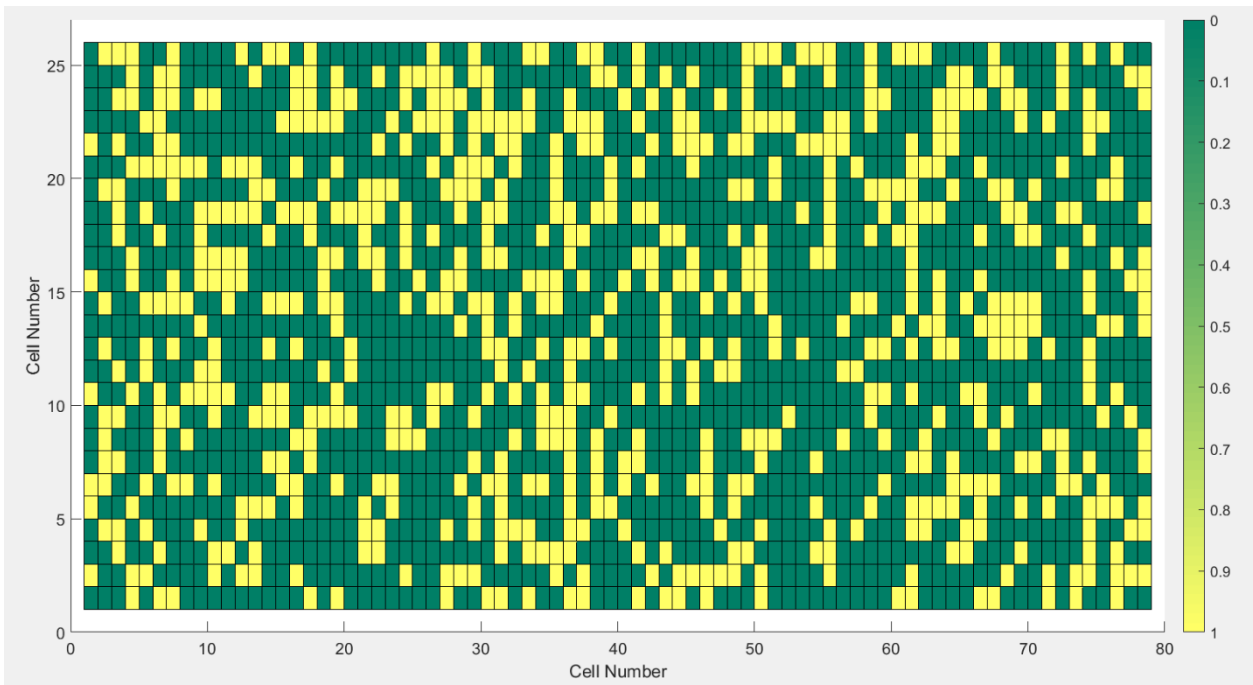
Figure 46. Possible random epoxy coating defect locations (abundant)

6.2.2 Joint Deterioration and Global Deck Results

Results of the time-to-failure for the sample 8-meter by 24-meter deck are compared for four scenarios:

- Non-probabilistic inputs without consideration of joint deterioration
- Non-probabilistic inputs with consideration of joint deterioration
- Probabilistic inputs without consideration of joint deterioration
- Probabilistic inputs with consideration of joint deterioration

All four scenarios include the effects of a membrane and overlay installed at construction with service lives of 10 years.

The purpose of comparing model results with and without joint deterioration included is to directly quantify the influence of joint deterioration (see Section 4.3) on time-to-failure, and to determine whether its impact is a worthwhile subject of investigation in future modeling efforts. Figure 47 and Figure 48 show the same deck not including and including the influence of joint deterioration. For the non-probabilistic model without joint deterioration, the time-to-failure for each cell is binary and only depends on the presence of a defect. However, if joint deterioration influences the rate of corrosion, the time-to-failure decreases non-linearly when approaching the ends of the deck. The mean time-to-failure decreases from 59 years to 47 years for a bridge with joints that are installed at the time of deck construction and are not maintained. For the probabilistic model without joint deterioration, there is an equal probability of failure in each cell and the average time-to-failure is not dependent on location. Similar to the non-probabilistic model, if joint deterioration is considered, the average time-to-failure is no longer constant between the ends of the bridge and mid span. This phenomenon is observed graphically in Figures 49 and 50, where the end strips of the deck in Figure 50 are lighter in color than those of Figure 49, indicating shorter service lives near the joints.
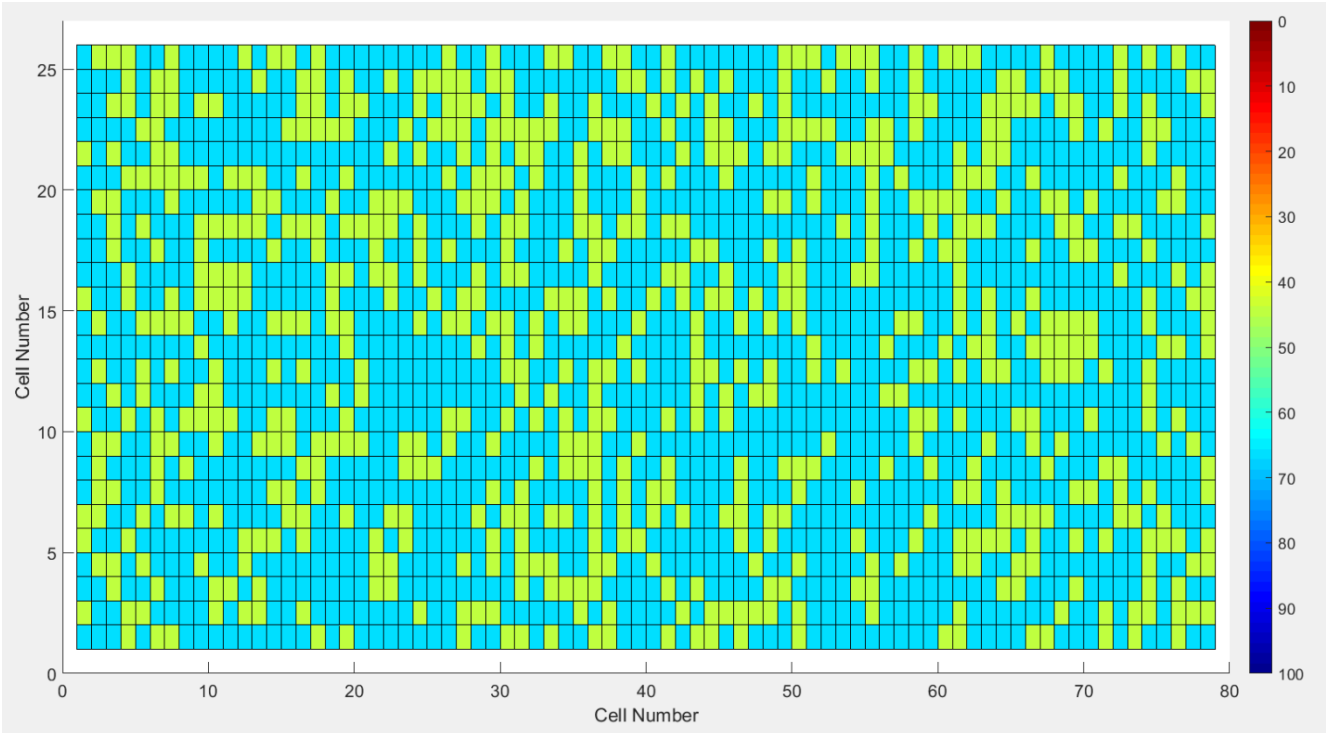
Figure 47. Non-probabilistic cell failure map without consideration of joint deterioration
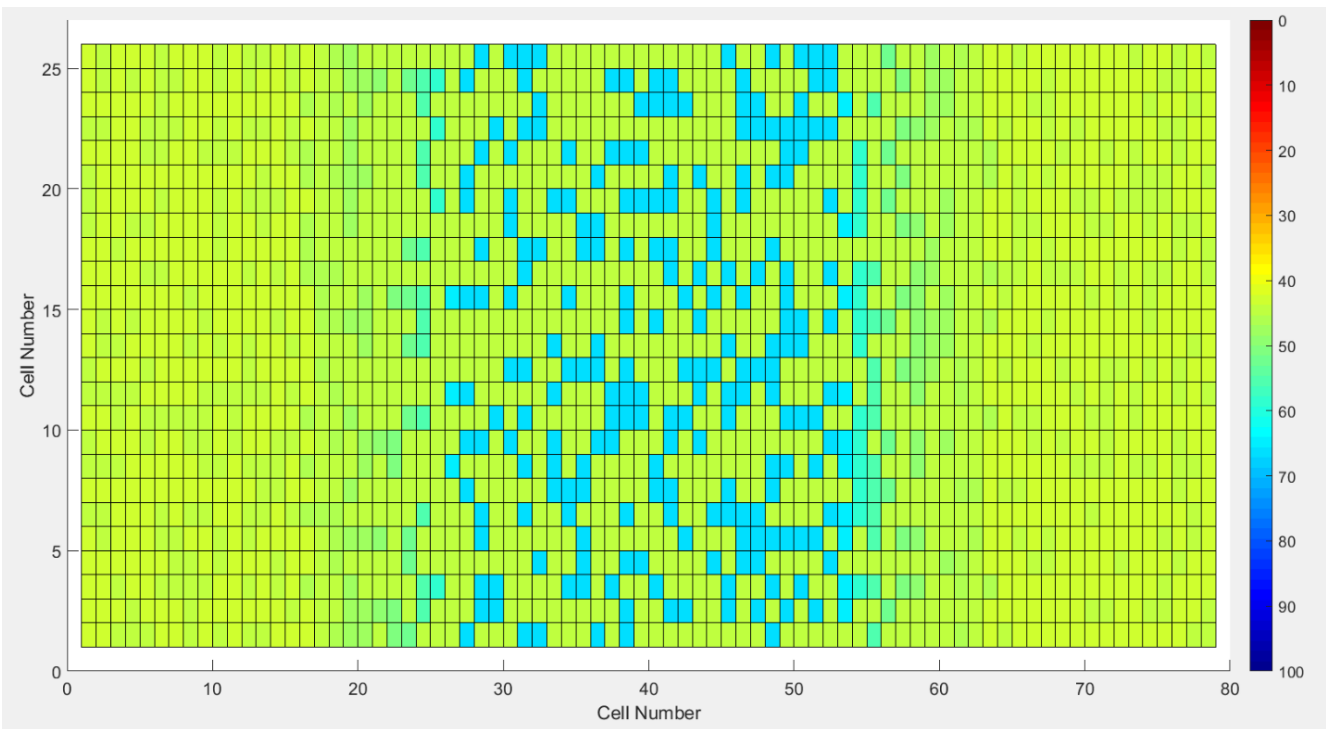
Figure 48. Non-probabilistic cell failure map with consideration of joint deterioration
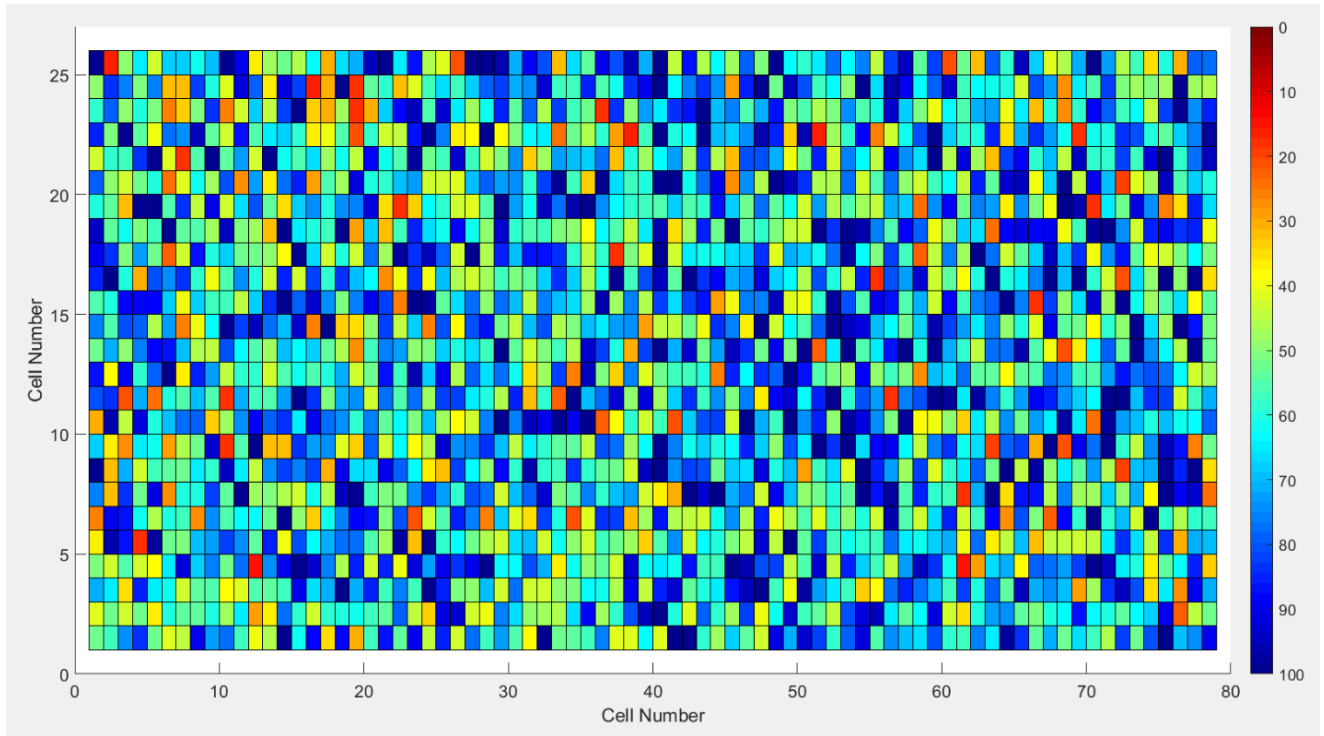
Figure 49. Probabilistic cell failure map without consideration of joint deterioration
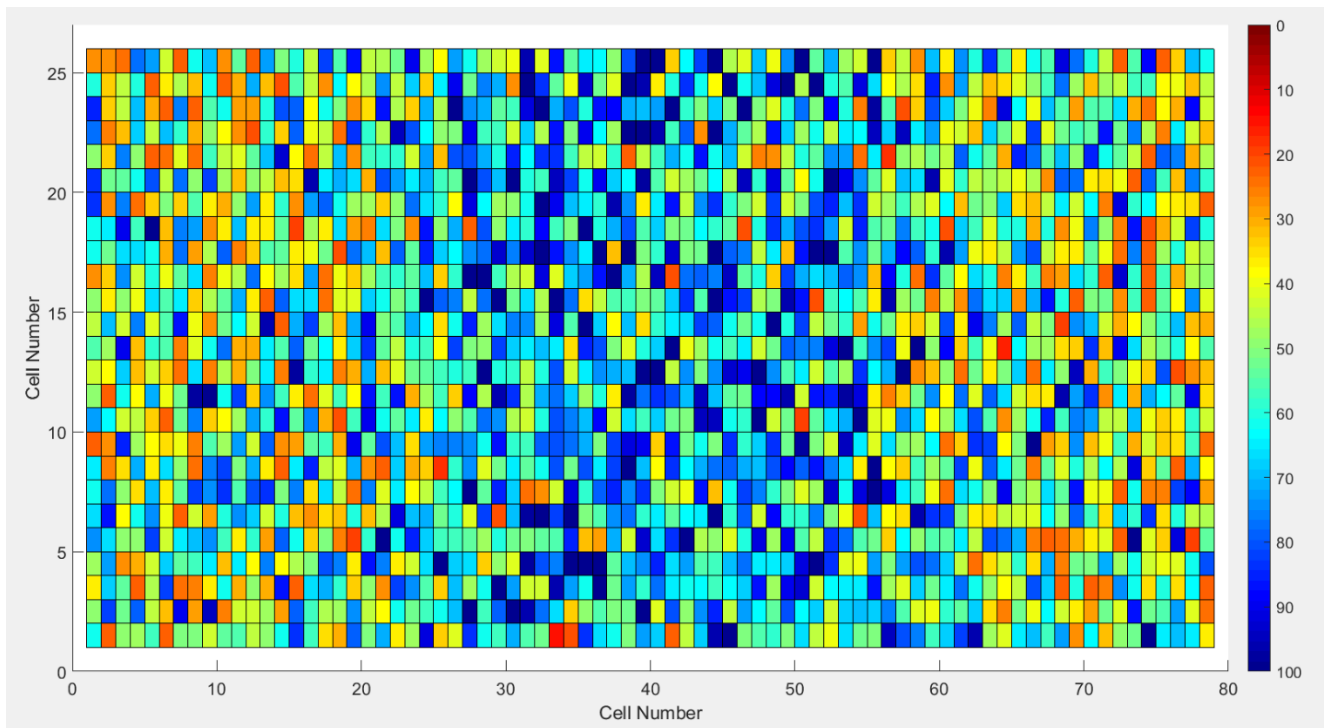
Figure 50. Probabilistic cell failure map with consideration of joint deterioration

Table 13 compares the mean T1, T2, and T3 for each of the four scenarios. A single simulation was conducted for each non-probabilistic scenario, since results do not change between multiple simulations. For each of the probabilistic scenarios, ten simulations were conducted and results reflect the mean times across all ten simulations. This means that the probabilistic results represent the average times of 19,500 cell simulations (10 deck simulations of 1,950 cells each). Non-probabilistic inputs are the same as those used in Chapter 3 (see Table 6). Probabilistic inputs are consistent with those in Table 12. The average time to corrosion initiation is unaffected by the presence of joint deterioration, as expected. In the present model, joint deterioration only affects the rate of corrosion within the deck, which changes the time to cracking initiation (T2) and cell failure (T3).

Table 13. Mean end-of-stage times for global deck model

	Time from Deck Construction to End of Stage (years)			
	Non-Probabilistic		Probabilistic	
	No joint influence	With joint influence	No joint influence	With joint influence
Mean T1	44	44	51	51
Mean T2	54	46	61	56
Mean T3	59	47	65	58

Additionally, the sample deck should be evaluated for a system with bare steel reinforcement and no protective systems to act as a control. Figure 51 displays the probabilistic results of the sample deck with the same input parameters, sans the inclusion of epoxy coating, the 3-inch asphalt layer, and waterproofing membrane. Joint deterioration is still included. The mean T1, T2, and T3 are 18 years, 23 years, and 25 years, respectively. As expected, the average time-to-failure decreases significantly when corrosion protection is absent. Only a handful of cells are expected to reach service lives of greater than 50 years.
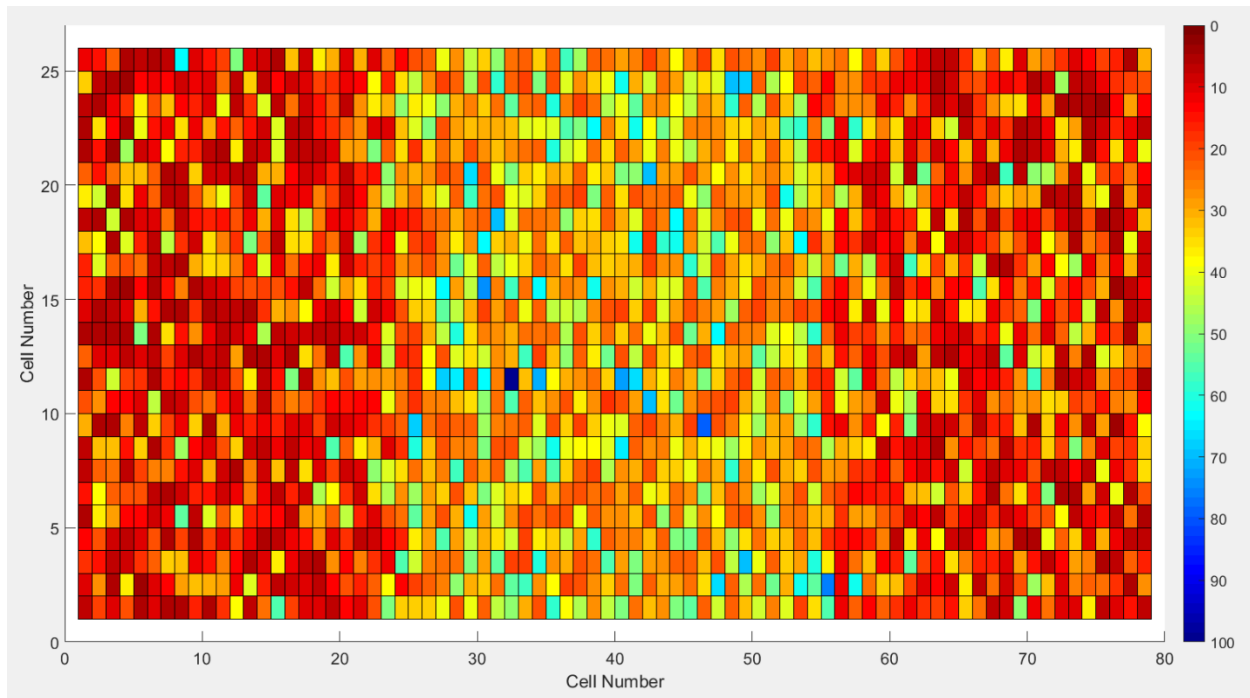
Figure 51. Probabilistic cell failure map for unprotected deck with consideration of joint deterioration

The mean time-to-failure is useful for predicting service life at the project scale. More useful to bridge management, however, is a timeline of the percent of deck failure. A percentage of failed cells throughout the 100-year period of interest yields bridge condition in any given year, and describes the overall rate of deterioration at the global scale. In addition, the percentage of deck failure allows model predictions to be mapped to NBI ratings, which are sometimes quantified by the percentage of deck cracking, spalling, or delamination. These aspects of model application and validation are discussed in Chapter 7.

6.2.3 Effect of Joint Replacement on Average Time to Failure

The effect of joint installation on the average time to failure of an entire deck should be investigated. Since the condition of the joint will only affect the service life of nearby cells, it is expected that the influence of joint maintenance on deck service life is dependent on bridge length. For the purpose of comparison, the 8-meter by 24-meter sample deck is used again to examine changes in service life due to joint replacement. In this case, the waterproofing membrane and asphalt overlay are installed at construction and not replaced throughout deck service life to match the conditions used in the previous section and obtain a direct comparison.

108

Figure 52 shows the time to failure for all cells in a deck with both joints being installed at construction and subsequently replaced every 7 years. Table 14 demonstrates the difference in average time to failure between the deck with no joint replacement (see Figure 48) and the deck with a 7-year joint replacement cycle.
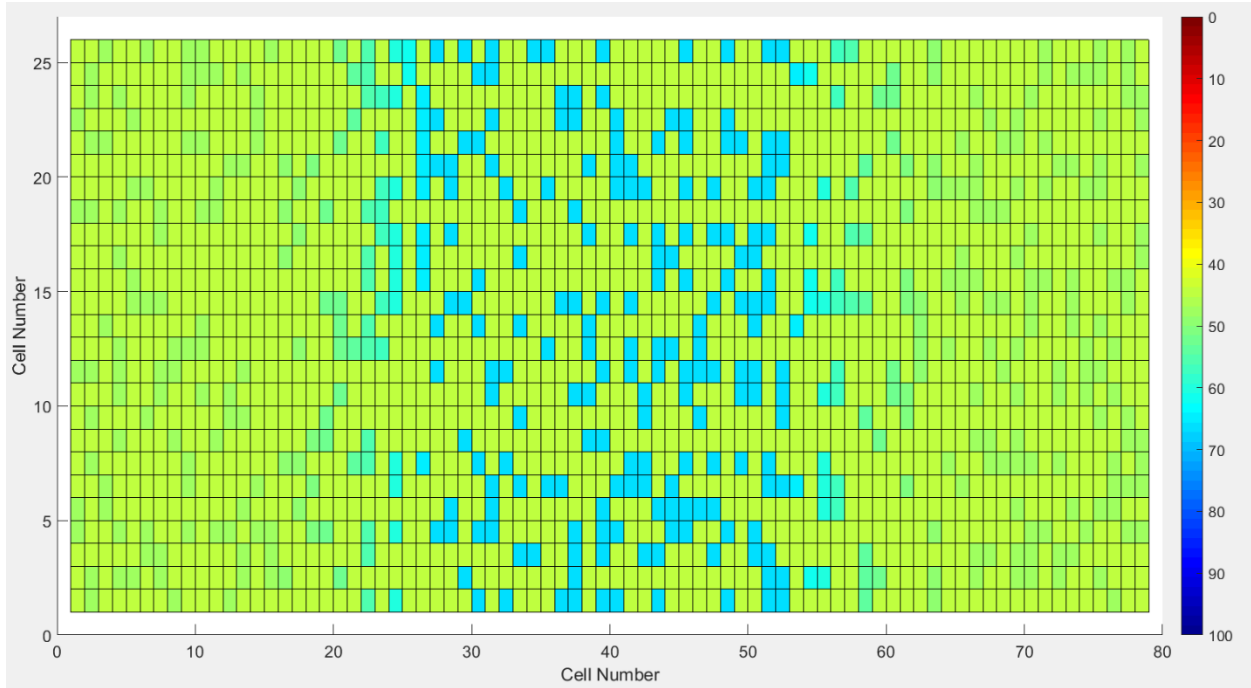
Figure 52. Non-probabilistic cell failure map with seven-year joint replacement cycle

Table 14. Mean end-of-stage times for global deck model with joint replacement

Time from Deck Construction to End of Stage (years)		
	No Joint Replacement	7-year Joint Replacement Cycle
Mean T1	44	44
Mean T2	46	47
Mean T3	47	48

As expected, the average time to corrosion initiation is unchanged. However, even with a joint being replaced at $T = 42$ years, the time to crack initiation and cell failure is hardly affected. At 44 years, when corrosion initiates, the newest joint installed at 42 years has already deteriorated

109

to 77.1% of its original condition. This causes a decrease in the half-cell potential from -362 mV to -430 mV and subsequent increase in rate of corrosion from 0.86 $\mu A/cm^2$ to 2.0 $\mu A/cm^2$. Thus, the newly installed joint does little to inhibit corrosion of nearby cells.

In order for joint replacement to significantly extend deck service life, a new joint would be needed almost immediately before or after corrosion initiation. Alternatively, joint maintenance such as cleaning may be a more viable method of preventing increased corrosion rates near joints. Further investigation is needed to model the effect of joint condition and maintenance on rate of corrosion in nearby cells. The cause of high corrosive activity near joints has not been well defined from a mechanistic standpoint. Additionally, joint replacement is not typically governed by deck condition, but by the condition of the joint.

7. MODEL APPLICATION

In previous chapters, a model for predicting bridge deck deterioration due to rebar corrosion was developed. The effect of joint deterioration and maintenance actions on baseline model inputs was also observed. The next step is to validate the model predictions through comparison to historical bridge data. In the following sections, results and limitations of bridge validation using existing historical data are examined and necessary steps for model application to bridge management in the future are proposed.

7.1 Cumulative Damage and Service Life

7.1.1 Full Deck Simulations

The present model is capable of estimating RC deck condition throughout the 100-year period of interest by indicating the number or percentage of cells having experienced failure at any given time. This percentage can be plotted as a cumulative damage index (CDI) for the entire bridge, from which bridge condition ratings can be identified. To obtain the expected CDI bounds and measure reproducibility of the model, twelve model simulations were conducted on the sample deck with probabilistic inputs and properties consistent with those in Chapter 6 (see Table 12). Figure 53 shows the CDIs for each simulation. After ten simulations with random numbers of epoxy coating defects were complete, the number of cells with defects appeared to be the strongest predictor of CDI shape and average time to cell failure. Two simulations labeled "All Defects" and "No Defects" were then conducted to represent extreme conditions of initial rebar damage in the deck, whereas the previous ten simulations were conducted to represent typical rebar damage conditions. The simulation labeled "All Defects" represents an expected cumulative damage index for a deck with non-uniform corrosion in every cell, such that the number of epoxy coating defects far exceeds the allowable number as mandated by ASTM. This CDI is considered to be the most conservative damage estimate for the given deck. Alternatively, the simulation labeled "No Defects" represents a bridge deck with no defects in the epoxy coating, such that all rebar experiences uniform corrosion following complete loss of epoxy coating adhesion. This CDI indicates the least conservative damage estimate, since at least some non-uniform corrosion is likely to occur in the deck. The remaining simulations, which fall between these two bounds, represent a random number of epoxy coating defects as dictated by the lognormal distribution with

a mean of 0.65 defects/foot and standard deviation of 0.70 defects/foot. A summary of each simulation is shown in Table 15. In Table 15, $\%Det_{(t=52)}$ represents the percent of total deck deterioration in year 52, where the largest range of estimated deterioration was observed across all twelve simulations. Between the minimum and maximum number of defects, a difference in percent deck area deteriorated of 14.9% was observed in year 52.
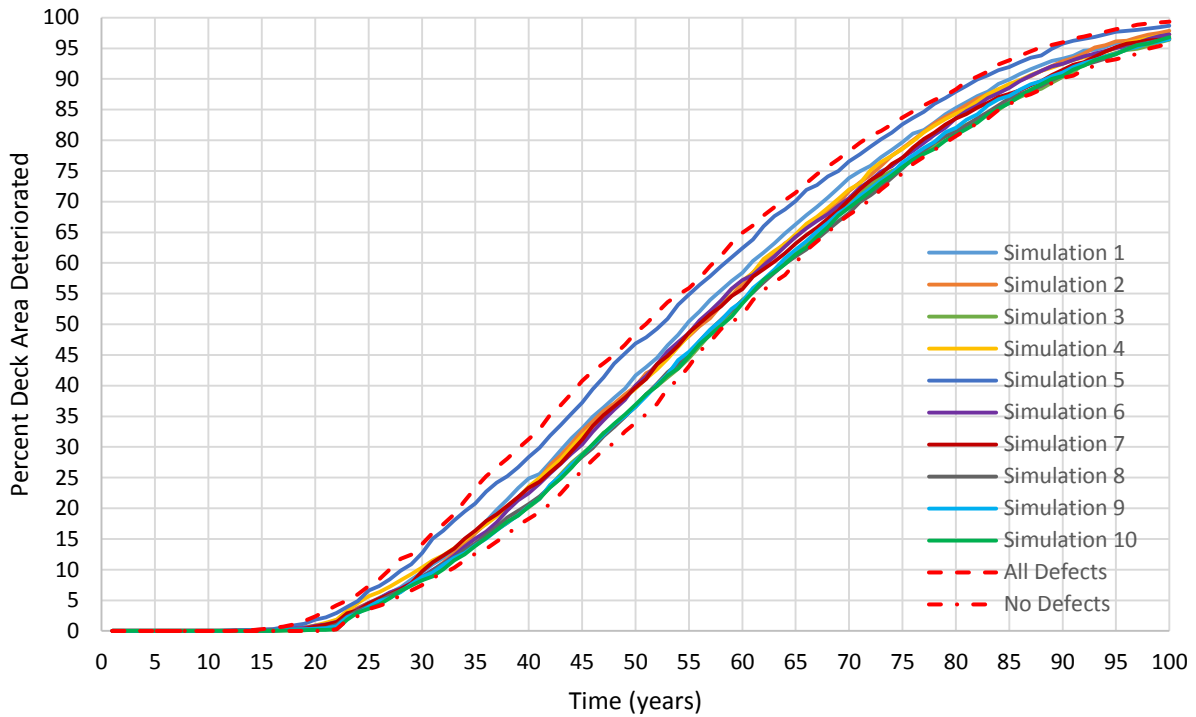
Figure 53. Cumulative damage of the sample deck

Table 15. Cumulative damage variation for sample deck model simulations

Simulation No.	Number of Cells with Epoxy Coating Defects	%Det$_{(t=52)}$
1	949/1950 (49%)	44.5
2	689/1950 (35%)	42.9
3	125/1950 (6%)	40.0
4	734/1950 (38%)	42.7
5	1350/1950 (69%)	49.3
6	624/1950 (32%)	43.5
7	502/1950 (26%)	43.5
8	360/1950 (19%)	40.3
9	294/1950 (15%)	40.2
10	139/1950 (7%)	40.0
No Defects	0/1950 (0%)	37.0
All Defects	1950/1950 (100%)	51.9

Since the presence of an epoxy coating defect assumes that no loss of adhesion is necessary to initiate corrosion, and that non-uniform corrosion will accelerate damage near a defect, the number of defects in a deck acts as a simple indicator of expected bridge condition. The number of defects can thus be used to estimate the CDI for any given bridge without the need to run multiple simulations. To test this hypothesis, five additional simulations (labeled 11 to 15) were conducted on the sample deck with the same probabilistic input distributions sans the number of defects, which was held constant at the mean of 0.65 defects per foot of transverse rebar. For an 8-meter by 12-meter deck, 632 defects are present. The location of each defect remained random and uniform for each simulation. Figure 54 shows five CDIs for a constant number of defects. It can be observed that there is almost no change among simulations in the rate of global deck deterioration, even though properties such as rebar size, concrete cover, chloride concentrations/thresholds, and relative humidity are random according to the distributions described in Table 12.
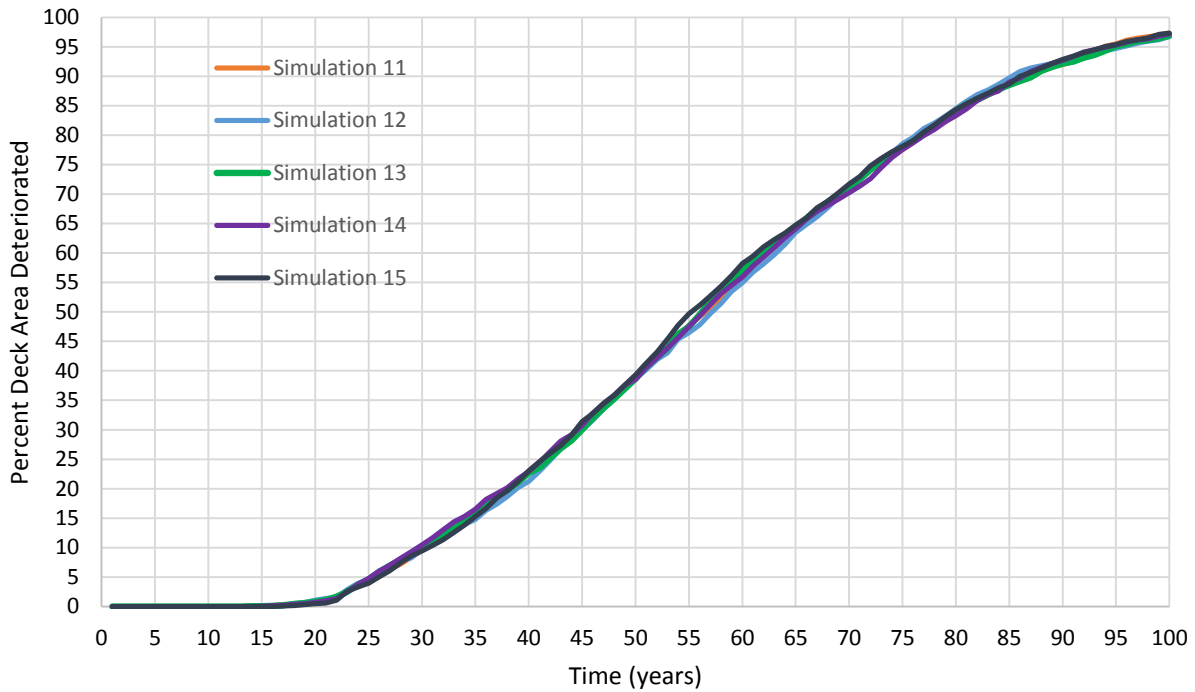
Figure 54. Cumulative damage of the sample deck with constant number of epoxy coating defects

By plotting the number of defects against the percentage of deck deterioration in a single year, an approximate relationship between number of defects and deck condition can be defined for the sample deck. This relationship is shown in Figure 55. Each horizontal row of points represents a single simulation, and the times to reach several different levels of deterioration are plotted. Although the approximations shown may only represent bridges with similar properties to the sample deck, a similar analysis could be conducted for other bridges or groups of bridges with different dimensions, rebar sizes, and/or cover/protection mechanisms. These bridge groups are described in Section 7.3.
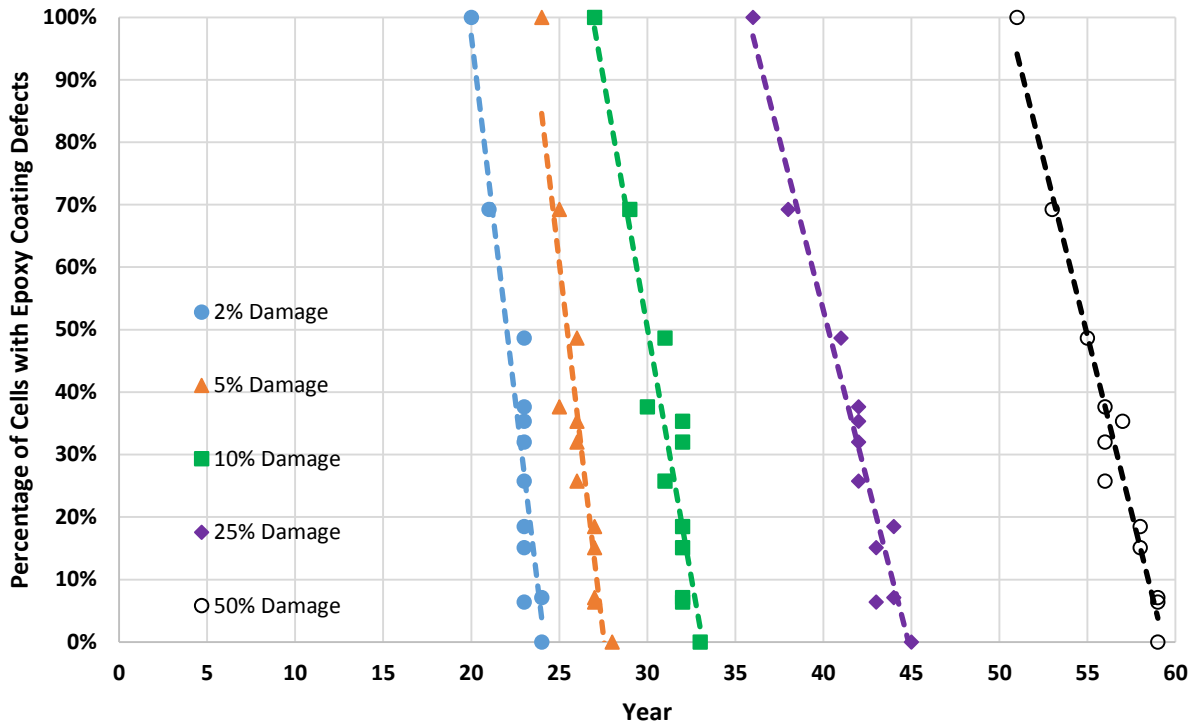
Figure 55. Deterioration as a function of time and percentage of cells with epoxy coating defects

7.1.2 Mapping to Element Ratings

Once a timeline of deck deterioration has been established, its relation to historical bridge inspection data can be assessed. In order to validate the predictions made by the model, data from the deck CDI should be mapped to the NBI or CoRe element ratings that govern historical bridge records. The FHWA Recording and Coding Guide (FHWA 1995) only provides qualitative indicators of deck condition. Although ratings are often based on subjective condition descriptors, quantitative indicators in the form of percent deck cracking/delamination are also in use by some departments of transportation. The Michigan Department of Transportation provides numerical support for deck ratings, where bridge condition can be represented by spalling and/or delamination (MDOT 2016). These ratings are shown in Figure 56. Similarly, the Delaware Department of Transportation indicates NBI ratings by percentage of deck that is water saturated or deteriorated (DelDOT 2008). Delaware's condition ratings are shown in Figure 57. The percentage area of deck deterioration to warrant different ratings can vary significantly between guides. For example, for a deck rating of 3, MDOT indicates that at least 25% of the deck area is

115

spalled, whereas DelDOT suggests that as much of 60% of the deck has deteriorated. However, the type or extent of damage that constitutes deterioration is not always consistent between departments or inspectors.

Code	Description
N	NOT APPLICABLE. Code N for culverts and other structures without decks, e.g., filled arch bridge.
9	NEW CONDITION. No noticeable or noteworthy deficiencies which affect the condition of the surface.
8	GOOD CONDITION. Minor cracking less than 1/32" wide (0.8mm) with no spalling, scaling or delamination.
7	GOOD CONDITION. Open cracks less than 1/16" wide (1.6mm) at a spacing of 10 ft or more, light shallow scaling allowed.
6	FAIR CONDITION. Surface has considerable number of open cracks greater than 1/16" wide (1.6mm) at a spacing of 5 ft or less. Surface area exhibits 2% or less of spalled or delaminated areas, including repaired areas. Medium scaling on the surface is 1/4" to 1/2" (6.4 mm to 13 mm) in depth.
5	FAIR CONDITION. Between 2% and 10% of the surface area is spalled or delaminated. There can be excessive cracking in the surface. Heavy scaling 1/2" to 1" in depth (13 mm to 26 mm) can be present.
4	POOR CONDITION. Large areas of the surface, 10 - 25% is spalled or delaminated.
3	SERIOUS CONDITION. More than 25% of the surface area is spalled.
2	CRITICAL CONDITION. Emergency surface repairs required by the crews.
1	IMMINENT FAILURE CONDITION. Bridge is closed to traffic, but corrective action may put the bridge back in service.
0	FAILED CONDITION. Bridge closed.

Figure 56. NBI ratings for a concrete bridge deck in Michigan (MDOT 2011)

Concrete Deck Condition Rating (Item 58)

Code	Condition of Deck Item
N	Use for all culverts
9	**Excellent condition** – No noticeable or noteworthy deficiencies which affect the condition of the deck item. Usually new decks.
8	**Very good condition** – Minor transverse cracks with no deterioration, i.e. delamination, spalling, scaling or water saturation.
7	**Good condition** – Sealable deck cracks, light scaling (less than ¼" depth). No spalling or delamination of deck surface but visible tire wear. Substantial deterioration of curbs, sidewalks, parapets, railing or deck joints (need repair). Drains or scuppers need cleaning.
6	**Satisfactory condition** – Medium scaling (¼" to ½" in depth). Excessive number of open cracks in deck (5 ft intervals or less). Extensive deterioration of the curbs, sidewalks, parapets, railing or deck joints (requires replacing deteriorated elements).
5	**Fair condition** – Heavy scaling (½" to 1" in depth). Excessive cracking and up to 5% of the deck area is spalled; 20 – 40% is water saturated and/or deteriorated. Disintegrating of deck edges or around scuppers. Considerable leaching through deck. Some partial depth failures, i.e. rebar exposed (repairs needed).
4	**Poor condition** – More than 50 % of the deck area is water saturated and/or deteriorated. Leaching throughout deck. Substantial partial depth failures (replace deck soon).
3	**Serious condition** – More than 60% of the deck area is water saturated and/or deteriorated. Use this rating if severe or critical signs of structural distress are visible and the deck is integral with the superstructure. A full depth failure or extensive partial depth failures (repair or load post immediately).
2	**Critical condition** – Some full depth failures in the deck (close the bridge until the deck is repaired or holes covered).
1	**"Imminent" failure condition** – Substantial full depth failures in the deck (close the bridge until deck is repaired or replaced).
0	**Failed condition** – Extensive full depth failures in the deck (close bridge until the deck is replaced).

Figure 57. NBI ratings for a concrete bridge deck in Delaware (DelDOT 2008)

The Colorado Department of Transportation utilizes an element rating system in addition to the NBI coding guide, where element condition ratings are based on a five-point scale rather than the 0-9 rating used for NBI (CDOT 1998). However, quantitative support is provided for each rating and each type of bridge protection is provided with an individual coding guide (i.e. bare or coated rebar; protected or unprotected concrete). Table 16 shows the CDOT rating scale for a concrete bridge deck with an AC overlay, waterproofing membrane, and epoxy coated rebar. Condition ratings are reverse relative to standard NBI ratings, such that a higher condition-state number indicates a worse bridge condition.

Table 16. Condition-state ratings in Colorado (Adapted from CDOT 1998)

Condition State	Percent Distressed Deck Area
1	0%
2	$< 2\%$
3	$< 10\%$
4	$> 10\%$ and $< 25\%$
5	$> 25\%$

By applying the CDOT element coding guide indicators, the CDIs for the sample deck in Figure 53 can be used to determine a range of times when the sample deck can be expected to exist at a given condition state. The range of expected years since construction that the sample deck is in each condition state or transitioning between states is described in Table 17, and displayed in Figure 58. As anticipated, there is overlap in each period due to the range of CDIs. This overlap can be described as a condition state transition. Deterioration of the sample deck may begin between 12 and 22 years, and the deck may reach a 5 condition state between 36 and 45 years, depending on the number of epoxy coating defects. To reduce the transition times and obtain more precise condition state predictions, an analysis using the number of defects (similar to that in the previous section) can be performed. However, the approximate number of epoxy coating defects would need to be known. In the event that the number of defects is unknown, the average of 632/1950 (32% of cells) may be used.
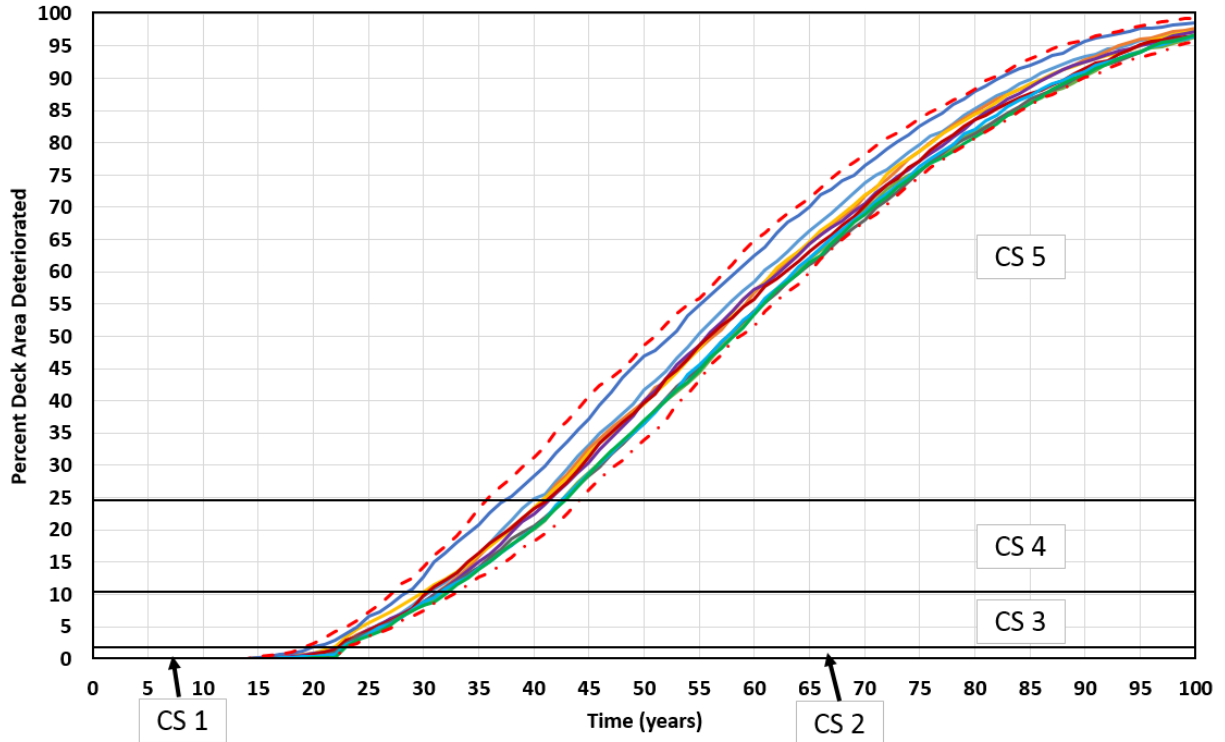
Figure 58. Cumulative damage vs. condition state for the sample deck

Table 17. Condition-state transitions for probabilistic simulations of the sample deck

Condition State	Years Since Construction
1	0 – 22
Transition 1-2	12 – 22
2	12 – 23
Transition 2-3	19 – 23
3	19 – 33
Transition 3-4	27 – 33
4	27 – 44
Transition 4-5	36 – 44
5	36 - 100+

At the local (cell) level, service life is defined as the time until cracking exceeds 0.3 mm and time T3 is reached. At the deck level, cells are still considered deteriorated ("failed") when time T3 is reached, but the definition of service life is adjusted to account for the timeline of deck

119

deterioration. The service life of a deck can be defined as the year when the percentage of cells experiencing cracking widths greater than 0.3 mm exceeds 25%. In other words, condition state 5 represents the end of the deck life. For the sample deck described above, the service life thus ranges between 36 and 44 years. For the sample deck with an average number of defects, the service life can be expected to end at 42 years.

7.2 Cumulative Damage with Maintenance

CDIs presented in the previous section are representative of a bridge deck being allowed to deteriorate without interference. Realistically, maintenance actions applied periodically to the deck will alter the shape of the CDI and timings of condition-state transitions. In Chapter 5, three scenarios for waterproofing membrane and asphalt overlay replacement cycles were proposed such that a single cell with mean-value inputs could reach a 100-year service life. Each scenario can be applied to a probabilistic full deck simulation of the same sample deck, in order to observe the changes in condition-state timings. Joint replacement on a seven-year cycle may also be included to represent standard repair practice.

In order to produce a direct comparison, a single simulation is conducted for each maintenance scenario using the average number of defects as shown in Figure 54. The same probabilistic distributions are used in each simulation, but the number of defects is held constant at the average number of 632/1950 (32%). Table 18 documents the estimated time for each scenario to change condition states. As expected, all maintenance strategies predict an extension on deck service life. Although it performs worse than the uniform maintenance strategy after roughly 70 years, the preventive maintenance strategy may significantly delay condition-state transitions early in the bridge life. Since the deck has reached an unacceptable level of deterioration before 70 years in all three cases, performance in the last 30 years of the 100-year period is not useful for extending bridge life. The dispersed maintenance scenario performs the worst overall, with a predicted service life of nearly 15 years less than its preventive counterpart. This is likely due to the very few number of waterproofing membranes installed, which allows for higher concrete saturation in all phases of deterioration.
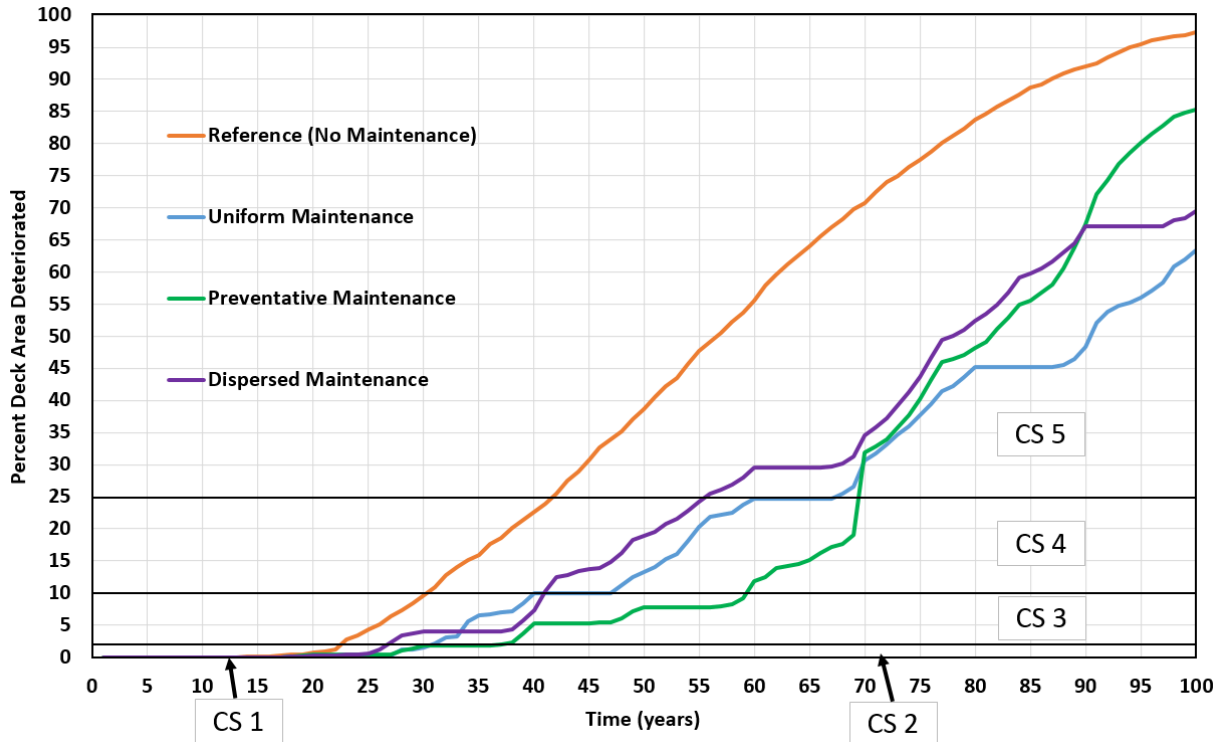
Figure 59. Cumulative damage vs. condition state for the sample deck with maintenance

Table 18. Condition states for the sample deck with maintenance

Condition State	Years Since Construction			
	Reference – No Maintenance	1 – Uniform Maintenance	2 – Preventive Maintenance	3 – Dispersed Maintenance
1	0 - 14	0 - 18	0 - 18	0 - 18
2	14 - 23	18 - 31	18 - 38	18 - 27
3	23 - 31	31 - 47	38 - 60	27 - 41
4	31 - 42	47 - 60	60 - 69	41 - 56
5	42+	60+	69+	56+

The main advantage of conducting preventive maintenance is a longer deck service life with fewer repairs. In comparison to uniform maintenance, performing preventive maintenance may extend service life by 9 or more years while using only one additional waterproofing membrane and four fewer asphalt overlay replacements.

121

If a single bridge deck is to reach the end of the 100-year period without being replaced, a uniform maintenance schedule can be used with more closely spaced repair intervals throughout the 100-year period. Referred to as "repetitive maintenance", this scenario predicts that the deck is only 20 percent deteriorated at 100 years. To obtain such a low deterioration rate, both the waterproofing membrane and asphalt overlay would be replaced simultaneously every 9 years until 99 years. The result of a repetitive maintenance strategy on the sample deck is shown in Figure 60. The mean time to corrosion initiation for each cell is 74 years, and the mean time to cell failure is 94 years.
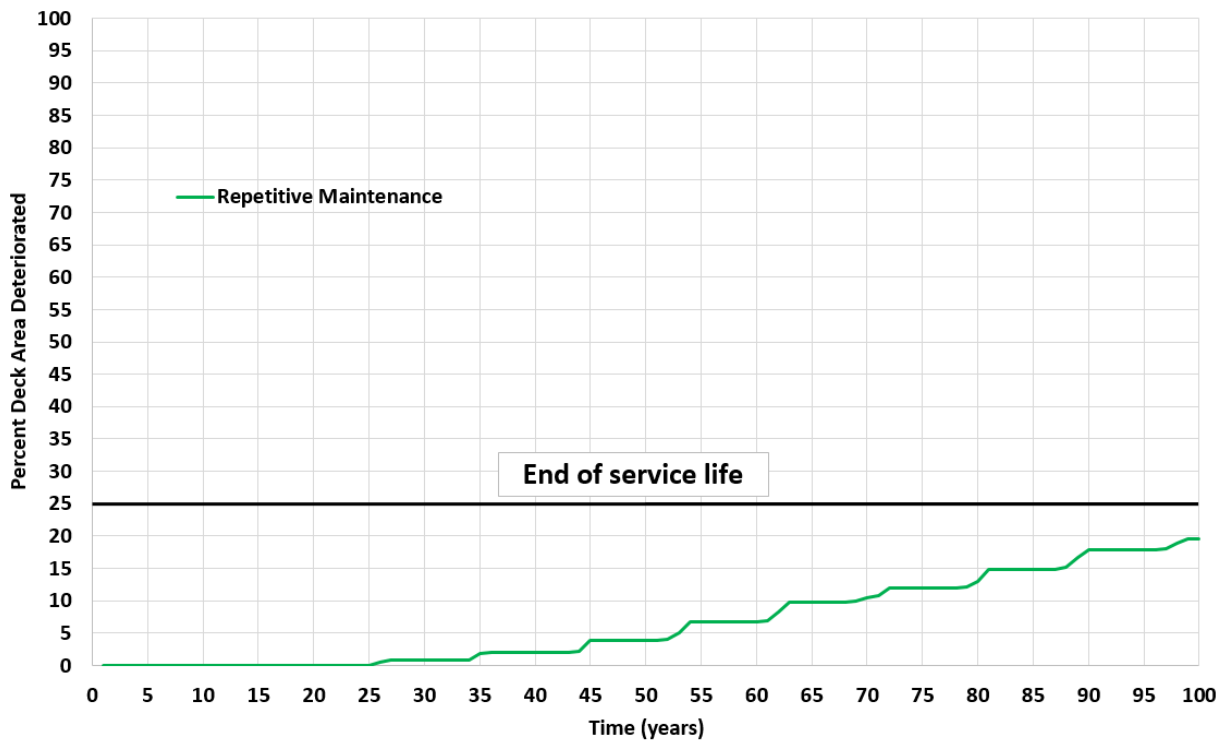
Figure 60. Cumulative damage of the sample deck with repetitive maintenance

7.3 Model Application

7.3.1 Bridge Categories

Application of probabilistic inputs and maintenance history to the deck model has demonstrated that individual bridge decks may not experience the same rate of deterioration due to variability in the model inputs. For example, an icy bridge deck in a mountainous region with high traffic loads

cannot be expected to deteriorate at the same rate as a bridge deck in a rural plains region with higher temperatures and lower traffic. Ideally, each bridge deck could be analyzed in the proposed deterioration model using inputs that represent that bridge alone. However, for thousands of bridges being maintained by a department of transportation, analyzing each bridge at the project level is unrealistic. In order to effectively predict deterioration, bridge decks with similar properties can be grouped together and a single analysis can be conducted for each group. Several suggested ways in which Colorado bridge decks may be categorized and the associated changes in model inputs are described in Table 19. This list is not comprehensive, and may vary depending on conditions specific to a state or other region.

Table 19. Potential bridge deck categories

Category	Model Inputs Affected
Location	Plains region: lower C_0 Mountainous region: higher C_0
Traffic	High traffic: shorter membrane/AO life Low traffic: longer membrane/AO life
Age	1970s and earlier: black steel rebar Post 1970s: epoxy coated rebar
Maintenance Cycle	Membrane replacement: lower i_{corr} Asphalt replacement: lower Cl^- concentration

To create bridge groups, each category can be combined. For example, one bridge group may describe bridges built prior to 1970 in mountainous regions with high traffic. This bridge group would have high mean surface chloride concentrations with short protective system life and black steel rebar. In this manner, service life predictions can be made for all bridges within a network without conducting an analysis for each individual bridge. Analyses based on design practices in the year(s) built may also be conducted to reflect changes in bridge design in recent decades. Properties such as cover depth and rebar size/spacing may depend on the era of construction, and protective systems such as membranes and overlays have evolved over time as well.

7.3.2 Limitations of Model Validation

Model validation is a necessary but challenging step in applying results of the deterioration model to bridge management. Since condition-state ratings can be approximated using the mechanistic model results, a direct comparison between model results and historical bridge condition states can be made. However, bridge condition states recorded during inspection reflect the effects of maintenance without a record of which maintenance actions were performed. As a result, the timing and type of maintenance applied to the bridge deck is unknown. For example, bridge WEL-031.0-074.0A in Colorado transitions from a 7 NBI rating in 1993 to a 3 rating in 2009. The window of NBI history does not include the initial conditions/rating of the deck (9 or 8), and the maintenance history or lack thereof is not documented in the inventory.

Previous attempts have been made to validate mechanistic models using inspection histories (Hu et al. 2013), but maintenance actions were not considered. As shown in Figure 59, condition state history may change significantly depending on maintenance. Model validation should be performed if and when a more comprehensive history of maintenance is available. In addition, NBI data that may be used for validation is only available from 1993 to present. The 23-year window may not be long enough to observe the full service life of an individual deck. Instead, condition state transitions between only two or three states may be observed. For modern bridge deck designs with longer expected service lives, 23-year inspection histories may not be able to fully depict deterioration. As a result of these limitations, model validation based on historical inspection ratings is not performed in the present analysis. Additional limitations and suggested steps towards model validation and implementation are discussed in Chapter 8.

8. CONCLUSIONS

As many aging highway bridges in the United States approach service lives of half a century or more, an understanding of how and when bridges will reach unserviceable states is of increasing importance. Bridge management is centered on the dynamic between inspection, management, and funding. In order to improve current bridge management practice and increase the overall condition of the nation's bridge infrastructure, two approaches are available: The level of funding may be increased, or funds may be allocated more efficiently. This report has sought to address the second option by demonstrating the capability of mechanistic-deterioration models to predict bridge deterioration in advance. If bridge condition can be determined as a function of design and environmental factors, funds can be allocated to maintenance that most cost-effectively extend service life. In this report, the following steps were taken with the goal of improving mechanistic models for bridges:

1. Reinforced concrete (RC) bridge decks were selected as the bridge element for study of mechanistic modeling due to their prevalent use throughout the United States and frequent need for repair. Various causes of bridge deck deterioration were investigated, and concrete cracking due to steel reinforcement corrosion was determined to be the deterioration mode most worthwhile of further investigation.

2. Similar to previous research, deterioration was divided into three stages representing corrosion initiation (T1), crack initiation (T2), and cell failure (T3). Analytical models that represent each stage were selected from the literature and combined to create a baseline model that predicts concrete cracking in a block of surrounding concrete (cell).

3. The baseline cell model was modified to reflect modern concrete bridge deck design practices including epoxy coated rebar (ECR), waterproofing membranes, and asphaltic overlays. A preliminary adhesion model based on previous experimental study was proposed to represent the condition of ECR as a function of environmental relative humidity and waterproofing membrane condition. Random defects in the epoxy coating were used to indicate non-uniform corrosion.

4. Ways in which the coupled effects of deterioration between two elements (decks and joints) can be modeled analytically were investigated. Joint deterioration was considered an

independent mechanism, and the effects of joint deterioration on the rate of corrosion damage in nearby deck cells was modeled. Gaps in the relationship between joint and bridge condition were addressed, and connections between joint condition, half-cell potentials, and corrosion rate were made by combining previous research.

5. The effects of deck maintenance techniques including membrane, asphalt, and joint replacement on model inputs and outputs were examined. Three maintenance strategies including uniform, preventive, and dispersed replacement timings were developed with the goal of extending cell service life to 100 years.

6. Uncertainty in model inputs was addressed by assigning probabilistic distributions to each input and evaluating deck condition as a function of multiple cells through time. Cumulative damage indexes (CDIs) were developed for a sample 8-meter by 12-meter deck and mapped to condition-state ratings based on percent deck area damaged. Model predictions were not validated due to a lack of maintenance histories.

The investigation yielded the following main conclusions:

1. Information is available to model the deterioration of bridge decks for very simplistic scenarios, including up to two modes of deterioration (i.e. corrosion and carbonation, Hu et al. 2013), but work is still necessary to make mechanistic models useful in the future. Rather than a replacement for current statistical models in use by departments of transportation, mechanistic models may be used as a supplement to fill in gaps where bridge-condition information is missing.

2. Use of mechanistic modeling in practice may improve the allocation of maintenance funding if the effects of various maintenance strategies on service-life extension can be demonstrated. Preventive maintenance, by applying fewer waterproofing membrane and asphalt overlay installations in early stages of deck life, may be able to increase deck service life over that achieved by uniform maintenance throughout deck service life, which may be considered both preventive and reactive. In most cases, the first stage of deterioration before corrosion initiation is significantly longer than stages of pressure build-up and crack propagation. It is hard to get meaningful service life extension in the intermediate and reactive stages, and the windows for maintenance between these stages are small.

126

3. Existence of non-uniform or rapid corrosion in bridge decks may not be exclusive to bare spots on rebar, but the presence of an epoxy coating defect remains the best indicator of accelerated damage. Variation in predicted deck condition relies more on the presence of non-uniform or pitting corrosion than variability in any other model input, including chloride concentrations or relative humidity.

Although the present model is capable of predicting bridge deck condition at any time as a function of many variables, data is still needed to make the model accurate and useful for bridge management. Model results should be treated as preliminary estimations until experimental data is available to refine the proposed relationships and validate predictions. Limitations and challenges for model implementation of the present model include:

1. Incompatibility between sub-models. Models which represent all stages of degradation are available in commercial software (STADIUM, Life-365, Conclife) and in the literature (Balafas and Burgoyne 2010), but only provide predictions for a simplified scenario. More sophisticated models that may provide higher accuracy and resolution in the individual stages are available, but are not consistent among researchers. Attempting to combine these models inevitably creates some discontinuity between stages due to different assumptions and model parameters (i.e. concrete compressive strength) made by individual researchers.
2. Lack of experimental or field data for model inputs. As demonstrated in Chapter 4, the rate of chloride diffusion through multiple media has a significant impact on model predictions, but no information was found which addressed the diffusion of chlorides in asphalt. The efficiency of protective systems such as waterproofing membranes and epoxy coated rebar is not well known. The ability of each system to inhibit corrosion as a function of time is a relatively unknown, but necessary, relationship for improving the accuracy of mechanistic models.
3. Service life as a function of crack width. Once cracks exceed an allowable width, service life ends and the cell may no longer be maintained within the context of the model. Service on "failed" concrete cells may still extend service life, and this aspect of maintenance should be included in future efforts.

Finally, as confidence in model predictions has improved and more data becomes available, steps towards **implementation** may include:

1. Bridge groups are created as a function of different categories such as location and traffic load to describe potential input distributions for new and previously constructed decks within a network.
2. Full deck simulations are conducted using the model for each group to obtain CDI bounds and approximate condition state transition times.
3. Model results are validated using historical bridge inspection results and maintenance histories.
4. LCCA is conducted to evaluate cost efficiency of various maintenance strategies on each bridge group.
5. Tables that provide cost-effective design and maintenance plans for bridge managers are developed for future use.

REFERENCES

AASHTO. (1994). Manual for Condition Evaluation of Bridges MCE-1. Washington, DC: American Association of State Highway and Transportation Officials.

AASHTO (2002). Standard Specification for Highway Bridges.

AASHTO. (2016). AASHTOWare Bridge. Retrieved from: http://www.aashtoware.org/Bridge/Pages/default.aspx

Agrawal, A.K., Kawaguchi, A., & Chen, Z. (2010). Deterioration rates of typical bridge elements in New York. J. Bridge Eng., 15(4), 419-429.

Ahmad, S. (2003). Reinforcement corrosion in concrete structures, its monitoring and service life prediction – a review. Concrete & Cement Composites, 25, 459-471.

Andrade, C., Alonso, C., & Molina, F.J. (1993). Cover cracking as a function of bar corrosion: Part I – Experimental test. Materials and Structures, 26(8), 453-464.

Ann, K.Y., & Song, H. (2007). Chloride threshold level for corrosion of steel in concrete. Corrosion Science, 49, 4113-4133.

ASCE. (2013). 2013 Report Card for America's Infrastructure.

ASTM-A775/A775M. (2016). Standard Specification for Epoxy-Coated Steel Reinforcing Bars.

ASTM-C876-15. (2016). Standard Test Method for Corrosion Potentials of Uncoated Reinforcing Steel in Concrete.

Balafas, I., & Burgoyne, C. (2011). Modeling the structural effects of rust in concrete cover. J. Eng. Mech., 137(3), 175-185.

Basheer, P. A. M., Chidiact, S. E., & Long, A. E. (1996). Predictive models for deterioration of concrete structures. Construction and Building Materials, 10(1), 27-37.

Bazant, Z., Chern, J., Rosenberg, A., & Gaidis, J. (1988). Mathematical model for freeze-thaw durability of concrete. Journal of the American Ceramic Society, 71(9), 776-783.

Bazant, Z. P., & Baweja, S. (1995a). Creep and shrinkage prediction model for analysis and design of concrete structures-model B3. Materials and Structures, 28, 357-365.

Brown, M.C. (2002). Corrosion protection service life of epoxy coated reinforcing steel in Virginia bridge decks. Virginia Polytechnic Institute and State University.

Caicedo, J., Wieger, G., Ziehl, P., & Rizos, D. (2011). Simplifying bridge expansion joint design and maintenance. FHWA Report No. SC-11-03.

Cao, C., & Cheung, M. (2014). Non-uniform rust expansion for chloride-induced pitting corrosion in RC structures. Construction and Building Materials, 51, 75-81.

CDOT (1998). Pontis Bridge Inspection Coding Guide. Staff Bridge.

CDOT (2014). Bridge Rating Manual. Staff Bridge.

Chen, E., & Leung, C. (2015). Finite element modeling of concrete cover cracking due to non-uniform steel corrosion. Engineering Fracture Mechanics, 134, 61-78.

CurrentResults (2016). Annual Average Humidity in Colorado. Retrieved from https://www.currentresults.com/Weather/Colorado/humidity-annual.php.

Czarnecki, B., & Day, R. (2008). Service life predictions for new and rehabilitated concrete bridge structures. Life-Cycle Civil Engineering, 8, 311-316.

DelDOT (2008). DelDOT Bridge Inspection Policies and Procedures.

Dhir, R.K., Jones, M.R., & McCarthy, M.J. (1993). Quantifying chloride-induced corrosion from half-cell potential. Cement and Concrete Research, 23(6), 1443-1454.

Djerbi, A., Bonnet, S., Khelidj, A., & Baroghel-bouny, V. (2008). Influence of transverse crack on chloride diffusion into concrete. Cement and Concrete Research, 38, 877-883.

Fanous, F., & Wu, H. (2005). Performance of coated reinforcing bars in cracked bridge decks. J. Bridge Eng., 10(3), 255-261.

FHWA. (1995). Recording and Coding Guide for the Structural Inventory and Appraisal of the Nation's Bridges. Report No. FHWA-PD-96-001.

FHWA. (2012). Bridge Inspector's Reference Manual. Report No. FHWA NHI 12-049.

FHWA (2015). National Bridge Inventory. Retrieved: https://www.fhwa.dot.gov/bridge/nbi.cfm.

Frangopol, D., Kong, J., & Gharaibeh, E. (2001). Reliability-based life-cycle management of highway bridges. J. Comput. Civ. Eng., 15(1), 27-34.

Geenen, FM. (1991). Characterization of organic coatings with impedance measurements: a study of coating structure, adhesion and underfilm corrosion (Doctoral dissertation, TU Delft, Delft University of Technology).

Hu, N., Haider, S., & Burgueño, R. (2013). Development and validation of deterioration models for concrete bridge decks – Phase 2: mechanics-based degradation models. MDOT Report No. RC-1587b.

Huang, Y., Adams, T., & Pincheira, J. (2004). Analysis of life-cycle maintenance strategies for concrete bridge decks, 9(3), 250-258.

Irfan, M., Khurshid, M., & Labi, S. (2009). Determining the service life of thin hot-mix asphalt overlay by means of different performance indicators. Transportation Research Record, 2108, 37-45.

Isgor, O.B., & Razaqpur, A.G. (2004). Finite element modeling of coupled heat transfer. Moisture transport and carbonation processes in concrete structures. Cement & Concrete Composites, 26, 57-73.

Jang, B., & Oh, B. (2010). Effects of non-uniform corrosion on the cracking and service life of reinforced concrete structures. Cement and Concrete Research, 40, 1441-1450.

Jiang, J., & Yuan, Y. (2013). Relationship of moisture content with temperature and relative humidity in concrete. Magazine of Concrete Research, 65(11), 685-692.

Kassir, M., & Ghosn, M. (2002). Chloride-induced corrosion of reinforced concrete bridge decks. Cement and Concrete Research, 32, 139-143.

Keßler, S., Angst, U., Zintel, M., & Gehlen, C. (2015). Defects in epoxy-coated reinforcement and their impact on the service life of a concrete structure. Structural Concrete, No. 3.

Kim, Y., and Yoon, D.K. (2010). Identifying critical sources of bridge deterioration in cold regions through the constructed bridges in North Dakota. J. Bridge Eng., 15(5), 542-552.

Kirkpatrick, T., Weyers, R., Anderson-Cook, C., & Sprinkel, M. (2002). Probabilistic model for the chloride-induced corrosion service life of bridge decks. Cement and Concrete Research, 32, 1943-1960.

Krauss, P., Lawler, J., & Steiner, K. (2009). Guidelines for selection of bridge deck overlays, sealers, and treatments. National Cooperative Highway Research Program, Project 20-07.

Liu, Y., & Weyers, R. E. (1998). Modeling the time-to-corrosion cracking in chloride contaminated reinforced concrete structures. ACI Materials Journal, 95(6).

Luping, T., & Gulikers, J. (2007). On the mathematics of time-dependent apparent chloride diffusion coefficient in concrete. Cement and Concrete Research, 37, 589-595.

MDOT (2016). National Bridge Inventory Rating Scale – State of Michigan.

Manning, D. (1996). Corrosion performance of epoxy-coated reinforcing steel: North American experience. Construction and Building Materials, 10(5), 349-365.

Morcous, G. (2006). Performance prediction of bridge deck systems using Markov chains. J. Perform. Constr. Facil., 20(2), 146-155.

Morcous, G., Lounis, Z., & Cho, Y. (2010). An integrated system for bridge management using probabilistic and mechanistic deterioration models: Application to bridge decks. J. Civ. Eng., 14(4), 527-537.

NCHRP. (1996). Report No. 12-28(02)B. Bridge Management Systems Software.

Neves, L., Frangopol, D., & Petcherdchoo, A. (2006). Probabilistic lifetime-oriented multiobjective optimization of bridge maintenance: combination of maintenance types. J. Struct. Eng., 132(11), 1821-1834.

ODOT (2005). Washing bridges to reduce chloride. Report No. SPR 304-031.

Pan, T., & Wang, L. (2011). Finite-element analysis of chemical transport and reinforcement corrosion-induced cracking in variably saturated heterogeneous concrete. J. Eng. Mech., 137(5), 334-345.

Phares, B., Washer, G., Rolander, D., Graybeal, B., & Moore, M. (2004). Routine highway bridge inspection condition documentation accuracy and reliability. Journal of Bridge Engineering, 9(4), 403-413.

Pincheira, J., Aramayo, A., Fratta, D., & Kim, K. (2015). Corrosion performance of epoxy-coated bars in four bridge decks subjected to deicing salts: 30-year perspective. J. Perform. Constr. Facil., 29(4), 1-1.

Pyć, Wioleta (1998). Field performance of epoxy-coated reinforcing steel in Virginia bridge decks. Virginia Polytechnic Institute and State University.

Rahim, A.M., Jansen, D., Abo-Shadi, N., & Simek, J. (2007). Use of high molecular weight methacrylate to seal bridge deck cracks: overview of research. Transportation Research Board, No. 07-0144.

Robelin, C.A., & Madanat, S. (2007). History-dependent bridge deck maintenance and replacement optimization with Markov decision processes. J. Infrastruct. Syst., 13(3), 195-201.

Roelfstra, G., Hajdin, R., Adey, B., & Brühwiler, E. (2004). Condition evolution in bridge management systems and corrosion-induced deterioration. J. Bridge Eng., 9(3), 268-277.

Safiuddin, Md., & Soudki, K.A. (2011). Sealer and coating systems for the protection of concrete bridge structures. International Journal of the Physical Sciences, 6(37), 8188-8199.

Šavija, B., Luković, M., Pacheco, J., & Schlangen, E. (2013). Cracking of the concrete cover due to reinforcement corrosion: A two-dimensional lattice model study. Construction and Building Materials, 44, 626-638.

Sohanghpurwala, A., & Scannell, W. (1998). Verification of effectiveness of epoxy-coated rebars. Pennsylvania Department of Transportation. Project No. 94-05.

Sohanghpurwala, A. (2006). Manual on service life of corrosion-damaged reinforced concrete bridge superstructure elements. NCHRP Report No. 558.

Song, H., Shim, H., Petcherdchoo, A., & Park, S. (2009). Service life prediction of repaired concrete structures under chloride environments using finite difference method. Cement & Concrete Composites, 31, 120-127.

Stewart, M., & Rosowsky, D. (1998). Time-dependent reliability of deteriorating reinforced concrete bridge decks. Structural Safety, 20, 91-109.

Thomas, M., & Bamforth, P. (1999). Modelling chloride diffusion in concrete; effect of fly ash and slag. Cement and Concrete Research, 29, 487-495.

Transportation Research Board (TRB). (2006). Control of Cracking in Concrete: State of the Art. TRB's Transportation Research Circular E-C107.

Urs, N., B.S., M., Jayaram, H., & Hedge, M.N. (2015). Residual life assessment of concrete structure – a review. International Journal of Engineering and Technical Research, 3(3).

US Climate Data (2016). Climate of Denver, Colorado. Retrieved from http://www.usclimatedata.com/climate/denver/colorado/united-states/usco0105.

Washer, G., Nasrollahi, M., Applebury, C., Connor, R., Ciolko, A., Kogler, R., . . . Forsyth, D. (2014). Proposed guideline for reliability-based bridge inspection practices.

Xi, Y., Abu-Hejleh, N., Asiz, A., & Suwito, A. (2004). Performance evaluation of various corrosion protection systems of bridges in Colorado. CDOT Research Branch. Report No. DTD-R-2004-1.

Yehia, S., Abudayyeh, O., Fazal, I., & Randolph, D. (2008). A decision support system for concrete bridge deck maintenance. Advances in Engineering Software, 39, 202-210.